Chapter 2
Dynamics of a Moving and Oscillating Moving Load Acting on a Pre-strained Bi-material Layered Systems

In this chapter the problems related to the dynamics of a moving and oscillating moving load acting on the pre-stressed layered systems such as covering layer + half-plane, covering layer + half-space, bi-layered slab resting on a rigid foundation are studied. The studies are carried out within the scope of the piecewise homogeneous body model by utilizing of the three-dimensional linearized theory of the elastic waves in initially stressed bodies (TDLTEWISB). The cases where the initial stress-strain state is determined within the framework of the classical linear theory of elasticity and within the framework of the nonlinear theory of elasticity for highly elastic materials are considered. Materials of the constituents are modeled as isotropic as well as orthotropic ones. The problems considered in this chapter can also be classified as two and three dimensional ones. Numerical results on the critical velocity for each noted above cases are presented and discussed. The cases where the materials of the constituents are linear viscoelastic are also considered and analyzed.

Throughout this chapter, we will assume that if repeated subscripts are only in one side of equations, then they indicate a summation over their ranges.

2.1 Background of Related Investigations

We consider a brief review of the investigations related to the dynamics of the moving load acting on layered elastic systems. We start this review with the investigation made by Achenbach et al. (1967) in which the dynamical response of the system consisting of a covering layer + half-plane to a moving load has been studied. The equations of motion of the covering layer (plate) are described within the scope of the Timoshenko theory, but the equation of motion of the half-plane is described within the scope of the exact linear theory of elastodynamics. The plane-strain state is considered as is the load sinusoidal varying along the load-moving direction: the line load is also examined. It has been assumed that the velocity of the moving load is constant. For the sinusoidal varying load, it was established that for the system considered the resonance type effect occurs in the case where a load of certain wave length moves with a velocity equal to the velocity of free waves of that

S.D. Akbarov, *Dynamics of Pre-Strained Bi-Material Elastic Systems*,
DOI 10.1007/978-3-319-14460-3_2

wave length. For the sinusoidal varying loading the sought values are expressed through $(\Delta(c))^{-1}$, where $\Delta(c) = 0$ is a dispersion equation of the previously mentioned waves (here c is a wave velocity). However, under action of the moving line load, the sought values are expressed through $\int_0^\infty (\bullet)(\Delta(x))^{-1} dx$, and therefore the existence of the resonance type effect, expressed through the dispersion equation $\Delta(x) = 0$ must have a double real root, i.e. this root must satisfy the equations $\Delta(x) = 0$ and $d\Delta(x)/dx = 0$, simultaneously. As is normal in such cases, the phase velocity has a minimum and this velocity is known as the critical velocity. It is obvious that the mentioned phase velocity equals the group velocity. The numerical examination for the line load has been made for cases involving a relatively soft plate, i.e. for the case where $(G_1/\rho_1)/(G/\rho) < 1.0$; $G_1(G)$ and $\rho_1(\rho)$ are the shear modulus and density, respectively, of the covering plate (half-plane) material and a relatively stiff plate, i.e. for the case where $(G_1/\rho_1)/(G/\rho) > 1.0$. It is established that the critical velocity determined in the foregoing manner arises only for the cases where $(G_1/\rho_1)/(G/\rho) > 1.0$, i.e. for a relatively stiff plate.

The investigation started by Achenbach et al. (1967), over time, has been improved and developed continuously; the latest investigations of this development, the subjects of which are near to the subject of the present chapter, are described in papers by Dieterman and Metrikine (1997) and by Metrikine and Vrouwenvelder (2000) and other references listed in these papers. In the paper by Dieterman and Metrikine (1997) the critical velocity of a point-loaded harmonic varying load moving uniformly and acting on the free face plane of the plate resting on the rigid foundation is investigated. The motion of the plate is described by the 3D equations of the linear theory of elastic waves. The critical velocity is determined as that velocity which is equal to the group velocity. Moreover, in the paper by Dieterman and Metrikine (1997) it is noted that the elastic layer is taken as a model train-sleeper excitation. The corresponding boundary value problem is solved by employing exponential Fourier transforms over time and for the spatial coordinates. According to the analyses of the obtained numerical results, it is established that the harmonic variation of the moving load causes two critical velocities to exist; one is lower, but the other is higher, than the Rayleigh wave velocity in the plate material. Note that similar results are also obtained in papers by Akbarov and Salmanova (2009), Akbarov and Ilhan (2009) and Akbarov et al. (2014, 2015) which will be discussed in the present chapter.

In the paper by Metrikine and Vrouwenvelder (2000) the surface ground vibrations for a 2D model are considered, consisting of an elastic layer (possessing a small viscosity), and a beam located inside the layer. It is supposed that the layer and the beam are infinitely long in the horizontal direction and rest on the rigid foundation. The motion of the beam is written within the scope of the Euler-Bernoulli model. Moreover, it is assumed that the motion of the structure is caused by a point load, which moves uniformly along the beam: three types of this load are considered, namely a constants load, a harmonically varying load and, a stationary random load. Note that all investigations carried out by Metrikine and Vrouwenvelder (2000) are also based on knowledge of the critical velocity which is determined from the investigation of the straight line (known as a "kinematic

invariant" (see Vesnitskii and Metrikine 1993) and dispersion curves of the corresponding wave propagation. Moreover, under action of the external harmonically varying load the mentioned dispersion curves are plotted both for positive and "negative wavenumbers", because the harmonically varying load can radiate waves with a negative phase velocity. It should also be noted, in all the investigations discussed above, that the surface displacements are studied as well. But the stress distribution in the constituents of the system considered, and stresses acting on the interface planes, have essentially not been studied. Moreover, in the foregoing studies the reference particularities of these systems are not taken into account, one of which is the initial stresses (or strains) in the component of those.

The source of these initial stresses or strains could be sharp changes in environmental conditions (i.e. temperature changes which can cause roadbeds, aircraft runways, etc. to be initially stressed); alternately, the source of the initial stresses could be the manufacturing and assembly procedures of the systems considered, the action of the geostatic and geodynamic forces in the Earth's crust (which is modelled as a lower layer or as a half-plane in the corresponding investigations) etc. In fact, it is necessary to take these initial stresses (strains) into account within the study of the dynamic response of vehicle-tracking systems to a moving load. In these cases the excitation of the moving vehicle on the system mentioned is modelled as the action moving load or oscillating moving load on that system.

The first attempt to account for the initial stresses on the values of the critical velocity of the moving load was made in a paper by Kerr (1983) where a system consisting of an ice plate resting on a water layer was considered. In this case the motion of the plate is described within the scope of the Kirchhoff theory and it is established that the initial stretching (compression) causes an increase (decrease) in the values of the critical velocity.

It is obvious that more accurate and trustworthy results for the types of problems related to initially stressed systems can be attained within the scope of the TDLTEWISB. The construction of the TDLTEWISB field equations and their applications to wave propagation problems are detailed in works by Green et al. (1952), Biot (1965), Truesdell and Noll (1965), Eringen and Suhubi (1975), Guz (1999, 2002, 2004), and others. Under the mentioned construction, one considers two states of a deformable solid. The first is regarded as the initial or unperturbed state, and the second is a perturbed state with respect to the unperturbed. By "the state of a deformable solid" is meant both motion and equilibrium (as a particular case of motion). It is assumed that all values in a perturbed state can be represented as a sum of the values in the initial state and perturbations. The latter is also assumed to be small in comparison with the corresponding values in the initial state. It is also assumed that both initial (unperturbed) and perturbed states are described by the equations of non-linear solid mechanics. Due to the fact that perturbations are small, the relationships for the perturbed state in the vicinity of appropriate values for the unperturbed state are linearized and then subtract from them the relationships for the unperturbed state. The results are the equations of the TDLTEWISB. Since equations contain the initial state variables, the TDLTEWISB describes the influence of the initial stresses on the perturbations. In particular cases

in sections of the present chapter the procedure described above on the obtaining of the equations and relations of the TDLTEWISB will be given in detail.

It should be noted that there are some versions of the TDLTEWISB which were developed in the monographs by Guz (1999, 2004). These versions of the TDLTEWISB are distinguished from each other with respect to the magnitude of the initial strains. The version of the TDLTEWISB developed for highly elastic materials, according to which the initial strains in the bodies are determined within the scope of the non-linear theory of elasticity without any restrictions on the magnitude of the initial strains is called the large (or finite) initial deformation version. The version of the TDLTEWISB, according to which, an initial stress-strain state in bodies is determined within the scope of the geometrically non-linear theory of elasticity and under which changes to the elementary areas and volumes as a result of the initial deformation are not taken into account, is called the first version of the initial deformation theory of the TDLTEWISB. The second version of the small initial deformation theory of the TDLTEWISB is the version, according to which, an initial stress-strain state in bodies is determined within the scope of the classical linear theory of elasticity.

Nevertheless, within the framework of the TDLTEWISB, before of the author's and his students' works, a few studies have been done by Babich et al. (1986, 1988, 2008a, b) on the dynamic response to the moving load of a pre-strained layered half-space. Note that in the paper by Babich et al. (1986), as in the paper by Achenbach et al. (1967), the dynamic response was considered for a system consisting of a covering layer and pre-strained half-plane. The motion of the covering layer was described by the Timoshenko plate theory, but the motion of the half-plane by the finite initial deformation version of the TDLTEWISB. The solution of the corresponding boundary-value problem was found by employing Fourier transforms by spatial coordinate. Numerical investigations were performed in the case where the constitutive relations for the half-plane material were given by the harmonic potential. The speed of the moving load was assumed constant, and the subsonic case had been taken into consideration. These numerical investigations led to further study of the parameters' influence on the critical velocity in the second study by Babich et al. (1988) utilizing the complex potentials of the TDLTEWISB. As in the paper by Achenbach et al. (1967), the numerical results obtained in the papers by Babich et al. (1986, 1988) show that a critical velocity occurs for a relatively stiff plate. In the further investigations by Babich et al. (2008a, b) the investigations carried out in the previous two papers of these authors were developed for the case where the velocity of the moving load is supersonic. This development was made for an incompressible (Babich et al. 2008a) as well as for compressible (Babich et al. 2008b) materials. Note that all investigations carried out in these papers were made for 2D problems (plane-strain state).

That is all which were studied before investigations carried out by Akbarov et al. (2007), Akbarov and Salmanova (2009), Akbarov and Ilhan (2008, 2009) and Akbarov et al. (2011, 2014, 2015) in which not only the motion of the half-plane or substrate, but also the motion of the pre-stressed covering layer is described by employing of the TDLTEWISB and it is supposed that the initial stresses exist not

only in the half-plane, but also in the covering layer. Moreover, in these papers not only the finite initial deformation version, but also the small initial deformation version of the TDLTEWISB is employed. The detail description and analyze of the results obtained in the mentioned papers by the author of the present monograph and his students and some new results related to the cases where the materials of the covering layer + half-plane systems are viscoelastic ones are the subject of the present chapter.

2.2 Critical Velocity of a Moving Load Acting on the Pre-stressed Layer Resting on a Pre-stressed Half-Plane

In the present section the problem related to the dynamics of the moving load acting on the system consisting of the pre-stressed covering layer and pre-stressed half-plane is studied. It is assumed that the materials of the constituents are isotropic. The investigations are carried out by utilizing the second version of the small initial deformation theory of the TDLTEWISB and are based on the results obtained in the paper by Akbarov et al. (2007).

2.2.1 Formulation of the Problem

Let us consider a pre-stressed half-plane with a pre-stressed layer. The points of the layer and half-plane are specified by Lagrangian coordinates in a Cartesian reference frame $Ox_1x_2x_3$ (Fig. 2.1). Before assembling, the layer and the half-plane had been stressed separately in the Ox_1 axis direction, so that a uniaxial homogeneous initial stress state exists in each of them. The covering layer and the half-plane occupy the regions $\{-h < x_2 < 0\}$ and $\{-\infty < x_2 < -h\}$ respectively in the case where $-\infty < x_1 < +\infty$ and $-\infty < x_3 < +\infty$. The Ox_3 axis is perpendicular to the figure plane and therefore is not shown in Fig. 2.1.

The stresses, strains and displacements related to the layer and half-plane are denoted by the superscripts (1) and (2), respectively. The quantities related to the initial stresses are denoted by the superscripts $(m)0$, where $m = 1, 2$.

The linear elastic materials of the layer and the half-plane are taken to be homogeneous, isotropic and moderately rigid. The initial stresses $\sigma_{ij}^{(m)0}$ in the constituents are determined within the scope of the classical linear theory of elasticity and can be written in the form

$$\sigma_{11}^{(m)0} = const_m; \sigma_{ij}^{(m)0} = 0 \quad \text{at} \quad ij \neq 11. \tag{2.1}$$

Since the initial strains are small, it is assumed that the coordinates of the layer and half-plane points in the natural and initial states coincide.

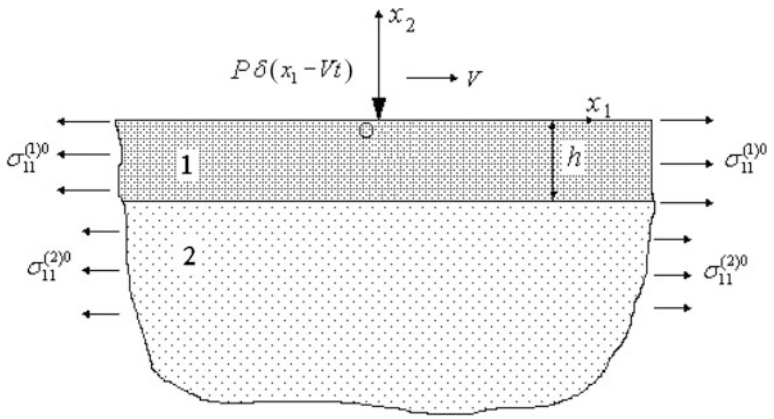

Fig. 2.1 Geometry of a pre-stressed half-plane (denoted by number *2*) covered with a pre-stressed layer (denoted by number *1*)

Thus, within the framework of foregoing assumptions, we assume that on the free upper face of the covering layer a lineal located force with intensity P acts and this force moves in the Ox_1 axis direction with a constant speed V (Fig. 2.1). It is required to determine the dynamical response of the layered system under consideration to this moving loading. Under this determination we will consider only the subsonic regime, i.e. we will assume that

$$V < \min\left\{c_2^{(1)}\sqrt{1+\frac{\sigma_{11}^{(1)0}}{\mu^{(1)}}}, c_2^{(2)}\sqrt{1+\frac{\sigma_{11}^{(2)0}}{\mu^{(2)}}}\right\}, c_2^{(m)} = \sqrt{\mu^{(m)}/\rho^{(m)}}, \quad m = 1, 2, \tag{2.2}$$

where $c_2^{(m)}$, $\mu^{(m)}$ and $\rho^{(m)}$ are the speed of distortion waves, the shear modulus and density of the material of the mth constituent.

According to the foregoing discussions, we can assume that the plane-strain state occurs in the system under consideration. In the mentioned case the equation of the second version of the small initial deformation theory of the TDLTEWISB are

$$\frac{\partial \sigma_{ij}^{(m)}}{\partial x_i} + \sigma_{11}^{(m)0}\frac{\partial^2 u_j^{(m)}}{\partial x_1^2} = \rho^{(m)}\frac{\partial^2 u_j^{(m)}}{\partial t^2}, \quad i;\ j;\ m = 1, 2, \tag{2.3}$$

$$\sigma_{ij}^{(m)} = \lambda^{(m)}\theta^{(m)}\delta_i^j + 2\mu^{(m)}\varepsilon_{ij}^{(m)}, \theta^{(m)} = \varepsilon_{11}^{(m)} + \varepsilon_{22}^{(m)} \tag{2.4}$$

$$\varepsilon_{ij}^{(m)} = \frac{1}{2}\left(\frac{\partial u_i^{(m)}}{\partial x_j} + \frac{\partial u_j^{(m)}}{\partial x_i}\right). \tag{2.5}$$

In Eq. (2.3) repeated index i is summed over its range.

Now we consider briefly the obtaining of the Eq. (2.3). For this purpose, first, we write the geometrical non-linear equations of motion

$$\frac{\partial}{\partial x_i}\left[\sigma_{in}\left(\delta_j^n+\frac{\partial u_j}{\partial x_n}\right)\right]=\rho\frac{\partial^2 u_j}{\partial t^2}. \tag{2.6}$$

Replacing the stresses σ_{in} and the displacements u_j in Eq. (2.6) with $\sigma_{in}^0+\sigma_{in}$ and $u_j^0+u_j$ respectively, where σ_{in}^0 and u_j^0 relate to the initial stress state and satisfy the equilibrium equation

$$\frac{\partial}{\partial x_i}\left[\sigma_{in}^0\left(\delta_j^n+\frac{\partial u_j^0}{\partial x_n}\right)\right]=0, \tag{2.7}$$

σ_{in} and u_j are perturbations of stresses and displacements respectively; $\sigma_{in}^0+\sigma_{in}$ and $u_j^0+u_j$ satisfy the equation of motion (2.6), i.e.

$$\frac{\partial}{\partial x_i}\left[(\sigma_{in}^0+\sigma_{in})\left(\delta_j^n+\frac{\partial(u_j^0+u_j)}{\partial x_n}\right)\right]=\rho\frac{\partial^2 u_j}{\partial t^2} \tag{2.8}$$

According to the second version of the small initial deformation theory of the TDLTEWISB, we assume that $\partial u_j^0/\partial x_n \ll 1$ and $\delta_j^n+\partial u_j^0/\partial x_n\approx\delta_j^n$, and obtain $\partial\sigma_{ij}^0/\partial x_i=0$ instead of the Eq. (2.7), and linearizing the Eq. (2.8) with respect to σ_{in} and u_j, taking the expression (2.1) and the Eq. (2.7) (or the equation $\partial\sigma_{ij}^0/\partial x_i=0$) into consideration we obtain the Eq. (2.3) from the Eq. (2.8). Under the mentioned linearization procedure it is assumed that the nonlinear terms, such as $\sigma_{in}\partial u_j/\partial x_n$ and $\sigma_{in}^0\partial u_j^0/\partial x_n$, as well as the term $\sigma_{in}\partial u_j^0/\partial x_n$ can be neglected with respect to the σ_{in} and $\sigma_{in}^0\partial u_j/\partial x_n$ in the Eq. (2.8).

Since, it is assumed that the elasticity relations are linear, therefore these relation for the initial stress-strain state and for the perturbations of stresses and strains are the same as shown in (2.4). Finally, writing the non-linear strain-displacement relations

$$\varepsilon_{ij}=\frac{1}{2}\left(\frac{\partial u_i}{\partial x_j}+\frac{\partial u_j}{\partial x_i}+\frac{\partial u_n}{\partial x_j}\frac{\partial u_n}{\partial x_i}\right), \tag{2.9}$$

replacing ε_{ij}, u_i, u_j and u_n with $\varepsilon_{ij}^0+\varepsilon_{ij}$, $u_i^0+u_i$, $u_j^0+u_j$ and $u_n^0+u_n$ respectively, taking $\delta_j^n+\partial u_n^0/\partial x_j\approx\delta_j^n$ and $\delta_i^n+\partial u_n^0/\partial x_i\approx\delta_j^n$ into consideration, and linearizing the expression (2.9) with respect the u_i, u_j and u_n we obtain the Eq. (2.5).

As follows from the foregoing discussions that under consideration of the moving load problems, to take the initial stresses into account can be estimated as to take the non-linear dynamical effects into account which cannot be described within

the scope of the classical linear theory of elastodynamics. In connection with this, it can be concluded that the magnitude of the stresses and displacements caused by the moving load depends not only on the magnitude of the moving load and boundary-contact conditions related to the perturbations, mechanical and geometrical properties of the constituents of the system under consideration, but also on the values of the initial stresses. In other words, the classical superposition principle cannot be applied for the problem under consideration.

Thus, we turn to formulation of the problem and, according to the mentioned above, on the upper face of the covering layer, the following boundary conditions must be satisfied:

$$\sigma_{12}^{(1)}\Big|_{x_2=0} = 0, \ \sigma_{22}^{(1)}\Big|_{x_2=0} = -P\delta(x_1 - Vt). \tag{2.10}$$

where $\delta(x)$ is the Dirac delta function.

Consider two types (complete contact and incomplete contact with full slipping) of contact conditions on the interface plane between the covering layer and half-plane. For the complete contact case we assume that the relations

$$\sigma_{i2}^{(1)}\Big|_{x_2=-h} = \sigma_{i2}^{(2)}\Big|_{x_2=-h}, \ u_i^{(1)}\Big|_{x_2=-h} = u_i^{(2)}\Big|_{x_2=-h}, \quad i = 1, 2 \tag{2.11}$$

take place, but the incomplete contact conditions with full slipping are formulated as follows.

$$\sigma_{12}^{(1)}\Big|_{x_2=-h} = 0, \sigma_{12}^{(2)}\Big|_{x_2=-h} = 0, \sigma_{22}^{(1)}\Big|_{x_2=-h} = \sigma_{22}^{(2)}\Big|_{x_2=-h}, \ u_2^{(1)}\Big|_{x_2=-h} = u_2^{(2)}\Big|_{x_2=-h}. \tag{2.12}$$

In addition, we also assume that

$$\left|u_i^{(2)}\right| \to 0, \ \left|\sigma_{ij}^{(2)}\right| \to 0 \quad \text{as } x_2 \to -\infty. \tag{2.13}$$

This completes the formulation of the problem, according to which, the investigation of the dynamical response of the initially stressed covering layer + half-plane system to the moving load is reduced to the solution of the boundary-contact-value problem consisting of the Eqs. (2.3)–(2.5), boundary condition (2.10) and the contact condition (2.11) (for the complete contact case) or the contact condition (2.12) (for the incomplete contact with full slipping). In the case where the initial stresses are absent in the constituents of the system, i.e. in the case where $\sigma_{11}^{(1)0} = \sigma_{11}^{(2)0} = 0$, the foregoing formulation transforms to the formulation of the corresponding dynamic problem of the classical linear theory of elastodynamics.

2.2.2 Solution Method of the Corresponding Boundary-Contact-Value Problem

From Eqs. (2.3)–(2.5) we obtain the following equations of motion in terms of perturbations of displacements $u_i^{(m)}$:

$$\begin{aligned}
&(\lambda^{(m)} + 2\mu^{(m)} + \sigma_{11}^{(m)0})\frac{\partial^2 u_1^{(m)}}{\partial x_1^2} + \mu^{(m)}\frac{\partial^2 u_1^{(m)}}{\partial x_2^2} \\
&\quad + (\lambda^{(m)} + \mu^{(m)})\frac{\partial^2 u_2^{(m)}}{\partial x_1 \partial x_2} = \rho^{(m)}\frac{\partial^2 u_1^{(m)}}{\partial t^2}, \\
&(\lambda^{(m)} + \mu^{(m)})\frac{\partial^2 u_1^{(m)}}{\partial x_1 \partial x_2} + (\mu^{(m)} + \sigma_{11}^{(m)0})\frac{\partial^2 u_2^{(m)}}{\partial x_1^2} \\
&\quad + (\lambda^{(m)} + 2\mu^{(m)})\frac{\partial^2 u_2^{(m)}}{\partial x_2^2} = \rho^{(m)}\frac{\partial^2 u_2^{(m)}}{\partial t^2}.
\end{aligned} \tag{2.14}$$

By using the coordinate system

$$x_2' = x_2, x_1' = x_1 - Vt \tag{2.15}$$

which moves with the loading force and rewriting the Eq. (2.14) with the coordinates x_1' and x_2', we obtain:

$$\begin{aligned}
&\left(\frac{\lambda^{(m)}}{\mu^{(m)}} + 2 + \frac{\sigma_{11}^{(m)0}}{\mu^{(m)}} - \frac{V^2}{(c_2^{(m)})^2}\right)\frac{\partial^2 u_1^{(m)}}{\partial x_1^2} \\
&\quad + \frac{\partial^2 u_1^{(m)}}{\partial x_2^2} + \left(\frac{\lambda^{(m)}}{\mu^{(m)}} + 1\right)\frac{\partial^2 u_2^{(m)}}{\partial x_1 \partial x_2} = 0, \\
&\left(\frac{\lambda^{(m)}}{\mu^{(m)}} + 1\right)\frac{\partial^2 u_1^{(m)}}{\partial x_1 \partial x_2} + \left(1 + \frac{\sigma_{11}^{(m)0}}{\mu^{(m)}} - \frac{V^2}{(c_2^{(m)})^2}\right)\frac{\partial^2 u_2^{(m)}}{\partial x_1^2} \\
&\quad + \left(\frac{\lambda^{(m)}}{\mu^{(m)}} + 2\right)\frac{\partial^2 u_2^{(m)}}{\partial x_2^2} = 0,
\end{aligned} \tag{2.16}$$

where the primes on x_1 and x_2 are omitted. In this case, the second condition in (2.10) transforms to the following one

$$\sigma_{22}^{(1)}\Big|_{x_2} = -P\delta(x_1), \tag{2.17}$$

but the other relations in (2.10)–(2.13) remain valid in the new coordinates determined by (2.15).

In order to solve system of equations in (2.16), we apply the Fourier transform

$$f_F(s,x_2)=\int\limits_{-\infty}^{+\infty} f(x_1,x_2)e^{-isx_1}dx_1. \tag{2.18}$$

to these equations, boundary and contact conditions in (2.17), (2.10)–(2.13). As a result we have

$$\begin{aligned} -s^2a^{(m)}u_{1F}^{(m)}+\frac{d^2u_{1F}^{(m)}}{dx_2^2}+isb^{(m)}\frac{du_{2F}^{(m)}}{dx_2}=0,\\ isb^{(m)}\frac{du_{1F}^{(m)}}{dx_2}-s^2c^{(m)}u_{2F}^{(m)}+(b^{(m)}+1)\frac{d^2u_{2F}^{(m)}}{dx_2^2}=0, \end{aligned} \tag{2.19}$$

where

$$\begin{aligned} i=\sqrt{-1},a^{(m)}=\frac{\lambda^{(m)}}{\mu^{(m)}}+2+\frac{\sigma_{11}^{(m)0}}{\mu^{(m)}}-\frac{V^2}{(c_2^{(m)})^2},\\ b^{(m)}=\frac{\lambda^{(m)}}{\mu^{(m)}}+1,c^{(m)}=1+\frac{\sigma_{11}^{(m)0}}{\mu^{(m)}}-\frac{V^2}{(c_2^{(m)})^2}. \end{aligned} \tag{2.20}$$

After some mathematical manipulations, we obtain from (2.19) the equations

$$\begin{aligned} &(b^{(m)}+1)\frac{d^4u_{2F}^{(m)}}{dx_2^4}+(s^2(b^{(m)})^2-s^2c^{(m)}-s^2a^{(m)}(b^{(m)}+1))\frac{d^2u_{2F}^{(m)}}{dx_2^2}\\ &+s^4a^{(m)}c^{(m)}u_{2F}^{(m)=0}\ ,\quad \frac{du_{1F}^{(m)}}{dx_2}=-is\frac{c^{(m)}}{b^{(m)}}u_{2F}^{(m)}+i\frac{(b^{(m)}+1)}{dx_2^2}. \end{aligned} \tag{2.21}$$

Taking the condition (2.13) into account, the solution to the Eq. (2.21) is found as follows.

$$\begin{aligned} u_{2F}^{(1)}=F_1^{(1)}e^{k_1^{(1)}x_2}+F_2^{(1)}e^{-k_1^{(1)}x_2}+F_3^{(1)}e^{k_2^{(1)}x_2}+F_4^{(1)}e^{-k_2^{(1)}x_2},\\ u_{2F}^{(2)}=F_1^{(2)}e^{k_1^{(2)}x_2}+F_3^{(2)}e^{k_2^{(2)}x_2}, \end{aligned} \tag{2.22}$$

where

$$\begin{aligned} k_1^{(m)}=\sqrt{\frac{A^{(m)}}{2}+\sqrt{\left(\frac{A^{(m)}}{2}\right)^2-B^{(m)}}},k_2^{(m)}=\sqrt{\frac{A^{(m)}}{2}-\sqrt{\left(\frac{A^{(m)}}{2}\right)^2-B^{(m)}}},\\ A^{(m)}=\frac{s^2b^{(m)}-s^2c^{(m)}-s^2a^{(m)}(b^{(m)}+1)}{b^{(m)}+1},B^{(m)}=\frac{s^4a^{(m)}c^{(m)}}{b^{(m)}+1}. \end{aligned} \tag{2.23}$$

We obtain the following expressions for $u_{1F}^{(m)}$ from the second equation in (2.21).

$$\begin{aligned} u_{1F}^{(1)} &= i\Big[F_1^{(1)}\alpha_1^{(1)}e^{k_1^{(1)}x_2} + F_2^{(1)}\alpha_2^{(1)}e^{-k_1^{(1)}x_2} + F_3^{(1)}\alpha_3^{(1)}e^{k_2^{(1)}x_2} + F_4^{(1)}\alpha_4^{(1)}e^{-k_2^{(1)}x_2}\Big], \\ u_{1F}^{(2)} &= i\Big[F_1^{(2)}\alpha_1^{(2)}e^{k_1^{(2)}x_2} + F_3^{(2)}\alpha_3^{(2)}e^{k_2^{(2)}x_2}\Big]. \end{aligned} \tag{2.24}$$

where

$$\begin{aligned} \alpha_1^{(1)} &= -s\frac{c^{(1)}}{k_1^{(1)}} + \frac{(b^{(1)}+1)k_1^{(1)}}{sb^{(1)}}, \alpha_2^{(1)} = s\frac{c^{(1)}}{k_1^{(1)}} - \frac{(b^{(1)}+1)k_1^{(1)}}{sb^{(1)}}, \\ \alpha_3^{(1)} &= -s\frac{c^{(1)}}{k_2^{(1)}} + \frac{(b^{(1)}+1)k_2^{(1)}}{sb^{(1)}}, \alpha_4^{(1)} = s\frac{c^{(1)}}{k_2^{(1)}} - \frac{(b^{(1)}+1)k_2^{(1)}}{sb^{(1)}}, \\ \alpha_1^{(2)} &= -s\frac{c^{(2)}}{k_1^{(2)}} + \frac{(b^{(2)}+1)k_1^{(2)}}{sb^{(2)}}, \alpha_3^{(2)} = -s\frac{c^{(2)}}{k_2^{(2)}} + \frac{(b^{(2)}+1)k_2^{(2)}}{sb^{(2)}}. \end{aligned} \tag{2.25}$$

Finally, substituting (2.22) and (2.24) into the Fourier transforms of the expressions (2.4) and (2.5) we attain the expressions written below for the Fourier transforms of the stresses.

$$\begin{aligned} \sigma_{11F}^{(1)} &= F_1^{(1)}(\lambda^{(1)}(s\alpha_1^{(1)} + k_1^{(1)}) + 2\mu^{(1)}s\alpha_1^{(1)})e^{k_1^{(1)}x_2} \\ &\quad + F_2^{(1)}(\lambda^{(1)}(s\alpha_2^{(1)} - k_1^{(1)}) + 2\mu^{(1)}s\alpha_2^{(1)})e^{-k_1^{(1)}x_2} \\ &\quad + F_3^{(1)}(\lambda^{(1)}(s\alpha_3^{(1)} + k_2^{(1)}) + 2\mu^{(1)}s\alpha_3^{(1)})e^{k_2^{(1)}x_2} \\ &\quad + F_4^{(1)}(\lambda^{(1)}(s\alpha_4^{(1)} - k_2^{(1)}) + 2\mu^{(1)}s\alpha_4^{(1)})e^{-k_2^{(1)}x_2}, \\ \sigma_{11F}^{(2)} &= F_1^{(2)}(\lambda^{(2)}(s\alpha_1^{(2)} + k_1^{(2)}) + 2\mu^{(2)}s\alpha_1^{(2)})e^{k_1^{(2)}x_2} \\ &\quad + F_3^{(2)}(\lambda^{(2)}(s\alpha_3^{(2)} + k_2^{(2)}) + 2\mu^{(2)}s\alpha_3^{(2)})e^{k_2^{(2)}x_2}, \\ \sigma_{22F}^{(1)} &= F_1^{(1)}(\lambda^{(1)}(s\alpha_1^{(1)} + k_1^{(1)}) + 2\mu^{(1)}k_1^{(1)})e^{k_1^{(1)}x_2} \\ &\quad + F_2^{(1)}(\lambda^{(1)}(s\alpha_2^{(1)} - k_1^{(1)}) - 2\mu^{(1)}k_1^{(1)})e^{-k_1^{(1)}x_2} \\ &\quad + F_3^{(1)}(\lambda^{(1)}(s\alpha_3^{(1)} + k_2^{(1)}) + 2\mu^{(1)}k_2^{(1)})e^{k_2^{(1)}x_2} \\ &\quad + F_4^{(1)}(\lambda^{(1)}(s\alpha_4^{(1)} - k_2^{(1)}) - 2\mu^{(1)}k_2^{(1)})e^{-k_2^{(1)}x_2}, \\ \sigma_{22F}^{(2)} &= F_1^{(2)}(\lambda^{(2)}(s\alpha_1^{(2)} + k_1^{(2)}) + 2\mu^{(2)}k_1^{(2)})e^{k_1^{(2)}x_2} \\ &\quad + F_3^{(2)}(\lambda^{(2)}(s\alpha_3^{(2)} + k_2^{(2)}) + 2\mu^{(2)}k_2^{(2)})e^{k_2^{(2)}x_2}, \\ \sigma_{12F}^{(1)} &= i\mu^{(1)}\Big[F_1^{(1)}(\alpha_1^{(1)}k_1^{(1)} - s)e^{k_1^{(1)}x_2} + F_2^{(1)}(-\alpha_1^{(1)}k_1^{(1)} - s)e^{-k_1^{(1)}x_2} \\ &\quad + F_3^{(1)}(\alpha_3^{(1)}k_2^{(1)} - s)e^{k_2^{(1)}x_2} + F_4^{(1)}(-\alpha_4^{(1)}k_2^{(1)} - s)e^{-k_2^{(1)}x_2}\Big], \\ \sigma_{12F}^{(2)} &= i\mu^{(2)}\Big[F_1^{(2)}(\alpha_1^{(2)}k_1^{(2)} - s)e^{k_1^{(2)}x_2} + F_3^{(2)}(\alpha_3^{(2)}k_2^{(2)} - s)e^{k_2^{(2)}x_2}\Big]. \end{aligned} \tag{2.26}$$

Thus, we determine completely the expressions (2.22)–(2.26) of the Fourier transforms of the sought values. These expressions contain the unknowns constants $F_1^{(1)},\ldots,F_4^{(1)},F_1^{(2)}$ and $F_3^{(2)}$ for determination of which we use the boundary conditions (2.17), (2.10) and (2.13), and contact conditions in (2.11) (for the complete contact case) or (2.12) (for the contact with the full slipping case). Using the usual procedures we obtain the equation

$$\sum_{n=1}^{4} F_n^{(1)}\alpha_{nm} + F_1^{(2)}\alpha_{5m} + F_3^{(2)}\alpha_{6m} = -P\delta_2^m, \quad m = 1,2,\ldots,6 \tag{2.27}$$

from the mentioned conditions for the unknowns $F_1^{(1)},\ldots,F_4^{(1)},F_1^{(2)}$ and $F_3^{(2)}$, where δ_2^m is a Kronecker symbol. We here do not give the expressions for the coefficients α_{nm}, because these expressions can be easily determined from the Eqs. (2.22)–(2.26).

It is obvious that the noted unknowns can be expressed as follows.

$$\begin{aligned}&\left\{F_1^{(1)},\ldots,F_4^{(1)},F_1^{(2)},F_3^{(2)}\right\}\\ &\quad=\frac{1}{\det\|\alpha_{nm}\|}\left\{\det\left\|\beta_{nm}^{F_1^{(1)}}\right\|,\ldots,\det\left\|\beta_{nm}^{F_1^{(4)}}\right\|,\det\left\|\beta_{nm}^{F_1^{(2)}}\right\|,\det\left\|\beta_{nm}^{F_3^{(2)}}\right\|\right\}.\end{aligned} \tag{2.28}$$

Note that the matrix $\left\|\beta_{nm}^{F_1^{(1)}}\right\|$, …, $\left\|\beta_{nm}^{F_1^{(4)}}\right\|$, $\left\|\beta_{nm}^{F_1^{(2)}}\right\|$ and $\left\|\beta_{nm}^{F_3^{(2)}}\right\|$ are obtained from the matrix $\|\alpha_{nm}\|$ by replacing of the first,…, fourth, fifth and sixth columns with the column $\|0,-P,0,0,0,0\|^T$, respectively.

According to the foregoing discussions, the inverse of the Fourier transforms through which the originals of the sought values are determined, can be expresses as

$$\left\{\sigma_{11}^{(m)};\sigma_{22}^{(m)};u_2^{(m)}\right\}(x_1,x_2) = \int_0^\infty \frac{\left\{S_{11F}^{(m)};S_{22F}^{(m)};U_{2F}^{(m)}\right\}(s,x_2)\cos(sx_1)\mathrm{d}s}{\det\|\alpha_{nm}\|},$$

$$\left\{\sigma_{12}^{(m)};u_1^{(m)}\right\}(x_1,x_2) = \int_0^\infty \frac{\left\{S_{12F}^{(m)};U_{1F}^{(m)}\right\}(s,x_2)\sin\,(sx_1)\mathrm{d}s}{\det\|\alpha_{nm}\|}.$$

$$\sigma_{ijF}^{(m)} = \frac{S_{ijF}^{(m)}}{\det\|\alpha_{nm}\|}, u_{iF}^{(m)} = \frac{U_{iF}^{(m)}}{\det\|\alpha_{nm}\|}. \tag{2.29}$$

This completes the discussion of the solution method of the corresponding boundary-contact value problem related to the dynamics of the moving load acting on the system consisting of the pre-stressed covering layer and pre-stressed half-plane.

2.2.3 The Algorithm for Determination of the Critical Velocity

It should be noted that if we take the Fourier transform parameter s as a wave-number and the moving load velocity V as a wave propagation velocity, then the equation

$$\det\|\alpha_{nm}\| = 0 \tag{2.30}$$

coincides with the dispersion equation of the near-surface wave propagation in the Ox_1 axis direction in the system under consideration. Consequently, the solution to the Eq. (2.30) with respect to the parameter s for a fixed moving load velocity V is a singular point for the integrated expressions in (2.29). It is evident that the order of this singularity (denote it by r) plays basic role under calculation of the integrals (2.29). At $0 \leq r < 1$, the integrals in (2.29) can be calculated by the use of the well-known ordinary algorithms. At $r = 1$, the calculation of the integrals in (2.29) is performed in the Cauchy's principal value sense by utilizing a special algorithm related to this case. But for $r > 1$, the integrals in (2.29) are meaningless, and the velocity V of the moving load corresponding to this case is called the critical velocity (denote it by V_{cr}). At this velocity a resonance-type phenomenon takes place. For determination of the critical velocity V_{cr}, first, the Eq. (2.30) is solved with respect to the moving load velocity for each possible fixed value of the sh under selected values of the problem parameters, such as the initial stresses $\sigma_{11}^{(m)0}$, the ratio of the elasticity moduli $E^{(1)}/E^{(2)}$, Poisson's ratio $\nu^{(1)}$ and $\nu^{(2)}$. As a result, a relationship $V = V(sh)$ is obtained. According to the foregoing discussions and determination, the critical velocity correspond to one of the cases where

$$\frac{dV(sh)}{d(sh)} = 0. \tag{2.31}$$

Consequently, in general, the relationship $V = V(sh)$ may have a certain number local maximums or minimums under which the Eq. (2.31) satisfies. The moving load velocities related to these local maximums and minimums we denote by V_{cr1}, V_{cr2}, …, V_{crN}. In such cases it can be said that the moving load has N number critical velocities and each of these velocities can be taken into consideration, or it can be taken into consideration the critical velocity which is determined according to the relation

$$V_{cr} = \min\{V_{cr1}, V_{cr2}, \ldots, V_{crN}\} \tag{2.32}$$

only. If the relationship $V = V(sh)$ has not any point at which the Eq. (2.31) satisfies, then it is said that there is not any critical velocity of the moving load for the system under consideration.

On the main issues in problems for layered materials with moving loads in a subsonic state (2.2) is the determination of the critical velocity and the effect of the problem parameters on it. This issues is carried out through the solution to the Eq. (2.30). Another issues is the determination of the stress-strain state in the mechanical system under consideration at $V < V_{cr}$ which is carried out through the calculation of the integrals (2.29). The calculation is made by utilizing well-known ordinary algorithms.

Now, we consider numerical results pertinent to the problem discussed above.

2.2.4 Numerical Results and Discussions

Let us introduce the designations

$$\upsilon = \frac{V}{c_2^{(1)}}, \quad \upsilon_{12} = \frac{c_2^{(1)}}{c_2^{(2)}}, \quad e = \frac{E^{(1)}}{E^{(2)}}, \quad \eta_1 = \frac{\sigma_{11}^{(1)0}}{\mu^{(1)}} \quad \text{and} \quad \eta_2 = \frac{\sigma_{11}^{(2)0}}{\mu^{(2)}} \tag{2.33}$$

and assume that $\nu^{(1)} = \nu^{(2)} = 0.3$, where $E^{(m)}$ and $\nu^{(m)}$ are Young's modulus and Poisson's coefficient of the mth material. First, we consider the case where $\upsilon_{12} = 1$ and $\eta_1 = \eta_2 = 0$, and analyze graphs of the function $\upsilon = \upsilon(sh)$ found by solving Eq. (2.30). The numerical results obtained for various values of the e show that the function $\upsilon = \upsilon(sh)$ (or the function $V = V(sh)$) has minima, i.e. has a point at which the Eq. (2.31) satisfies, only in the case where $e > 1$. Graphs constructed for various values of the parameter e are shown in Fig. 2.2. It is seen that $\upsilon_{cr}(=V_{cr}/c_2^{(1)})$ decreases monotonically with growing e. The results show that the full slipping of the contact between the constituents causes to decrease the values of the critical velocity.

Consider numerical results illustrated the influence of the initial stresses in the constituents on the values of the critical velocity. For this purpose consider the data

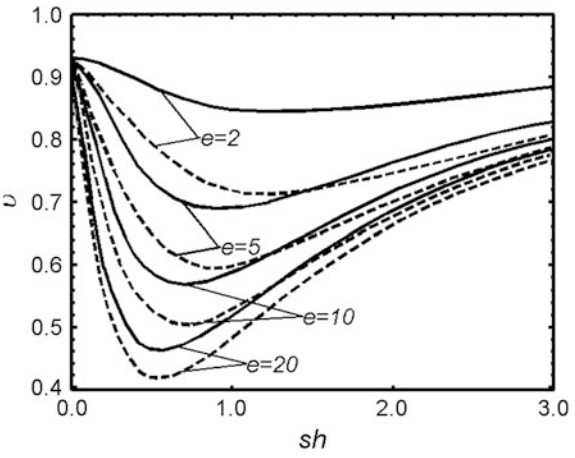

Fig. 2.2 Graphs of the relationship $\upsilon = \upsilon(sh)$ for the complete contact case (2.11) (*solid lines*) and for the incomplete contact with full slipping (2.12) (*dashed lines*) in the case where $\eta_1 = \eta_2 = 0$

given in Tables 2.1, 2.2 and 2.3 which show the values of the v_{cr} in the cases where $\{\eta_1 \geq 0; \eta_2 = 0, \eta_1 = 0; \eta_2 \geq 0\}$ and $\{\eta_1 = 0; \eta_2 \leq 0\}$ respectively under $v_{12} = 1$.

It follows from these tables that the initial stretching of the covering layer, as well as the initial stretching of the half-plane causes to increase of the values of the v_{cr}. In this case the influence of the initial stretching of the covering layer is more significant than that of the half-plane. Table 2.3 shows that the initial compressing of the half-plane causes to decrease of the values of the v_{cr}.

Let us consider now the case where $\rho^{(2)}/\rho^{(1)} = 0.5$, i.e. the case where $v_{12} = \sqrt{0.5e}$. In Table 2.4 the values of the critical velocity v_{cr} obtained in the present investigation for various e at $\eta_1 = \eta_2 = 0$ are compared with corresponding ones found by Babich et al. (1986) and a good agreement is seen to exist between them. Tables 2.5, 2.6 and 2.7 show the influence of the initial stresses, i.e. of the parameters η_1 and η_2 on the values of the v_{cr} in the case where $v_{12} = \sqrt{0.5e}$. It

Table 2.1 The influence of the initial stretching of the covering layer on the values of the v_{cr} for various e under complete contact case (2.11) (numerator) and under the incomplete contact with full slipping (2.12) (denominator) in the case where $\eta_2 = 0$ and $v_{12} = 1$

e	η_1			
	0	0.005	0.01	0.03
2	0.8414 0.7093	0.8468 0.7154	0.8521 0.7214	0.8723 0.7442
10	0.5664 0.5016	0.5764 0.5126	0.5863 0.5233	0.6240 0.5640

Table 2.2 The influence of the initial stretching of the half-plane on the values of the v_{cr} for various e under complete contact case (2.11) (numerator) and under the incomplete contact with full slipping (2.12) (denominator) in the case where $\eta_1 = 0$ and $v_{12} = 1$

e	η_2			
	0	0.005	0.01	0.03
2	0.8414 0.7093	0.8437 0.7123	0.8454 0.7153	0.8540 0.7266
10	0.5664 0.5016	0.5677 0.5034	0.5690 0.5052	0.5741 0.5121

Table 2.3 The influence of the initial compression of the half-plane on the values of the v_{cr} for various e under complete contact case (2.11) (numerator) and under the contact with full slipping (denominator) in the case where $\eta_1 = 0$ and $v_{12} = 1$

e	η_2			
	0	−0.005	−0.01	−0.03
2	0.8414 0.7093	0.8391 0.7062	0.8367 0.7031	0.8263 0.6898
10	0.5664 0.5016	0.5650 0.4998	0.5637 0.4979	0.6240 0.4900

Table 2.4 The comparison of the present results (numerator) with corresponding ones obtained in paper by Babich et al. (1986) (denominator) in the case where $\upsilon_{12} = \sqrt{0.5e}$ and $\eta_1 = \eta_2 = 0$

e	Complete contact	Contact with full slipping
2	0.841 0.839	0.709 0.719
10	0.428 0.427	0.373 0.372

Table 2.5 The influence of the initial stretching of the half-plane on the values of the υ_{cr} for various e under complete contact case (2.11) (numerator) and under the incomplete contact with full slipping (2.12) (denominator) in the case where $\eta_1 = 0$ and $\upsilon_{12} = \sqrt{0.5e}$

e	η_2			
	0.00	0.005	0.01	0.03
2	0.8414 0.7093	0.8437 0.7123	0.8454 0.7153	0.8541 0.7266
10	0.4284 0.3730	0.4307 0.3754	0.4329 0.3777	0.4415 0.3868

Table 2.6 The influence of the initial stretching of the covering layer on the values of the υ_{cr} for various e under complete contact case (2.11) (numerator) and under the incomplete contact with full slipping (2.12) (denominator) in the case where $\eta_2 = 0$ and $\upsilon_{12} = \sqrt{0.5e}$

e	η_1			
	0.00	0.005	0.01	0.03
2	0.8414 0.7093	0.8468 0.7154	0.8512 0.7214	0.8723 0.7442
10	0.4284 0.3730	0.4319 0.3784	0.4348 0.3833	0.4358 0.3995

Table 2.7 The influence of the initial compression of the half-plane on the values of the υ_{cr} for various e under complete contact case (2.11) (numerator) and under the incomplete contact with full slipping (2.12) (denominator) in the case where $\eta_1 = 0$ and $\upsilon_{12} = \sqrt{0.5e}$

e	η_2			
	0.00	−0.005	−0.01	−0.03
2	0.8414 0.7093	0.8391 0.7062	0.8367 0.7031	0.8263 0.6898
10	0.4284 0.3730	0.4261 0.3706	0.4238 0.3682	0.4141 0.3582

follows from these tables that, in the qualitative sense, the effect of the parameters η_1 and η_2 on the values of the υ_{cr} is the same as in the case where $\upsilon_{12} = 1$.

Now we consider numerical results related to the stress distribution on the interface plane between the covering layer and half-plane. As an example, we consider the distribution of the normal stress, i.e. the stress

$$\sigma_{22}(x_1) = \sigma_{22}^{(1)}(x_1, -h) = \sigma_{22}^{(2)}(x_1, -h) \tag{2.34}$$

with respect to the dimensionless coordinate x_1/h. Note that the value of the stress (2.34) and other required quantities are calculated through the integrals (2.29). Under this calculation procedure the improper integrals in (2.29) are replaced with corresponding proper integrals by using the relation

$$\int_0^{\infty} (\bullet) ds \approx \int_0^{S_1^*} (\bullet) ds. \tag{2.35}$$

The values of the S_1^* in (2.35) are determined from the convergence criterion for the improper integrals. The numerical results show that the difference between the results obtained in the case where $S_1^* = 30$ and in the case where $S_1^* > 30$ is less than 10^{-5}. Therefore all numerical results which will be analyzed below are obtained in the case where $S_1^* = 30$. Note that under obtaining these results it is assumed that $\upsilon < \upsilon_{cr}$ (or $V < V_{cr}$) because the absolute values of the stresses and displacements in the constituents approach the infinity, for example, $|\sigma_{22}| \to \infty$ as $\upsilon \to \upsilon_{cr}$ for each x_1 at which $\sigma_{22}(x_1) \neq 0$.

Thus, we consider Fig. 2.3 which illustrate the graphs of the distribution of the $\sigma_{22}(x_1)$ (2.34) with respect to the x_1/h for various values of the parameter e under $\upsilon = 0.3$ and $\upsilon_{12} = \sqrt{0.5e}$ in the complete contact case (2.11) (solid lines) and in the incomplete contact with full slipping case (2.12) (dashed lines). It follows from these graphs that the absolute maximum of the $\sigma_{22}(x_1)$ is reached at $x_1/h = 0$. It is also seen that $|\sigma_{22}|$ decrease with e. In this case the values of the $|\sigma_{22}|$ obtained for the incomplete contact with full slipping case are greater than those for the complete contact case between the covering layer and half-plane, and the influence of the type of the contact conditions on $\sigma_{22}(x_1)$ increase with e.

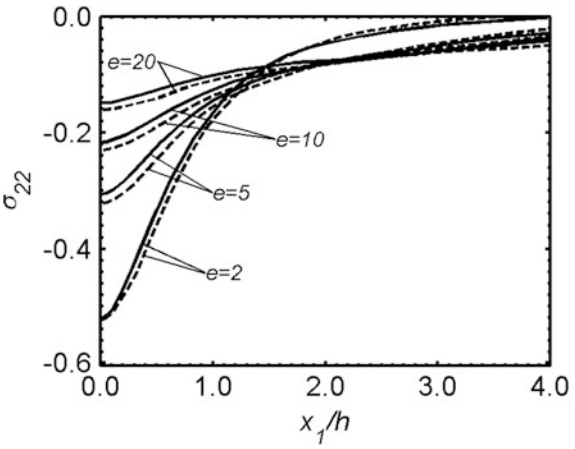

Fig. 2.3 The distribution of the normal stress $\sigma_{22}(x_1)$ (2.34) with respect to the x_1/h in the complete contact case (2.11) (*solid lines*) and in the incomplete contact with full slipping (2.12) (*dashed lines*) for various e at $\upsilon = 0.3$ and $\eta_1 = \eta_2 = 0$

This completes analyze of the numerical results related to the problem considered in the present section. It should be noted that the mentioned problem is very simplest one among the problem which will be studied in the present chapter. Therefore the investigations carried out and the results obtained in the present section can be taken as introduction to the study of the more complicate problems related to the dynamics of the moving load acting on the pre-stressed layered system. Nonetheless, the numerical results obtained in the present section allow us to make the following conclusions.

2.2.5 Conclusions

Thus, in the present section the dynamical response of a system consisting of a pre-stressed covering layer and a pre-stressed half-plane to a moving load has been investigated. An algorithm for determining the critical velocity of the moving load was developed.

The numerical results obtained allow us to draw the following conclusions:

- In the cases under considerations, i.e. in the cases where (i) $\rho^{(2)} = \rho^{(1)}$ and (ii) $\rho^{(2)}/\rho^{(1)} = 0.5$ under $v^{(1)} = v^{(2)}(=0.3)$ a critical velocity arises only in the cases where Young's modulus of the covering layer $E^{(1)}$ is greater than that of the underlying half-plane $E^{(2)}$. Many other numerical results which have not discussed here show that this conclusion holds not only in the cases (i) and (ii), but also for any other cases for which $E^{(1)}/E^{(2)} > 1$. Consequently, the condition $E^{(1)}/E^{(2)} > 1$ is enough for appearing of the critical velocity;
- the critical velocity decreases with growing the ratio $E^{(1)}/E^{(2)}$;
- the initial stretching of the covering layer and of the half-plane increases the critical velocity;
- the critical velocity decreases with growing initial compression of the half-plane;
- the critical velocity at complete contact conditions is greater than that at incomplete contact conditions with full slipping.

2.3 Dynamical Response of a Pre-stressed System Comprising a Substrate, Bond and Covering Layer to the Moving Load

In many cases, a system comprising a substrate and a covering layer is not adequate for simulating the track beds of high-speed trains, cars, trucks, etc., because there usually is a bond layer between the covering layer and substrate. Mechanical and geometrical parameters of this layer can significantly affect the dynamical response of track beds to a moving load. Therefore, in the present section, the investigation

initiated in the previous section is continued for a system comprising a substrate, bond and covering layers.

The results presented in the present section is based on paper by Dincsoy et al. (2009).

2.3.1 Formulation of the Problem

Let us consider a pre-stressed composite system consisting of a substrate, bond and covering layers. The points of the layers and substrate are specified by Lagrange coordinates in a Cartesian reference frame $Ox_1x_2x_3$ (Fig. 2.4). Before assembling, the layers and the substrate have been stressed (stretched or compressed) separately in the Ox_1 axis direction, so that a uniaxial homogeneous initial stress state determined by expression (2.1), exists in each of them. The covering and bond layers, and the half-plane occupy the regions $\{-h_1 < x_2 < 0\}$, $\{-(h_1 + h_2) < x_2 < -h_1\}$ and $\{-\infty < x_2 < -(h_1 + h_2)\}$ respectively in the case where $-\infty < x_1 < +\infty$ and $-\infty < x_3 < +\infty$. The Ox_3 axis is perpendicular to the figure plane and therefore is not shown in Fig. 2.4.

The quantities related to the covering layer, bond layer and substrate will be denoted by the superscripts (1), (2) and (3) respectively and the initial stresses will be denoted by the superscript $(m)0$ where $m = 1, 2, 3$.

Thus, within the assumptions accepted in the previous sections we investigate the response of the system shown in Fig. 2.4 to the lineal located moving load with intensity P acting on the free face plane of the covering layer. As in the previous section, we will consider the subsonic regime, i.e. we assume that

$$V < \min(c_2^{(1)}, c_2^{(2)}, c_2^{(3)}), c_2^{(m)} = \sqrt{\mu^{(m)}/\rho^{(m)}}, \quad m = 1, 2, 3, \tag{2.36}$$

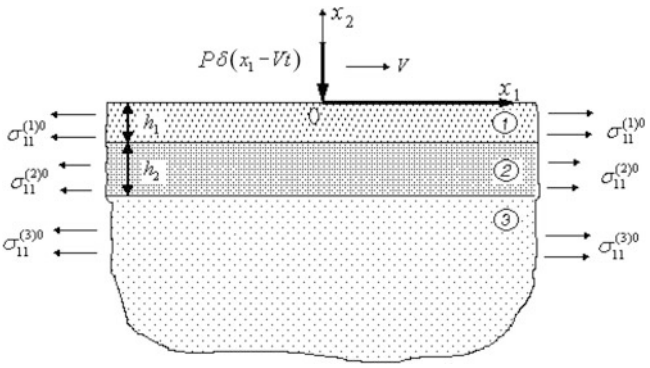

Fig. 2.4 Geometry of the system consisting of the substrate, bond and covering layers indicated by numbers *3*, *2* and *1* respectively

where $c_2^{(m)}$, $\mu^{(m)}$ and $\rho^{(m)}$ are the speed of distortion waves, the shear modulus and density of the material of the mth constituent. Moreover, we assume that the field Eqs. (2.3)–(2.5) are satisfied within each constituents of the system under consideration and on the upper face plane of the covering layer the boundary condition (2.10) occurs.

As in the previous section, we consider two types (complete and full slipping) of contact conditions on the interfaces between the covering and bond layers, and between the bond layer and substrate. For the complete contact conditions we assume that the following relations satisfy.

$$\begin{aligned}
&\sigma_{i2}^{(1)}\Big|_{x_2=-h_1} = \sigma_{i2}^{(2)}\Big|_{x_2=-h_1}, u_i^{(1)}\Big|_{x_2=-h_1} = u_i^{(2)}\Big|_{x_2=-h_1}, \quad i=1,2\\
&\sigma_{i2}^{(2)}\Big|_{x_2=-(h_1+h_2)} = \sigma_{i2}^{(3)}\Big|_{x_2=-(h_1+h_2)},\\
&u_i^{(2)}\Big|_{x_2=-(h_1+h_2)} = u_i^{(3)}\Big|_{x_2=-(h_1+h_2)},
\end{aligned} \tag{2.37}$$

The contact conditions with full slipping are formulated as follows:

$$\begin{aligned}
&\sigma_{22}^{(1)}\Big|_{x_2=-h_1} = \sigma_{22}^{(2)}\Big|_{x_2=-h_1}, u_2^{(1)}\Big|_{x_2=-h_1} = u_2^{(2)}\Big|_{x_2=-h_1},\\
&\sigma_{12}^{(1)}\Big|_{x_2=-h_1} = 0, \sigma_{12}^{(2)}\Big|_{x_2=-h_1} = 0, \sigma_{22}^{(2)}\Big|_{x_2=-(h_1+h_2)} = \sigma_{22}^{(3)}\Big|_{x_2=-(h_1+h_2)},\\
&u_2^{(2)}\Big|_{x_2=-(h_1+h_2)} = u_2^{(3)}\Big|_{x_2=-(h_1+h_2)}, \sigma_{12}^{(2)}\Big|_{x_2=-(h_1+h_2)} = 0,\\
&\sigma_{12}^{(3)}\Big|_{x_2=-(h_1+h_2)} = 0.
\end{aligned} \tag{2.38}$$

In addition, we assume that the following decay conditions are satisfied:

$$\left|u_i^{(3)}\right|, \left|\sigma_{ij}^{(3)}\right| \to 0 \quad \text{as} \quad x_2 \to -\infty. \tag{2.39}$$

This completes the formulation of the problem. It should be noted that, at $\sigma_{11}^{(m)0} = 0$ $(m = 1, 2, 3)$, we return to the corresponding problem of the classical linear theory of elastodynamics.

2.3.2 Method of Solution

As in the previous section, using the coordinate transform (2.15), we obtain the Eq. (2.16) and boundary condition (2.17) (instead of the second boundary condition in (2.10)). The contact conditions (2.37) and (2.38), and boundary condition (2.39) are also valid for the new system of coordinates (2.15). Applying the Fourier

transform (2.18) to the all equations and boundary, and contact conditions, we obtain corresponding ones for the Fourier transforms of the sought values. As a result we have the Eqs. (2.19) and (2.20) with respect of the Fourier transforms of the displacements. Solution to these equations are presented as in (2.22), i.e. these solutions are

$$\begin{aligned} u_{2F}^{(n)} &= F_1^{(n)} e^{k_1^{(n)} x_2} + F_2^{(n)} e^{-k_1^{(n)} x_2} + F_3^{(n)} e^{k_2^{(n)} x_2} + F_4^{(n)} e^{-k_2^{(n)} x_2}, \quad n = 1, 2, \\ u_{2F}^{(3)} &= F_1^{(3)} e^{k_1^{(3)} x_2} + F_3^{(3)} e^{k_2^{(3)} x_2}. \end{aligned} \tag{2.40}$$

where $k_1^{(m)}$ and $k_2^{(m)}$ $(m = 1, 2, 3)$ are determined by expressions given in (2.23).

Taking the Eq. (2.40) into consideration, we obtain corresponding expressions for $u_{1F}^{(m)}$ and $\sigma_{ijF}^{(m)}$. These expressions are the same with those given in (2.24), (2.25) and (2.12). However, under using the Eqs. (2.24)–(2.26) it is necessary to take the corresponding change of the upper index into consideration.

Thus, we determine completely the expressions of the Fourier transforms of the sought values which contain the unknowns $F_1^{(1)}, \ldots, F_4^{(1)}, F_1^{(2)}, \ldots, F_4^{(2)}, F_1^{(3)}$ and $F_3^{(3)}$ for determination of which we use the boundary conditions (2.17), (2.10) and (2.39), and contact conditions in (2.37) (for the complete contact case) or in (2.38) (for the contact with full slipping). Employing the usual procedures we obtain the equation

$$\sum_{n=1}^{4} F_n^{(1)} \alpha_{n,m} + \sum_{n=5}^{8} F_n^{(2)} \alpha_{n,m} + F_1^{(3)} \alpha_{9,m} + F_3^{(3)} \alpha_{10,m} = -P\delta_m^2, \tag{2.41}$$

where $m; n = 1, 2, \ldots, 10$ and δ_m^2 is a Kronecker symbol, from the mentioned conditions for the unknowns $F_1^{(1)}, \ldots, F_4^{(1)}, F_1^{(2)}, \ldots, F_4^{(2)}, F_1^{(3)}$ and $F_3^{(3)}$. We here do not give the expressions for the coefficients $\alpha_{n,m}$, because they can be easily determined from the Eqs. (2.22)–(2.26).

Thus, according to (2.41), we can write the following expressions for the foregoing unknowns.

$$\begin{aligned} \left\{ F_1^{(1)}, \ldots, F_4^{(1)}, F_1^{(2)}, \ldots, F_4^{(2)}, F_1^{(3)}, F_3^{(3)} \right\} = \frac{1}{\det \left\| \alpha_{n,m} \right\|} \left\{ \det \left\| \beta_{n,m}^{F_1^{(1)}} \right\|, \ldots, \right. \\ \left. \det \left\| \beta_{n,m}^{F_1^{(4)}} \right\|, \det \left\| \beta_{n,m}^{F_1^{(2)}} \right\|, \ldots, \det \left\| \beta_{n,m}^{F_4^{(2)}} \right\|, \det \left\| \beta_{n,m}^{F_1^{(3)}} \right\|, \det \left\| \beta_{n,m}^{F_3^{(3)}} \right\| \right\} \end{aligned} \tag{2.42}$$

where $n; m = 1, 2, \ldots, 10$ and the matrices $\left\| \beta_{n,m}^{F_1^{(1)}} \right\|$, …, $\left\| \beta_{n,m}^{F_3^{(3)}} \right\|$ are obtained from the matrix $\left\| \alpha_{n,m} \right\|$ by replacing first, …, tenth columns with the column $(0, -P, 0, 0, 0, 0, 0, 0, 0, 0)^T$, respectively.

After the foregoing determination of the unknowns in Eq. (2.41), the inverse of the Fourier transforms of the sought values are presented by the expressions in (2.29). It should be noted that, as in the previous section, the singular points of the integrated expressions in the integrals in (2.29) coincide with roots of the equation

$$\det\left\|\alpha_{n,m}\right\| = 0, \quad n;m = 1,2,\ldots,10. \tag{2.43}$$

The Eq. (2.43) is solved with respect to the moving load velocity V for each possible fixed values of the Fourier transform parameter s and as a result of this solution the relation $V = V(sh_1)$ is obtained. According to the character of this relation, i.e. according to the Eqs. (2.31) and (2.32) the critical velocity of the moving load is determined.

2.3.3 Numerical Results and Discussions

We introduce the designations

$$\upsilon = \frac{V}{c_2^{(1)}}, e_1 = \frac{E^{(1)}}{E^{(2)}}, e_2 = \frac{E^{(3)}}{E^{(2)}}, H = \frac{h_2}{h_1}, \eta_m = \frac{\sigma_{11}^{(m)0}}{\mu^{(m)}}, \quad m = 1,2,3, \tag{2.44}$$

and assume that $\rho^{(2)}/\rho^{(1)} = 0.5$, $\rho^{(3)}/\rho^{(2)} = 0.5$ and $\nu^{(1)} = \nu^{(2)} = \nu^{(3)} = 0.3$. Note that the notation υ in (2.44) coincides with the same notation in (2.33).

Let us analyze the relationship between υ and sh_1 which are obtained from the solution of the Eq. (2.43). According to the well-known mechanical consideration, in the case where $H \to \infty$ this relationship must approach the corresponding one obtained in the previous section under $e = e_1$, where the notation e is determined by

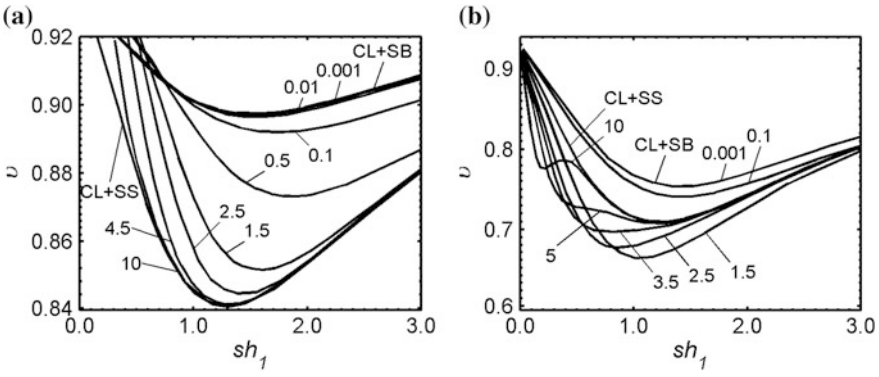

Fig. 2.5 Graphs of the relationship between the υ and sh_1 for the complete contact case (**a**) and for the contact with full slipping (**b**) constructed for various $H = h_1/h_2$ (*number at curves*)

(2.33). We denote this case as *CL + SS*. Also, according to the well-known mechanical consideration, in the case where $H \rightarrow 0$ the relationship $v = v(sh_1)$ must approach the corresponding one obtained in the previous section under $e = e_1/e_2 = E^{(1)}/E^{(3)}$. We use a notation *CL + SB* for denoting this case. These predictions are proven with the graphs given in Fig. 2.5 which are constructed in the case where $e_1 = 2$, $e_2 = 1.5$ and $\eta_1 = \eta_2 = \eta_3 = 0$ for various values of the H for the complete contact case (2.37) (Fig. 2.5a) and for the contact with full slipping (2.38) (Fig. 2.5b). Note that the graph of the $v = v(sh_1)$ constructed for the system *CL + SS* and related to the case where $e_1 = 2$ and shown in Fig. 2.5a coincide with the corresponding one given in Fig. 2.2. Moreover, the graphs illustrated in Fig. 2.5 approach, as predicted above, the graph related to the case denoted by *CL + SB* with decreasing of the H.

Now, let us look at the effect of the parameter e_1 on the relationship between v and sh_1. The corresponding graphs are given in Fig. 2.6 in the case where $H = 1.0$, $e_2 = 2$ and $\eta_1 = \eta_2 = \eta_3 = 0$ for the complete contact case (2.37) (solid lines) and for the contact with full slipping (2.38) (dashed lines). A comparison of these graphs with those given in Fig. 2.2 shows that the existence of a bond layer whose elastic modulus is greater than that of the substrate increases the values of the $v = v(sh_1)$.

Analyses of the foregoing and other large number of other numerical results, not illustrated here, allow us to conclude that there are values of the problem parameters at which (i) the function $v = v(sh_1)$ has no local maxima or minima; (ii) the function $v = v(sh_1)$ has only one local maximum or minimum at $sh_1 \neq 0$ and $sh_1 \neq \infty$; (iii) the function $v = v(sh_1)$ has one or more local maxima or minima at $sh_1 \neq 0$ and $sh_1 \neq \infty$. As noted in the previous section, in case (i) a critical velocity does not exist; in case (ii) a critical velocity exists and corresponds to the local maximum or minimum of the function $v = v(sh_1)$; in case (iii) a critical velocity exists and corresponds to the absolute minimum of v.

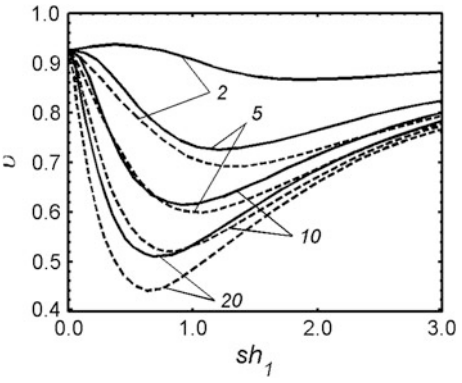

Fig. 2.6 The influence of the parameter e_1 (*numbers at the curves*) on the graphs of the relationship between v and sh_1 for the complete contact case (*solid lines*) and for the contact with full slipping (*dashed lines*) under $H = 1$ and $e_2 = 2$

Table 2.8 Values of v_{cr} obtained for various values of e_1, e_2 and H in the complete contact case (numerator) and in the contact with full slipping (denominator)

(e_1, e_2)	H				
	0.001	0.5	1.5	10	30
(2, 4/3)	0.8972 0.7540	0.8732 0.6970	0.8517 0.6644	0.8414 0.7754	0.8414 0.7093
(5, 5/2)	0.8058 0.6824	0.7538 0.6303	0.7100 0.5839	0.6957 0.5931	0.6857 0.5931
(10, 5)	0.6856 0.5930	0.6405 0.5490	0.5976 0.5041	0.5664 0.5016	0.5664 0.5016

Table 2.9 Values of v_{cr} obtained for the system $CL + SS$ under various e_1 in the complete contact case (numerator) and in the contact with full slipping (denominator)

$e_1 = 2$	$e_1 = 5$	$e_1 = 10$	$e_1 = 4/3$	$e_1 = 5/2$
0.8414 0.7093	0.6857 0.5931	0.5664 0.5016	0.8972 0.7542	0.8059 0.6825

Now we analyze the influence of the problem parameters on the values of the critical velocity v_{cr} determined in the foregoing manner.

Table 2.8 shows the influence of the parameters e_1, e_2 and H on the values of the v_{cr} under $\eta_1 = \eta_2 = \eta_3 = 0$. The corresponding values of the v_{cr} related to the system $CL + SS$, the system considered in the previous section and consisting of the covering layer and half-plane, are given in Table 2.9. According to the mechanical consideration, it can be predicted that the values of the v_{cr} obtained for the system under consideration must approach the corresponding ones obtained for the system $CL + SS$ ($CL + SB$) in the case where $e = e_1$ (in the case where $e = e_1/e_2$) with H (as $H \to 0$). This prediction is proven completely by data given in Tables 2.8 and 2.9.

Data given in Table 2.10 illustrated the influence of the parameters e_1 and e_2 on the values of the v_{cr} in the case where $H = 1$ under $\eta_1 = \eta_2 = \eta_3 = 0$. It follows from these data that an increase in the values of the e_1 (in the values of the e_2) causes to decrease (to increase) the values of the v_{cr}. This conclusion is also agree

Table 2.10 The influence of the parameters e_1 and e_2 on the values of v_{cr} under $H = 1$ in the complete contact case (numerator) and in the contact with full slipping (denominator)

e_1	e_2			
	2	5	10	20
2	0.8661 0.6930	0.8756 0.7442	0.8784 0.7649	0.8798 0.7760
5	0.7260 0.5991	0.8669 0.6523	0.8706 0.6742	0.8724 0.6861
10	0.6142 0.5206	0.8253 0.5745	0.8325 0.5973	0.8361 0.6098
20	0.5106 0.4431	0.7777 0.4965	0.7906 0.5198	0.7970 0.5329

Table 2.11 The influence of the initial stretching of the constituents, i.e. of the parameters η_1, η_2 and η_3 on the values of υ_{cr} under $e_1 = 2$, $e_5 = 5$ and $H = 1$ in the complete contact case (numerator) and in the contact with full slipping (denominator)

Cases	η_1, η_2, η_3			
	0	0.005	0.01	0.05
$\eta_1 \neq 0$, $\eta_2 = \eta_3 = 0$	0.8756 / 0.7442	0.8821 / 0.7503	0.8884 / 0.7563	0.9353 / 0.7994
$\eta_2 \neq 0$, $\eta_1 = \eta_3 = 0$	0.8756 / 0.7442	0.8764 / 0.7456	0.8773 / 0.7469	0.8835 / 0.7575
$\eta_3 \neq 0$, $\eta_1 = \eta_2 = 0$	0.8756 / 0.7442	0.8758 / 0.7454	0.8759 / 0.7465	0.8767 / 0.7536

with the mechanical consideration. Moreover, other numerical results which are not given here show that this conclusion occurs not only for the case where $H = 1$, but also for the case where $H \neq 1$ and $0 < H < \infty$.

The influence of the initial stretching of the constituents of the system under consideration on the υ_{cr} is illustrated by the data given in Table 2.11, which were obtained for $e_1 = 2$, $e_2 = 5$ and $H = 1$. As evident from this table, the initial stretching increases υ_{cr}, the effect caused by the pre-stretching of the covering layer on the values of the υ_{cr} being the greatest.

Now we consider the case where the materials of the covering layer and half-plane are the same and the modulus of elasticity of the bond layer is greater than that of the materials of the covering layer and half-plane, i.e. we consider the case where $e_1 = e_2 < 1$. As an example, we analyze the case where $e_1 = e_2 = 0.1$.

Thus, according to the results obtained in the previous section, in the case where $e_1 = e_2 = 0.1$, if there exists a point of the relationship $\upsilon = \upsilon(sh_1)$ at which $d\upsilon/d(sh_1) = 0$, then this point must disappear as $H \to \infty$. This reasoning is proven

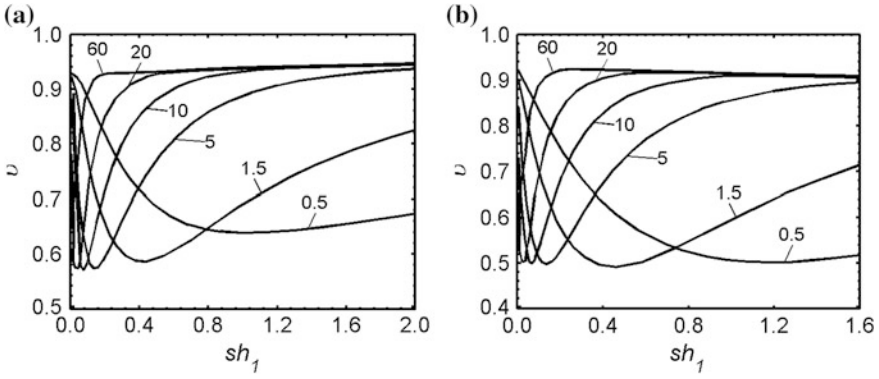

Fig. 2.7 Graphs of the relationship between υ and sh_1 constructed for various H (*numbers at curves*) in the complete contact case (**a**) and in the contact with full slipping (**b**) under $e_1 = e_2 = 0.1$ and $\eta_1 = \eta_2 = \eta_3 = 0$

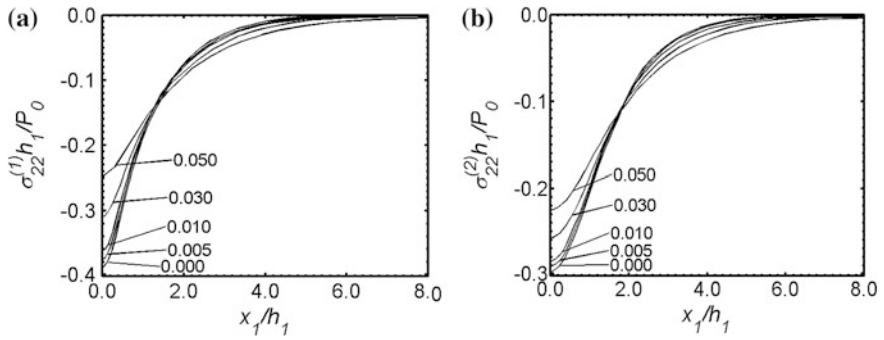

Fig. 2.8 The quantities $(\sigma_{22}^{(1)}h_1/P)\Big|_{x_2=-h_1}$ (**a**) and $(\sigma_{22}^{(2)}h_1/P)\Big|_{x_2=-(h_1+h_2)}$ (**b**) in relation to x_1/h_1 for the complete contact case (2.37) under various values of η_1 (*numbers at curves*)

with the graphs given in Fig. 2.7 which show the graphs of the function $v = v(sh_1)$ constructed for various H under $e_1 = e_2 = 0.1$, $\eta_1 = \eta_2 = \eta_3 = 0$ for the complete contact case (Fig. 2.7a) and for the contact with full slipping (Fig. 2.7b). Moreover, these graphs show that, at $e_1 = e_2 = 0.1$ there exists such a value $H = H^*$ that the local minimum of the relationship $v = v(sh_1)$ disappear if $H > H^*$.

Finally, let us consider some examples for the quantities $\sigma_{22}^{(1)}h_1/P$ at $x_2 = -h_1$ and $\sigma_{22}^{(2)}h_1/P$ at $x_2 = -(h_1 + h_2)$ in relation to x_1/h_1 under completer contact case (2.37). The corresponding graphs are given in Fig. 2.8 for various values of η_1 under $H = 1$, $e_1 = 2$, $e_2 = 5$ and $\eta_2 = \eta_3 = 0$. As is seen, the absolute values of $\sigma_{22}^{(1)}h_1/P$ (Fig. 2.8a) in the vicinity of the point $x_1/h_1 = 0$ are greater than the corresponding value of $\sigma_{22}^{(2)}h_1/P$ (Fig. 2.8b), and the initial stretching of the covering layer decreases the stresses significantly.

2.3.4 Conclusions

Thus, in the present section, with utilizing the TDLTEWISB, the dynamical response of a system consisting of a pre-stressed substrate, pre-stressed bond and pre-stressed covering layers to a moving load has been investigated. The numerical results obtained for the critical velocity of the moving load allow us to draw the following conclusions:

- in the case where $e_1 > e_2$ and $e_2 > 1$, there exists a critical velocity and the lower (upper) limit of this critical velocity is the critical velocity obtained for the $CL + SS$ ($CL + SB$) in the case where $e = e_1$ (in the case $e = e_2$);
- in the foregoing case the critical velocity decreases with increasing the thickness of the bond layer;

- in the case where $e_1 < 1$ and $e_1 = e_2$, the critical velocity exists if $H < H^*$, i.e. if the bond layer is not too thick;
- the pre-stretching of the layers and substrate increases the critical velocity;
- the most significant effect on the critical velocity is caused by the pre-stretching of the covering layer.

2.4 Dynamics of a Finite Pre-strained Bi-layered Slab Resting on a Rigid Foundation Under the Action of an Oscillating Moving Load

The subject of the present section is the study of the dynamical response of the finite pre-strained bi-layered slab to the oscillating moving load acting to this slab. A bi-layered slab (with a soft lower and stiff upper layer) resting on a rigid foundation is usually used for modeling floating-slab track systems with continuous slabs which are widely used to control vibration from underground trains (see, for instance, Hussein and Hunt 2006). This system is composed of the track which is mounted on a concrete slab on rubber bearings, glass fibers or steel springs. Consequently, the principal components relevant to this system are rails, rail pads, the floating slab and slab bearings. The track-bed is modeled as a rigid foundation, as the stiffness of the slab bearings is normally much less than the stiffness of the track-bed. At the same time, the system consisting of a bi-layered slab resting on a rigid foundation can be considered, in a certain sense, as the generalization of the system consisting of a covering layer + half-plane which has been used in the previous section and in relevant investigations reviewed in Sect. 2.1 of the present chapter. For example, this system generalization accounts for the waves reflected from the supporting ground.

It should be noted that in many cases the layers of the slab are strained before the action on that the oscillating moving load. These strains and stresses which are called initial stresses or strains, can be caused by manufacturing and assembly procedures. Moreover, the source of the initial strains could be sharp changes in environmental conditions (i.e. temperature changes) which can cause roadbeds, aircraft runways, etc. to be initially stressed. The action of the geostatic and geodynamic forces in the Earth's crust (which is modeled as a lower layer or as a half-plane in the corresponding investigations) can also cause the initial strains the magnitude of which can reach a large quantities.

As noted by Hussein and Hunt (2006), Dieterman and Metrikine (1997), Metrikine and Vrouwenvelder (2000), Madsus and Kaynia (2000) and as it follows from the direct observation, in reality highly-speed trains, cars and other high speed transportation vehicles modeled as moving loads are accompanied by their own oscillations. Consequently, the model consisting of a finite pre-strained bi-layered slab resting on a rigid foundation under action of an oscillating moving load has real application possibilities. Nevertheless, the investigations and analyses

presented in the present section and carried out by utilizing the large initial deformation version of the TDLTEWISB will be made without any concretization of the fields of application. However, the obtained results can be used in each aforementioned field under suitable selection of the values of the dimensionless problem parameters. Under obtaining these results it is assumed that the materials of the layers of the slab are highly elastic and these layers are finitely pre-strained. At the same time, it is assumed that the mechanical relations of these materials are defined by the harmonic potential.

This section is based on paper by Akbarov and Salmanova (2009) and throughout of that, as in the previous section, if repeated subscripts are only in one side of equations, then they indicate a summation over their ranges.

2.4.1 Formulation of the Problem and Some Remarks on the Equations and Relations of the TDLTEWISB

A bi-layered slab resting on a rigid foundation is considered herein (Fig. 2.9). Assume that in the natural state the thickness of the upper and lower layers are $H^{(2)}$ and $H^{(1)}$ respectively. In the natural state we determine the positions of the points of the layers by the Lagrange coordinates in the Cartesian system of coordinates $Ox_1x_2x_3$. Suppose that the layers of the slab have infinite length in the directions of the Ox_1 and Ox_3 axes. The Ox_3 axis extends along a direction perpendicular to the plane Ox_1x_2 in Fig. 2.9 and therefore is not shown in this figure.

We propose that the layers, before being compounded with each other and with a rigid foundation, be stretched separately along the Ox_1 axis direction and that in each of them, the homogeneous initial finite strain state appear. These initial strains are caused by the static forces acting in the Ox_1 axis direction at infinity and the action of these forces continues all further dynamic processes.

With the initial state of the layers of the slab we associate the Lagrangian Cartesian system of coordinates $Oy_1y_2y_3$ and suppose that the origin of this system

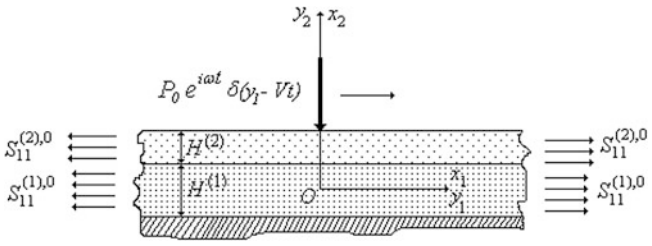

Fig. 2.9 The geometry of a bi-layered slab resting on a rigid foundation

coincides with the origin of the system $Ox_1x_2x_3$, and the coordinate axes Oy_1, Oy_2 and Oy_3 coincide with the coordinate axes Ox_1, Ox_2 and Ox_3, respectively.

Assuming that the material of the layers is compressible, the elasticity relations are given through the harmonic potential. Moreover, it is assumed that the values related to the upper and lower layers of the slab are denoted by upper indices (2) and (1), respectively. Furthermore, the values related to the initial state are denoted by the upper index 0. To simplify further discussions, a local system of coordinates $O^{(m)}x_1^{(m)}x_2^{(m)}x_3^{(m)}$ (in the natural state) and $O^{(m)}y_1^{(m)}y_2^{(m)}y_3^{(m)}$ (in the initial state) has been associated with the middle plane of the mth layer. The system of coordinates $O^{(m)}x_1^{(m)}x_2^{(m)}x_3^{(m)}(O^{(m)}y_1^{(m)}y_2^{(m)}y_3^{(m)})$ is attained from the system of coordinates $Ox_1x_2x_3(Oy_1y_2y_3)$ by parallel transfer along the $Ox_2(Oy_2)$ axis.

Thus, according to the foregoing, the initial state in the layers can be determined as follows:

$$\begin{aligned} u_i^{(m)} &= (\lambda_i^{(m)} - 1)x_i^{(m)}, \lambda_i^{(m)} = const_i^{(m)}, \\ y_i^{(m)} &= \lambda_i^{(m)} x_m^{(m)}, i = 1, 2\, \lambda_3^{(m)} = 1, y_3^{(m)} = x_3^{(m)}, \end{aligned} \tag{2.45}$$

where $u_i^{(m),0}$ is a component of the displacement vector in the mth layer in the initial strain state and $\lambda_i^{(m)}$ in an elongation factor which characterizes the change in the length of the line element in the Ox_1 axis direction. This parameter is determined by the expression $\lambda_i^{(m)} = \sqrt{1 + 2\varepsilon_i^{(m)}}$, where $\varepsilon_i^{(m)}$ is an ith principal value of the Green's strain tensor of the mth layer. The expression of the components of this tensor through the component of the displacement vector will be given below. Within this, let us investigate the mechanical behavior of the considered slab in the case where on the free face plane of the upper layer, the line-located normal time-harmonic moving force acts. This investigation will be made by the use of the coordinates associated with the initial state, i.e. by the use of coordinates $y_i^{(m)}$, in the framework of the large initial deformation version of the TDLTEWISB. The general scheme of construction of the equations and relations of the TDLTEWISB was described in Sect. 2.1 and some details of this construction for the second version of the small initial deformation theory of the TDLTEWISB was considered in Sect. 2.2 of the present chapter. The obtaining of the equations and relations related to the large initial deformation version of the TDLTEWISB we will consider below with respect to the problem under consideration.

Now we write the field equations and relations of the large initial deformation version of the TDLTEWISB for the compressible body under the plane-strain state in the Oy_1y_2 plane.

The equation of motion is

$$\frac{\partial Q_{ij}^{(m)}}{\partial y_i^{(m)}} = \rho^{(m)} \frac{\partial^2 u_j^{(m)}}{\partial t^2}, \tag{2.46}$$

and the mechanical relations are

$$Q_{ij}^{(m)} = \omega_{ij\alpha\beta}^{(m)} \frac{\partial u_\alpha^{(m)}}{\partial y_\beta^{(m)}}, \tag{2.47}$$

where

$$\begin{aligned}
&\omega_{1111}^{(m)} = \frac{\lambda_1^{(m)}}{\lambda_2^{(m)}}(\lambda^{(m)} + 2\mu^{(m)}),\ \omega_{2222}^{(m)} = \frac{\lambda_2^{(m)}}{\lambda_1^{(m)}}(\lambda^{(m)} + 2\mu^{(m)}),\\
&\omega_{1122}^{(m)} = \omega_{2211}^{(m)} = \lambda^{(m)},\ \omega_{1212}^{(m)} = \omega_{2121}^{(m)} = \frac{2\lambda_2^{(m)}\mu^{(m)}}{\lambda_1^{(m)} + \lambda_2^{(m)}},\\
&\omega_{1221}^{(m)} = \omega_{2112}^{(m)} = \frac{2(\lambda_2^{(m)})^2\mu^{(m)}}{\lambda_2^{(m)}(\lambda_1^{(m)} + \lambda_2^{(m)})}
\end{aligned} \tag{2.48}$$

In Eqs. (2.46)–(2.48) the following notation used: $Q_{ij}^{(m)}$ are the perturbations of the components of the Kirchhoff stress tensor in the mth layer related to the areas of the initial state, $u_j^{(m)}$ are the components of the perturbations of the displacement vector, and $\rho^{(m)}$, and $\lambda^{(m)}$, $\mu^{(m)}$ are the densities also related to the volume of the initial state and mechanical constants of the mth material.

Consider some relations of the non-linear theory of elasticity as a result of linearization of which the foregoing linearized equations and relations are obtained. The non-linear elasticity relations in the case under consideration are given through the harmonic potential which is presented as follows:

$$\Phi^{(m)} = \frac{1}{2}\lambda^{(m)}(s_1^{(m)})^2 + \mu^{(m)}s_2^{(m)} \tag{2.49}$$

where

$$\begin{aligned}
s_1^{(m)} &= \left(\sqrt{1 + 2\varepsilon_1^{(m)}} - 1\right) + \left(\sqrt{1 + 2\varepsilon_2^{(m)}} - 1\right) + \left(\sqrt{1 + 2\varepsilon_3^{(m)}} - 1\right),\\
s_2^{(m)} &= \left(\sqrt{1 + 2\varepsilon_1^{(m)}} - 1\right)^2 + \left(\sqrt{1 + 2\varepsilon_2^{(m)}} - 1\right)^2 + \left(\sqrt{1 + 2\varepsilon_3^{(m)}} - 1\right)^2.
\end{aligned} \tag{2.50}$$

In (2.50) $\varepsilon_i^{(m)}$ (i = 1, 2, 3) are principal values of the Green's strain tensor.

Let us consider briefly the definition of the stress and strain tensors in the large elastic deformation theory which are used in the present investigation. For this purpose we use the Lagrange coordinates x_i ($i = 1, 2, 3$) in the Cartesian system of coordinates $Ox_1x_2x_3$ and the position of the points after and before deformations we determine by the vectors $\mathbf{r}^*$ and $\mathbf{r}$ where $\mathbf{r}^* = \mathbf{r} + \mathbf{u}$. Here $\mathbf{u} = u_i\mathbf{g}_i$ is displacement vector expressed by the unit basic vector $\mathbf{g}_i$. Taking the relations $d\mathbf{r}^*.d\mathbf{r}^* = d\mathbf{r}.d\mathbf{r} + \mathbf{2}d\mathbf{r}.d\mathbf{u} + d\mathbf{u}.d\mathbf{u}$ (here the symbol **"."** means the scalar product of the vectors), $d\mathbf{u}.d\mathbf{u} = (\partial u_k/\partial x_i)(\partial u_k/\partial x_j)dx_idx_j$ and $\mathbf{2}d\mathbf{r}.d\mathbf{u} = 2(\partial u_k/\partial x_i)dx_kdx_i$ into account, it can be written that $d\mathbf{r}^*.d\mathbf{r}^* - d\mathbf{r}.d\mathbf{r} = 2\varepsilon_{ij}dx_idx_j$, where

$$\varepsilon_{ij} = \frac{1}{2}\left(\frac{\partial u_i}{\partial x_j} + \frac{\partial u_j}{\partial x_i} + \frac{\partial u_n}{\partial x_i}\frac{\partial u_n}{\partial x_j}\right) \tag{2.51}$$

This is a component of the Green's strain tensor $\tilde{\boldsymbol{\varepsilon}}$ which is symmetric.

Let us consider the definition of the Kirchhoff stress tensor. The use of various types of stress tensors in the large (finite) elastic deformation theory is connected with the reference of the components of these tensors to the unit area of the relevant surface elements in the deformed or un-deformed state, because, in contrast to the linear theory of elasticity, in the finite elastic deformation theory the difference between the areas of the surface elements taken before and after deformation must be accounted for in the derivation of the equation of motion and under satisfaction of the boundary conditions. According to the aim of the present investigation, we here consider two types of stress tensors denoted by $\tilde{\mathbf{q}}$ and $\tilde{\mathbf{S}}$ the components of which refer to the unit area of the relevant surface elements in the un-deformed state, but act on the surface elements in the deformed state. The components S_{ij} of the stress tensor $\tilde{\mathbf{S}}$ are determined through the strain energy potential $\Phi = \Phi(\varepsilon_{11}, \varepsilon_{12}, \ldots, \varepsilon_{33})$, where ε_{ij} is a component of the Green's strain tensor (2.51), but the use of the following expression:

$$S_{ij} = \frac{1}{2}\left(\frac{\partial}{\partial\varepsilon_{ij}} + \frac{\partial}{\partial\varepsilon_{ji}}\right)\Phi(\varepsilon_{11}, \varepsilon_{12}, \ldots, \varepsilon_{33}). \tag{2.52}$$

The components q_{ij} of the stress tensor $\tilde{\mathbf{q}}$ are determined by the expression

$$q_{ij} = \left(\delta_k^j + \frac{\partial u_j}{\partial x_k}\right)S_{ik}. \tag{2.53}$$

Here δ_k^i is the Kronecker symbol. The stress tensor $\tilde{\mathbf{q}}$ with components determined by expressions (2.52) and (2.53) is called the Kirchhoff stress tensor. According to expressions (2.51)–(2.53), the stress tensor $\tilde{\mathbf{S}}$ is symmetric, but the Kirchhoff stress tensor $\tilde{\mathbf{q}}$ is non-symmetric. Thus, with this we restrict ourselves to consideration of the definition of the stress and strain tensors in the finite elastic deformation theory. These definitions are given without any restriction related to the association of the selected coordinate systems to the natural or initial state.

However, in using the coordinate system associated with the initial deformed state, the initial strain state can be taken as an "un-deformed" state in the foregoing definitions.

Now we attempt to attain the Eqs. (2.46)–(2.48) by employing a linearization procedure. Throughout this procedure in order to simplify the writing of the mathematical symbols, as in the foregoing Eqs. (2.51)–(2.53) we will omit the upper index (m). Nevertheless, the results will be used simultaneously for each component of the system considered by supplying them with the upper index (1) and (2). But in order to denote the displacements, strains and stresses regarding the initial strain state as above we will use the upper index "0".

Thus, according to (2.45), (2.49)–(2.53), we attain that

$$S_{ii}^0 = [\lambda(\lambda_1 + \lambda_2 - 2) + 2\mu(\lambda_i - 1)](\lambda_i)^{-1}, S_{12}^0 = 0 \tag{2.54}$$

It follows from the statement of the problem that $S_{22}^0 = 0$, according to which, the following expression for λ_2 is attained:

$$\lambda_2 = [2\mu - \lambda(\lambda_1 - 2)](\lambda + 2\mu)^{-1} \tag{2.55}$$

In this way, for selected layer materials, the magnitude of the initial strains and the initial stresses in them can be determined only through the parameter λ_1. In this case the perturbation of the components of the non-symmetric Kirchhoff stress tensor q_{ij} (denoted by q'_{ij}) related to the areas of the natural state are determined by the following expression:

$$q'_{ij} = \left(\delta_k^j + \frac{\partial u_j^0}{\partial x_k}\right) S'_{ij} + S_{ik}^0 \frac{\partial u'_j}{\partial x_k} \tag{2.56}$$

where S'_{ik} is a perturbation of the components of the foregoing symmetric stress tensor $\tilde{\mathbf{S}}$.

Consider in more detail the linearization procedure of the non-linear mechanical relation (2.52). Under this consideration, as above, the perturbation of the considered any quantity g, as above, will be denoted as g'. First, we consider the obtaining the relation for the S'_{11} which is derived from the linearization of the expression

$$S_{11} = \lambda s_1 \frac{\partial s_1}{\partial \varepsilon_{11}} + \mu \frac{\partial s_2}{\partial \varepsilon_{11}} \tag{2.57}$$

Note that the Eq. (2.57) is written according to the expression of the strain energy function (2.49). Thus, it follows from the relation (2.57) that

$$S'_{11} = \lambda s_1^0 (\frac{\partial s_1}{\partial \varepsilon_{11}})' + \lambda s'_1 (\frac{\partial s_1}{\partial \varepsilon_{11}})^0 + \mu (\frac{\partial s_2}{\partial \varepsilon_{11}})' \tag{2.58}$$

Now we determine expressions for the s'_1, $(\partial s_1/\partial \varepsilon_{11})'$ and $(\partial s_2/\partial \varepsilon_{11})'$ which enter into (2.58).

From (2.50) we can write that

$$\frac{\partial s_1}{\partial \varepsilon_{11}} = \frac{\partial s_1}{\partial \varepsilon_1}\frac{\partial \varepsilon_1}{\partial \varepsilon_{11}} + \frac{\partial s_1}{\partial \varepsilon_2}\frac{\partial \varepsilon_2}{\partial \varepsilon_{11}}. \tag{2.59}$$

Taking the expressions

$$\begin{aligned} \varepsilon_1 &= \frac{\varepsilon_{11}+\varepsilon_{22}}{2} + \frac{1}{2}\sqrt{(\varepsilon_{11}-\varepsilon_{22})^2 + 4\varepsilon_{12}\varepsilon_{21}}, \\ \varepsilon_2 &= \frac{\varepsilon_{11}+\varepsilon_{22}}{2} - \frac{1}{2}\sqrt{(\varepsilon_{11}-\varepsilon_{22})^2 + 4\varepsilon_{12}\varepsilon_{21}} \end{aligned} \tag{2.60}$$

into consideration we can write the following mathematical calculations.

$$\begin{aligned} \varepsilon_1 = \varepsilon_1^0 + \varepsilon'_1 &= \frac{\varepsilon_{11}^0+\varepsilon_{11}^0}{2} + \frac{\varepsilon'_{11}+\varepsilon'_{11}}{2} + \frac{1}{2}\sqrt{(\varepsilon_{11}^0-\varepsilon_{11}^0)^2 + 2(\varepsilon_{11}^0-\varepsilon_{22}^0)(\varepsilon'_{11}-\varepsilon'_{22})} \\ &\approx \frac{\varepsilon_{11}^0+\varepsilon_{22}^0}{2} + \frac{\varepsilon'_{11}+\varepsilon'_{22}}{2} + \frac{\varepsilon_{11}^0-\varepsilon_{22}^0}{2}\sqrt{1+2\frac{\varepsilon'_{11}-\varepsilon'_{22}}{\varepsilon_{11}^0-\varepsilon_{22}^0}} \\ &\approx \frac{\varepsilon_{11}^0+\varepsilon_{22}^0}{2} + \frac{\varepsilon'_{11}+\varepsilon'_{22}}{2} + (\varepsilon_{11}^0-\varepsilon_{22}^0)\left(1+\frac{\varepsilon'_{11}-\varepsilon'_{22}}{\varepsilon_{11}^0-\varepsilon_{22}^0}\right) \\ &\approx \varepsilon_{11}^0 + \varepsilon'_{11} \Rightarrow \varepsilon_1^0 = \varepsilon_{11}^0, \varepsilon'_1 = \varepsilon'_{11}. \end{aligned} \tag{2.61}$$

Note that in the foregoing calculation procedure the terms in the order $O((\varepsilon'_{12})^2)$, $O((\varepsilon'_{11})^2)$ and $O((\varepsilon'_{22})^2)$ are ignored. In a similar manner we obtain that

$$\varepsilon_2^0 = \varepsilon_{22}^0,\ \varepsilon'_2 = \varepsilon'_{22}. \tag{2.62}$$

Moreover, doing the calculations

$$\begin{aligned} s_1 = s_1^0 + s'_1 &= \sqrt{1+2(\varepsilon_1^0+\varepsilon'_1)} - 1 + \sqrt{1+2(\varepsilon_2^0+\varepsilon'_2)} - 1 \\ &= \sqrt{1+2\varepsilon_1^0}\left(1+\frac{\varepsilon'_2}{1+2\varepsilon_1^0}\right) + \sqrt{1+2\varepsilon_2^0}\left(1+\frac{\varepsilon'_2}{1+2\varepsilon_2^0}\right) \\ &= \sqrt{1+2\varepsilon_1^0} + \sqrt{1+2\varepsilon_2^0} - 2 + \frac{\varepsilon'_1}{\sqrt{1+2\varepsilon_1^0}} + \frac{\varepsilon'_2}{\sqrt{1+2\varepsilon_2^0}}. \end{aligned} \tag{2.63}$$

and, according to (2.45), it is attained that

$$\varepsilon_1^0 = \varepsilon_{11}^0 = \frac{1}{2}(\lambda_1^2 - 1), \varepsilon_2^0 = \varepsilon_{22}^0 = \frac{1}{2}(\lambda_2^2 - 1). \tag{2.64}$$

Substituting (2.64) into (2.63), we obtain

$$s_1^0 = \lambda_1 + \lambda_2 - 2, s_1' = \frac{\varepsilon_{11}'}{\lambda_1} + \frac{\varepsilon_{22}'}{\lambda_2}. \tag{2.65}$$

Now we consider the linearization of the expression

$$\begin{aligned} \frac{\partial s_1}{\partial \varepsilon_{11}} &= \frac{\partial}{\partial \varepsilon_{11}}\left(\sqrt{1+2\varepsilon_1}\right) + \frac{\partial}{\partial \varepsilon_{11}}\left(\sqrt{1+2\varepsilon_2}\right) \\ &= \frac{1}{\sqrt{1+2\varepsilon_1}}\frac{\partial \varepsilon_1}{\partial \varepsilon_{11}} + \frac{1}{\sqrt{1+2\varepsilon_2}}\frac{\partial \varepsilon_2}{\partial \varepsilon_{11}}. \end{aligned} \tag{2.66}$$

We attempt to obtain the expressions for the derivatives $\partial\varepsilon_1/\partial\varepsilon_{11}$ and $\partial\varepsilon_2/\partial\varepsilon_{11}$. For this purpose, using the expression (2.60) we make the mathematical calculations

$$\begin{aligned} \frac{\partial \varepsilon_1}{\partial \varepsilon_{11}} &= \frac{1}{2} + \frac{1}{2}\frac{\varepsilon_{11} - \varepsilon_{22}}{\sqrt{(\varepsilon_{11} - \varepsilon_{22})^2 + 4(\varepsilon_{12})^2}} \\ &\approx \frac{1}{2}\left[1 + \frac{\varepsilon_{11}^0 - \varepsilon_{22}^0 + \varepsilon_{11}' - \varepsilon_{22}'}{\sqrt{(\varepsilon_{11}^0 - \varepsilon_{22}^0)^2 + 2(\varepsilon_{11}^0 - \varepsilon_{22}^0)(\varepsilon_{11}' - \varepsilon_{22}')}}\right] = 1 + O((\varepsilon_{11}')^2 + (\varepsilon_{22}')^2) \end{aligned}$$

and obtain that

$$\frac{\partial \varepsilon_1}{\partial \varepsilon_{11}} = 1 + O((\varepsilon_{11}')^2 + (\varepsilon_{22}')^2). \tag{2.67}$$

In a similar manner we obtain the relation

$$\frac{\partial \varepsilon_2}{\partial \varepsilon_{11}} = O((\varepsilon_{11}')^2 + (\varepsilon_{22}')^2). \tag{2.68}$$

Substituting (2.67) and (2.68) into the relation (2.66) and doing the corresponding mathematical calculations we obtain that

$$\left(\frac{\partial s_1}{\partial \varepsilon_{11}}\right)^0 = \frac{1}{\lambda_1}, \left(\frac{\partial s_1}{\partial \varepsilon_{11}}\right)' = -\frac{\varepsilon_{11}'}{\lambda_1^3}. \tag{2.69}$$

Also, we consider the linearization of the expression

$$\frac{\partial s_2}{\partial \varepsilon_{11}} = 2(\sqrt{1+2\varepsilon_1}-1)\frac{1}{\sqrt{1+2\varepsilon_1}}\frac{\partial \varepsilon_1}{\partial \varepsilon_{11}} + 2(\sqrt{1+2\varepsilon_2}-1)\frac{1}{\sqrt{1+2\varepsilon_2}}\frac{\partial \varepsilon_2}{\partial \varepsilon_{11}}. \tag{2.70}$$

Taking the relations (2.67) and (2.70) into consideration and doing the mathematical calculations which similar with the foregoing ones we determine that

$$\left(\frac{\partial s_2}{\partial \varepsilon_{11}}\right)' = 2\frac{\varepsilon'_{11}}{\lambda_1^3}. \tag{2.71}$$

Thus, substituting (2.65), (2.69) and (2.71) into the Eq. (2.58), we obtain:

$$S'_{11} = \frac{1}{\lambda_1^3}[\lambda(2-\lambda_2)+2\mu]\varepsilon'_{11} + \frac{\lambda}{\lambda_1\lambda_2}\varepsilon'_{22}, \tag{2.72}$$

According to the expressions (2.45) and (2.51) we can write that

$$\varepsilon'_{11} = \lambda_1\frac{\partial u'_1}{\partial x_1}, \varepsilon'_{22} = \lambda_2\frac{\partial u'_2}{\partial x_2}. \tag{2.73}$$

Substituting (2.73) into (2.72) we obtain:

$$S'_{11} = \frac{1}{\lambda_1^2}[\lambda(2-\lambda_2)+2\mu]\frac{\partial u'_1}{\partial x_1} + \frac{\lambda}{\lambda_1}\frac{\partial u'_2}{\partial x_2}. \tag{2.74}$$

According to the expressions (2.56) and (2.73) we can write that

$$q'_{11} = \lambda_1 S'_{11} + S^0_{11}\frac{\partial u'_1}{\partial x_1} \tag{2.75}$$

It follows from (2.74) and (2.75) that

$$q'_{11} = (\lambda+2\mu)\frac{\partial u'_1}{\partial x_1} + \lambda\frac{\partial u'_2}{\partial x_2} \tag{2.76}$$

We rewrite the relation (2.76) with the coordinates $y_1 = \lambda_1 x_1$ and $y_2 = \lambda_2 x_2$, and using the relation $Q'_{11} = q'_{11}/\lambda_2$, we obtain:

$$Q'_{11} = \frac{\lambda_1}{\lambda_2}(\lambda+2\mu)\frac{\partial u'_1}{\partial y_1} + \lambda\frac{\partial u'_2}{\partial y_2} \tag{2.77}$$

from which follows that

$$\omega_{1111} = \frac{\lambda_1}{\lambda_2}(\lambda + 2\mu), \omega_{1122} = \lambda. \tag{2.78}$$

The relations in (2.78) coincide with corresponding ones given in (2.48).

Also, consider the linearized relation for the shear stress S_{12}, that is, consider the linearization of the expression

$$\begin{aligned} S_{12} &= \frac{1}{2}\left(\frac{\partial}{\partial\varepsilon_{12}} + \frac{\partial}{\partial\varepsilon_{21}}\right)\Phi = \frac{1}{2}\left(\frac{\partial}{\partial\varepsilon_{12}} + \frac{\partial}{\partial\varepsilon_{21}}\right)(\frac{1}{2}\lambda s_1^2 + \mu s_2) \\ &= \frac{1}{2}\left(\lambda s_1 \frac{\partial s_1}{\partial\varepsilon_{12}} + \lambda s_1 \frac{\partial s_1}{\partial\varepsilon_{21}} + \mu\left(\frac{\partial s_2}{\partial\varepsilon_{12}} + \frac{\partial s_2}{\partial\varepsilon_{21}}\right)\right). \end{aligned} \tag{2.79}$$

Using the expressions in (2.60) and relations

$$\begin{aligned} &\frac{\partial s_k}{\partial\varepsilon_{12}} = \frac{\partial s_k}{\partial\varepsilon_1}\frac{\partial\varepsilon_1}{\partial\varepsilon_{12}} + \frac{\partial s_k}{\partial\varepsilon_2}\frac{\partial\varepsilon_2}{\partial\varepsilon_{12}}, \ \frac{\partial s_k}{\partial\varepsilon_{21}} = \frac{\partial s_k}{\partial\varepsilon_1}\frac{\partial\varepsilon_1}{\partial\varepsilon_{21}} + \frac{\partial s_k}{\partial\varepsilon_2}\frac{\partial\varepsilon_2}{\partial\varepsilon_{21}}, \quad k = 1, 2, \\ &\frac{\partial\varepsilon_1}{\partial\varepsilon_{12}} = \frac{\varepsilon_{21}}{\sqrt{(\varepsilon_{11} - \varepsilon_{22})^2 + 4\varepsilon_{12}\varepsilon_{21}}}, \ \frac{\partial\varepsilon_2}{\partial\varepsilon_{12}} = -\frac{\varepsilon_{21}}{\sqrt{(\varepsilon_{11} - \varepsilon_{22})^2 + 4\varepsilon_{12}\varepsilon_{21}}}, \\ &\frac{\partial\varepsilon_1}{\partial\varepsilon_{21}} = \frac{\varepsilon_{12}}{\sqrt{(\varepsilon_{11} - \varepsilon_{22})^2 + 4\varepsilon_{12}\varepsilon_{21}}}, \ \frac{\partial\varepsilon_2}{\partial\varepsilon_{21}} = -\frac{\varepsilon_{12}}{\sqrt{(\varepsilon_{11} - \varepsilon_{22})^2 + 4\varepsilon_{12}\varepsilon_{21}}}, \end{aligned} \tag{2.80}$$

according to (2.64) and to the foregoing linearization procedure, we can write the following linearized expressions from the relations in (2.80).

$$\begin{aligned} &(\frac{\partial\varepsilon_1}{\partial\varepsilon_{12}})' = \frac{\varepsilon'_{21}}{\varepsilon_1^0 - \varepsilon_2^0} = \frac{2\varepsilon'_{21}}{\lambda_1^2 - \lambda_2^2}, (\frac{\partial\varepsilon_2}{\partial\varepsilon_{12}})' = -\frac{\varepsilon'_{21}}{\varepsilon_1^0 - \varepsilon_2^0} = -\frac{2\varepsilon'_{21}}{\lambda_1^2 - \lambda_2^2}, \\ &(\frac{\partial\varepsilon_1}{\partial\varepsilon_{21}})' = \frac{\varepsilon'_{12}}{\varepsilon_1^0 - \varepsilon_2^0} = \frac{2\varepsilon'_{12}}{\lambda_1^2 - \lambda_2^2}, (\frac{\partial\varepsilon_2}{\partial\varepsilon_{21}})' = -\frac{\varepsilon'_{12}}{\varepsilon_1^0 - \varepsilon_2^0} - \frac{2\varepsilon'_{12}}{\lambda_1^2 - \lambda_2^2}, \\ &\frac{1}{2}(\lambda s_1 \frac{\partial s_1}{\partial\varepsilon_{12}} + \lambda s_1 \frac{\partial s_1}{\partial\varepsilon_{21}})' = -\lambda(\lambda_1 + \lambda_2 - 2)\frac{4\varepsilon_{12}}{(\lambda_1 + \lambda_2)\lambda_1\lambda_2}, \\ &(\frac{\partial s_2}{\partial\varepsilon_1}\frac{\partial\varepsilon_1}{\partial\varepsilon_{12}} + \frac{\partial s_2}{\partial\varepsilon_2}\frac{\partial\varepsilon_2}{\partial\varepsilon_{12}})' = \frac{8\varepsilon'_{12}}{(\lambda_1 + \lambda_2)\lambda_1\lambda_2}, \\ &S_{22}^0 = 0 = [\lambda(\lambda_1 + \lambda_2 - 2) + 2\mu(\lambda_2 - 1)](\lambda_2)^{-1} \\ &\quad \Rightarrow \lambda(\lambda_1 + \lambda_2 - 2) = -2\mu(\lambda_2 - 1). \end{aligned} \tag{2.81}$$

Taking the expressions in (2.81) into account we obtain

$$S'_{12} = \frac{4\mu\lambda_2}{\lambda_2\lambda_1(\lambda_1+\lambda_2)}\varepsilon'_{12} \tag{2.82}$$

from (2.79). According to (2.51), (2.56), $y_1 = \lambda_1 x_1$ and $y_2 = \lambda_2 x_2$, we can write that

$$\varepsilon'_{12} = \frac{\lambda_1\lambda_2}{2}\left(\frac{\partial u_1}{\partial y_2} + \frac{\partial u_2}{\partial y_1}\right), q'_{21} = \lambda_1 S'_{12},\ Q_{21} = q'_{21}/\lambda_1. \tag{2.83}$$

Consequently, it follows from (2.82) and (2.83) that

$$Q_{21} = \frac{2\mu\lambda_2}{\lambda_1+\lambda_2}\frac{\partial u_1}{\partial y_2} + \frac{2\mu\lambda_2}{\lambda_1+\lambda_2}\frac{\partial u_2}{\partial y_1} = \omega_{2112}\frac{\partial u_1}{\partial y_2} + \omega_{2121}\frac{\partial u_2}{\partial y_1}, \tag{2.84}$$

$$\omega^{(m)}_{2112} = \omega^{(m)}_{2121} = \frac{2\mu\lambda_2}{\lambda_1+\lambda_2}. \tag{2.85}$$

By supplying the foregoing expressions for ω_{2112} and ω_{2121} in (2.85) with the upper index (m) we attain the expressions for $\omega^{(m)}_{2112}$ and $\omega^{(m)}_{2121}$, respectively, given in Eq. (2.48). In a similar manner we can obtain the expressions of the remaining components $\omega^{(m)}_{ij\alpha\beta}$ which enter (2.47) and (2.48). Thus with this we restrict ourselves to consideration of the basic equations and relations within the scope of which the present investigation is carried out.

Consider the contact and boundary conditions. The considered system is excited by a line-located time-harmonic oscillating moving load on the upper layer, therefore the following conditions must be satisfied:

$$Q^{(2)}_{21}\Big|_{y_2^{(2)}=\lambda_2 H/2} = 0, \quad Q^{(2)}_{22}\Big|_{y_2^{(2)}=\lambda_2 H/2} = -P_0 e^{i\omega t}\delta(y_1 - Vt), \tag{2.86}$$

$$\begin{gathered}\left\{u_i^{(2)}; Q^{(2)}_{2i}\right\}\Big|_{y_2^{(2)}=-\lambda_2^{(2)}H^{(2)}/2} = \left\{u_i^{(1)}; Q^{(1)}_{2i}\right\}\Big|_{y_2^{(1)}=\lambda_2^{(1)}H^{(1)}/2}, \\ u_i^{(1)}\Big|_{y_2^{(1)}=-\lambda_2^{(1)}H^{(1)}/2} = 0.\end{gathered} \tag{2.87}$$

In (2.86) V and ω denote the velocity and frequency of the moving load with amplitude P_0.

This completes the formulation of the problem. It should be noted that in the case where $\lambda_i^{(m)} = 1.0\,(i = 1,2;\ m = 1,2)$ the formulation described above transforms into the corresponding one within the scope of the classical linear theory of elastodynamics.

2.4.2 Method of Solution

Below we will only deal with perturbation $u_i^{\prime(m)}$ and $Q_{ik}^{(m)}$, and will omit the upper prime in notation $u_i^{\prime(m)}$, i.e. instead of the notation $u_i^{\prime(m)}$ we will use the notation $u_i^{(m)}$.

By using the coordinate system

$$y_1' = y_1^{\prime(1)} = y_1^{\prime(2)} = y_1 - Vt,\ y_2^{\prime(m)} = y_2^{(m)}, \tag{2.88}$$

which moves with the loading force we represent the sought values as

$$g(y_1^{\prime(m)},\ y_2^{\prime(m)}, t) = \bar{g}(y_1^{\prime(m)}, y_2^{\prime(m)})e^{i\omega t} \tag{2.89}$$

From Eqs. (2.46)–(2.48), the following equations of motion in terms of displacement are obtained:

$$\omega_{kj\alpha\beta}^{\prime(m)} \frac{\partial^2 u_\alpha^{(m)}}{\partial y_k^{(m)} \partial y_\beta^{(m)}} - \frac{1}{(c_2^{(m)})^2}\left(V^2 \frac{\partial^2 u_j^{(m)}}{\partial (y_1^{(m)})^2} - 2i\omega V \frac{\partial u_j^{(m)}}{\partial y_1^{(m)}} - \omega^2 \frac{\partial^2 u_j^{(m)}}{\partial (y_2^{(m)})^2}\right), \quad j = 1, 2, \quad i = \sqrt{-1}, \tag{2.90}$$

where

$$\omega_{kj\alpha\beta}^{\prime(m)} = \frac{\omega_{kj\alpha\beta}^{(m)}}{\mu^{(m)}}, c_2^{(m)} = \sqrt{\frac{\mu^{(m)}}{\rho^{(m)}}}. \tag{2.91}$$

In Eq. (2.90), the upper prime in y_1 and y_2, and over bar in $u_1^{(m)}$ and $u_2^{(m)}$ are omitted. In this case, the second boundary condition in (2.86) is replaced by the following:

$$Q_{22}^{(2)}\Big|_{y_2^{(2)} = \lambda_2^{(2)} H^{(2)}/2} = -P_0 \delta(y_1). \tag{2.92}$$

Thus, the other conditions in (2.86) and (2.87) are also valid for the new coordinate system (2.88) and for the amplitude of the sought values.

Consider the solutions to Eq. (2.90). For this purpose, as in the previous sections, we employ the exponential Fourier transformation with respect to the y_1 coordinate defined as

$$f_F(s, y_2) = \int_{-\infty}^{+\infty} f(y_1, y_2) e^{-isy_1} dy_1 \tag{2.93}$$

in Eq. (2.90) and given the corresponding boundary and contact conditions. As a result of this transformation the following equations with respect to $u_{1F}^{(m)}(s, y_2^{(m)})$ and $u_{2F}^{(m)}(s, y_2^{(m)})$ are attained from (2.90):

$$\begin{aligned}(-\psi^{(m)} - \bar{s}^2\omega_{1111}^{\prime(m)})u_{1F}^{(m)} + \omega_{2112}^{\prime(m)}\frac{d^2u_{1F}^{(m)}}{d(\bar{y}_2^{(m)})^2} + (\omega_{1122}^{\prime(m)} + \omega_{2121}^{\prime(m)})i\bar{s}\frac{du_{2F}^{(m)}}{dy_2^{(m)}} = 0,\\ (-\psi^{(m)} - \bar{s}^2\omega_{1221}^{\prime(m)})u_{2F}^{(m)} + \omega_{2222}^{\prime(m)}\frac{d^2u_{2F}^{(m)}}{d(\bar{y}_2^{(m)})^2} + (\omega_{1212}^{\prime(m)} + \omega_{2211}^{\prime(m)})i\bar{s}\frac{du_{1F}^{(m)}}{dy_2^{(m)}} = 0,\end{aligned} \tag{2.94}$$

where

$$\begin{aligned}\psi^{(m)} = \frac{(c_2^{(2)})^2}{(c_2^{(m)})^2}(-\bar{s}^2c^2 + 2\Omega c\bar{s} - \Omega^2), \bar{y}_i^{(m)} = \frac{y_i^{(m)}}{H^{(2)}},\\ c = \frac{V}{c_2^{(2)}}, \Omega = \frac{\omega H^{(2)}}{c_2^{(2)}}, \bar{s} = sH^{(2)}.\end{aligned} \tag{2.95}$$

From the second equation in (2.94), it can be written that

$$\begin{aligned}\frac{du_{1F}^{(m)}}{d\bar{y}_2^{(m)}} = i\left(a^{(m)}u_{2F}^{(m)} + b^{(m)}\frac{d^2u_{2F}^{(m)}}{d(\bar{y}_2^{(m)})^2}\right),\\ \frac{d^3u_{1F}^{(m)}}{d(\bar{y}_2^{(m)})^3} = i\left(a^{(m)}\frac{d^2u_{2F}^{(m)}}{d(\bar{y}_2^{(m)})^2} + b^{(m)}\frac{d^4u_{2F}^{(m)}}{d(\bar{y}_2^{(m)})^4}\right).\end{aligned} \tag{2.96}$$

Similarly, it can also be written from the first equation in (2.94) that

$$(-\psi^{(m)} - \bar{s}^2\omega_{1111}^{\prime(m)})\frac{du_{1F}^{(m)}}{d\bar{y}_2^{(m)}} + \omega_{2112}^{\prime(m)}\frac{d^3u_{1F}^{(m)}}{d(\bar{y}_2^{(m)})^3} + (\omega_{1122}^{\prime(m)} + \omega_{2121}^{\prime(m)})i\bar{s}\frac{d^2u_{2F}^{(m)}}{d(y_2^{(m)})^2} = 0. \tag{2.97}$$

Substituting the expressions in Eq. (2.96) into Eq. (2.97), the equation

$$\frac{d^4u_{2F}^{(m)}}{d(y_2^{(m)})^4} + a_1^{(m)}\frac{d^2u_{2F}^{(m)}}{d(y_2^{(m)})^2} + b_1^{(m)}u_{2F}^{(m)} = 0, \tag{2.98}$$

is obtained, where

$$a^{(m)} = \frac{(-\psi^{(m)} - \bar{s}^2\omega_{1111}^{\prime(m)})}{(\omega_{1212}^{\prime(m)} + \omega_{2211}^{\prime(m)})\bar{s}},\ b^{(m)} = \frac{\omega_{2222}^{\prime(m)}}{(\omega_{1212}^{\prime(m)} + \omega_{2211}^{(m)})\bar{s}},$$
$$a_1^{(m)} = \left[b^{(m)}(-\psi^{(m)} - \bar{s}^2\omega_{1111}^{\prime(m)}) + a^{(m)}\omega_{2112}^{\prime(m)} + \bar{s}(\omega_{1122}^{\prime(m)} + \omega_{2121}^{\prime(m)})\right](\omega_{2112}^{\prime(m)}b^{(m)})^{-1} \quad (2.99)$$
$$b_1^{(m)} = a^{(m)}(-\psi^{(m)} - \bar{s}^2\omega_{1111}^{\prime(m)})(\omega_{2112}^{\prime(m)}b^{(m)})^{-1}.$$

Thus, we find the solution to Eq. (2.98) as follows:

$$u_{2F}^{(m)} = A_1^{(m)}e^{k_1^{(m)}y_2^{(m)}} + A_2^{(m)}e^{-k_1^{(m)}y_2^{(m)}} + A_3^{(m)}e^{k_2^{(m)}y_2^{(m)}} + A_4^{(m)}e^{-k_2^{(m)}y_2^{(m)}}, \quad (2.100)$$

where

$$k_1^{(m)} = \sqrt{-\frac{a_1^{(m)}}{2} + d_1^{(m)}},\quad k_2^{(m)} = \sqrt{-\frac{a_1^{(m)}}{2} - d_1^{(m)}},$$
$$d_1^{(m)} = \sqrt{-\frac{(a_1^{(m)})^2}{2} - b_1^{(m)}}. \quad (2.101)$$

As the subsonic case is considered, therefore it is assumed that the conditions

$$\max\left\{\left(\frac{V}{c_2^{(1)}}\right)^2, \left(\frac{V}{c_2^{(2)}}\right)^2\right\} < \min\left\{\omega_{ij\alpha\beta}^{\prime(1)}, \omega_{ij\alpha\beta}^{\prime(2)}\right\}. \quad (2.102)$$

satisfy each combination of the indices $ij\alpha\beta$. According to (2.102), it follows from (2.95), (2.99) and (2.101) that in the case where $\Omega = 0$ the values of $k_1^{(m)}$ and $k_2^{(m)}$ in (2.101) are real values and $k_1^{(m)} > 0$, $k_2^{(m)} > 0$. But in the case where $\Omega > 0$, the values of $k_1^{(m)}$ and $k_2^{(m)}$ can also be complex (most probably pure imaginary) numbers. Note that these statements have been taken into account in developing the calculation algorithm and in constructing the corresponding PC programs.

Thus, from (2.100), (2.96), (2.101) and (2.48) we have completely determined the Fourier transform of all values. The corresponding closed system of algebraic equations is obtained from boundary conditions (2.86)–(2.92) and contact conditions (2.87) for determination of the unknowns $A_1^{(1)}, A_2^{(1)}, \ldots, A_4^{(2)}$ which enter into these transforms. From the algebraic equations we find the aforementioned unknowns and, by employing the inverse transform

$$f(y_1, y_2) = \frac{1}{2\pi}\int_{-\infty}^{+\infty} f_F(s, y_2)e^{isy_1}ds \quad (2.103)$$

we determine the sought stresses and displacements.

2.4.3 General Remarks on the Doppler Effect

In the case where $\Omega = 0$ or in the case where $c = 0$ the integral (2.103) can be reduced to the calculation of either of the integrals $1/\pi \int_0^{+\infty} f_F(s, y_2)\cos(sy_1)ds$ (for $u_2^{(m)}$, $Q_{22}^{(m)}$, $Q_{11}^{(m)}$, $\varepsilon_{22}^{(m)}$, $\varepsilon_{11}^{(m)}$) or $1/\pi \int_0^{+\infty} f_F(s, y_2)\sin(sy_1)ds$ (for $u_1^{(m)}$, $Q_{21}^{(m)}$, $Q_{12}^{(m)}$, $\varepsilon_{12}^{(m)}$). However, in the case where $\Omega \times c \neq 0$, this reduction is violated by the term $2\Omega c\bar{s}$ which enters the expression $\psi^{(m)}$ in (2.95). Consequently, given the calculation of integrals (2.103) we must use the relation

$$\frac{1}{2\pi}\int\limits_{-\infty}^{+\infty}(\bullet)e^{isy_1}ds \approx \frac{1}{2\pi}\int\limits_{-S^*}^{+S^*}(\bullet)\cos(sy_1)ds + i\frac{1}{2\pi}\int\limits_{-S^*}^{+S^*}(\bullet)\sin(sy_1)ds. \quad (2.104)$$

The values of S^* in (2.104) are determined from the corresponding numerical convergence criterion. At the same time, we use the following notation:

$$\begin{gathered}
Q_{ijc}^{(m)} \approx \frac{1}{2\pi}\int\limits_{-S^*}^{+S^*} Q_{ijF}^{(m)}\cos(sy_1)ds,\ Q_{ijs}^{(m)} \approx \frac{1}{2\pi}\int\limits_{-S^*}^{+S^*} Q_{ijF}^{(m)}\sin(sy_1)ds,\\
u_{ic}^{(m)} \approx \frac{1}{2\pi}\int\limits_{-S^*}^{+S^*} u_{iF}^{(m)}\cos(sy_1)ds,\ u_{is}^{(m)} \approx \frac{1}{2\pi}\int\limits_{-S^*}^{+S^*} u_{iF}^{(m)}\sin(sy_1)ds,\\
\left\{\tilde{Q}_{22}^{(m)}, \tilde{Q}_{11}^{(m)}, \tilde{u}_2^{(m)}\right\} = \left\{\left|\tilde{Q}_{22}^{(m)}\right|e^{i\alpha_{22}^{(m)}}, \left|\tilde{Q}_{11}^{(m)}\right|e^{i\alpha_{11}^{(m)}}, \left|\tilde{u}_2^{(m)}\right|e^{i\alpha_2^{(m)}}\right\},\\
\left\{\tilde{Q}_{21}^{(m)}, \tilde{Q}_{12}^{(m)}, \tilde{u}_1^{(m)}\right\} = \left\{i\left|\tilde{Q}_{21}^{(m)}\right|e^{i\alpha_{21}^{(m)}}, i\left|\tilde{Q}_{12}^{(m)}\right|e^{i\alpha_{12}^{(m)}}, i\left|\tilde{u}_1^{(m)}\right|e^{i\alpha_1^{(m)}}\right\},
\end{gathered} \quad (2.105)$$

where

$$\begin{gathered}
\left|\tilde{Q}_{ij}^{(m)}\right| = \sqrt{\left(\tilde{Q}_{ijc}^{(m)}\right)^2 + \left(\tilde{Q}_{ijs}^{(m)}\right)^2},\ \left|\tilde{u}_i^{(m)}\right| = \sqrt{\left(\tilde{u}_{ic}^{(m)}\right)^2 + \left(\tilde{u}_{is}^{(m)}\right)^2},\\
\tan\alpha_{ij}^{(m)} = \frac{Q_{ijs}^{(m)}}{Q_{ijc}^{(m)}},\ \tan\alpha_i^{(m)} = \frac{u_{is}^{(m)}}{u_{ic}^{(m)}}.
\end{gathered} \quad (2.106)$$

After the foregoing mathematical preparation, the real values of the sought quantities are determined by the expression

$$\left\{Q_{ij}^{(m)}, u_i^{(m)}\right\} = \mathrm{Re}\left\{\tilde{Q}_{ij}^{(m)} e^{i\omega t}, \tilde{u}_i^{(m)} e^{i\omega t}\right\}, \tag{2.107}$$

according to which,

$$\begin{aligned} Q_{22}^{(m)} &= \left|\tilde{Q}_{22}^{(m)}\right| \cos(\alpha_{22}^{(m)} + \omega t),\ Q_{11}^{(m)} = \left|\tilde{Q}_{11}^{(m)}\right| \cos(\alpha_{11}^{(m)} + \omega t), \\ Q_{21}^{(m)} &= -\left|\tilde{Q}_{21}^{(m)}\right| \sin(\alpha_{21}^{(m)} + \omega t),\ Q_{12}^{(m)} = -\left|\tilde{Q}_{12}^{(m)}\right| \sin(\alpha_{12}^{(m)} + \omega t), \\ u_2^{(m)} &= \left|\tilde{u}_2^{(m)}\right| \cos(\alpha_2^{(m)} + \omega t),\ u_1^{(m)} = -\left|\tilde{u}_1^{(m)}\right| \sin(\alpha_1^{(m)} + \omega t). \end{aligned} \tag{2.108}$$

It follows from expressions (2.106) and (2.108) that the functions $\alpha_{ij}^{(m)}(y_1, y_2^{(m)})$ and $\alpha_i^{(m)}(y_1, y_2^{(m)})$ are odd functions with respect to y_1. At the same time, by direct calculation it is proven that

$$\begin{aligned} &\alpha_{ij}^{(m)}(y_1, y_2^{(m)}) < 0, \quad \alpha_i^{(m)}(y_1, y_2^{(m)}) < 0 \quad \text{for } y_1 > 0, \\ &\alpha_{ij}^{(m)}(y_1, y_2^{(m)}) > 0, \quad \alpha_i^{(m)}(y_1, y_2^{(m)}) > 0, \quad \text{for } y_1 < 0. \end{aligned} \tag{2.109}$$

For fixed $y_2^{(m)} (= y_2^{(m)^*})$ we can write

$$\begin{aligned} \alpha_{ij}^{(m)}(y_1, y_2^{(m)}) &= \left.\frac{\partial \alpha_{ij}^{(m)}}{\partial y_1}\right|_{y_1=0} y_1 + \tilde{\alpha}_{ij}^{(m)}(y_1, y_2^{(m)}), \\ \alpha_i^{(m)}(y_1, y_2^{(m)}) &= \left.\frac{\partial \alpha_i^{(m)}}{\partial y_1}\right|_{y_1=0} y_1 + \tilde{\alpha}_i^{(m)}(y_1, y_2^{(m)}). \end{aligned} \tag{2.110}$$

It follows from (2.109) and from the foregoing discussions that

$$k_i^{(m)} = \left.\frac{\partial \alpha_i^{(m)}}{\partial y_1}\right|_{y_1=0} < 0, \quad k_i^{(m)} = \left.\frac{\partial \alpha_i^{(m)}}{\partial y_1}\right|_{y_1=0} < 0. \tag{2.111}$$

According to Eqs. (2.106), (2.109)–(2.111), the expressions given in (2.108) can be presented through multiplication of two terms, one of which is $e^{i(k_{ij}^{(m)} y_1 + \omega t)}$ or $e^{i(k_i^{(m)} y_1 + \omega t)}$. This is similar to the expressions corresponding to the wave propagation along the Oy_1 axis. It should be noted that this "wave propagation" is considered in a moving frame of reference. In this case, as it moves, propagating a wave with angular frequency ω and wave-number $k_{ij}^{(m)}$, the observation point oscillates with angular frequency ω in a moving frame of reference. However, in a fixed frame of reference, according to the foregoing discussions and expressions, it oscillates with angular frequency $\tilde{\omega} = \omega - k_{ij}^{(m)} V$. This follows from the relationship

$$e^{i\omega t}e^{i\alpha_{ij}^{(m)}} = e^{i\omega t}e^{i(k_{ij}^{(m)}y_1+\tilde{\alpha}_{ij}^{(m)})} = e^{i\omega t}e^{i(k_{ij}^{(m)}(y_1'-Vt)+\tilde{\alpha}_{ij}^{(m)})}$$
$$= e^{i(\omega-k_{ij}^{(m)}V)t}e^{i(k_{ij}^{(m)}y_1'+\tilde{\alpha}_{ij}^{(m)})} \Rightarrow \tilde{\omega} = \omega - k_{ij}^{(m)}V.$$

Hence, according to the expressions and inequalities (2.109)–(2.111), for a fixed frame of reference, the oscillation frequency $\tilde{\omega}$ of the observation point determined by coordinates $y_1 > 0 (y_1 < 0)$ increases (decreases). This statement is known physically as the Doppler Effect. Consequently, the foregoing discussions and results agree with the well-known results of acoustic-physics and prove the validity of the mathematical modeling used for the problem considered.

With this we restrict here the discussions regarding the Doppler Effect. More detailed analysis of this effect for the problem considered can be the subject of other separate investigations.

2.4.4 *On the Algorithm Used for Obtaining Numerical Results*

Consider the description of the algorithm regarding the determination of the critical velocity, and the calculation of the integrals in expression (2.103). Numerical investigations show that, in general, within fixed values of the problem parameters for each value of V the quantities $u_{iF}^{(m)}$, $Q_{ijF}^{(m)}$ have singular points with respect to $sH^{(2)}$. The following is a consideration of the determination of these singular point.

Arguing as in the previous sections, the aforementioned singular points coincide with the roots of the equation

$$\det\left\|\alpha_{nm}(V(sH^{(2)})\right\| = 0, \quad n;\, m = 1, 2, \ldots, 8 \tag{2.112}$$

in $V(sH^{(2)})$, where $\alpha_{nm}(V(sH^{(2)})$ are the coefficients of the unknowns $A_1^{(1)}, \ldots, A_4^{(1)}$, $A_1^{(2)}, \ldots, A_4^{(2)}$ in these algebraic system of equations obtained from the boundary (2.86), (2.92) and contact (2.87) conditions for determination of these unknowns. Consequently, the order of singularity (denoted by r) of integrated values coincides with the order of the roots of Eq. (2.112). It is known that in the case where $0 \leq r < 1$ the integrals in (2.103) can be calculated by the use of normal well-known algorithms. In the case where $r = 1$, the calculation of integrals (2.78) and (2.104) are performed according to Cauchy's principal value sense. But in the case where $r > 1$ the integrals do not have any meaning and the velocity corresponding to the case is called the "critical velocity" at which a resonance type of phenomenon takes place. In this case the values of all parameters of the problem are fixed (except the load-moving velocity V) and for the given value of $sH^{(2)}$, the velocity V is determined from Eq. (2.112) as the root of this equation. In this way, the dependence between V and $sH^{(2)}$ is obtained, and, as in the previous sections, the critical

velocity corresponds to the case where $dV/d(sH^{(2)}) = 0$. A principal difference of the present algorithm for the solution to the Eq. (2.112) from those used in the previous sections is caused by the non-symmetry of the $\det\left\|\alpha_{nm}(V(sH^{(2)})\right\|$ in Eq. (2.112) with respect to the parameter $sH^{(2)}$. We recall that in the previous sections the left side of the related equations is symmetric with respect to the Fourier transformation parameter s. We attempt at this point to analyze an equivalency for the definition of the critical velocity described above and used in the previous two sections, and in papers by Dieterman and Metrikine (1997) and by Metrikine and Vrouwenvelder (2000). Note that in the paper by Dieterman and Metrikine (1997) the critical velocity is defined as the velocity for which the phase and group velocity are equal to each other. Note that the definition of the critical velocity used in the present and previous sections coincides with that proposed in the paper by Dieterman and Metrikine (1997). This conclusion can be proven as follows (below instead of notation V and s we will use the notation c and k, respectively, where c is a phase velocity and k is a wave number):

$$\begin{aligned} dc/d(sH^{(2)}) &= d(\omega/k)/d(kH^{(2)}) = d(\omega(kH^{(2)}) \\ &= 1/(kH^{(2)})^2(d\omega/dk) - (\omega/k)/(kH^{(2)})^2 = 0 \\ &\Rightarrow c_g = d\omega/dk = \omega/k = c_p. \end{aligned}$$

Consequently, as in the case where $\Omega = 0$, the physical meaning of the critical velocity is defined by the equation $dV/d(sH^{(2)}) = 0$ (because under $\Omega = 0$ Eq. (2.112) coincides with the dispersion equation of the system considered) which is equivalent to that proposed in paper by Dieterman and Metrikine (1997). At the same time, in paper by Metrikine and Vrouwenvelder (2000) the critical velocity is defined as a minimal phase velocity after which wave propagation starts to occur in the system analyzed. The determination $dV/d(sH^{(2)}) = 0$ of the critical velocity under $\Omega = 0$ also confirms that proposed in paper by Metrikine and Vrouwenvelder (2000), if the velocity satisfying the equation $dV/d(sH^{(2)}) = 0$ is a minimal velocity. It is obvious that sometimes the velocity satisfying this equation may be also a maximal phase velocity. Therefore, in the author's opinion, the definition and the physical meaning of the critical velocity based on the equality of the phase and group velocities is a more generalized one than the one based on the minimal phase velocity and also confirms the critical velocity definition used in the present and previous sections.

As has been mentioned above, the foregoing discussions concerning the critical velocity are for the case where $\Omega = 0$. However, in the case where $\Omega > 0$, in papers by Dieterman and Metrikine (1997) and by Metrikine and Vrouwenvelder (2000) the critical velocity is determined from the set of equations consisting of the dispersion equation plus the equation $\omega = kV \pm \Omega$ (the equation of the kinematic invariant) as well as the equation $d\omega/dk = V$ (i.e. the condition for the equality of the group velocity of radiated waves and the load velocity), and in this way two critical velocities are also determined from the equation $dV/d(sH^{(2)}) = 0$ one of

which corresponds to the values $sH^{(2)} < 0$, but the other one to the values $sH^{(2)} > 0$. It should be noted that in the case where $\Omega > 0$ the curves $V = V(sH^{(2)})$ determined from Eq. (2.112) do not coincide with the dispersion curves. Nevertheless, the expression $\psi^{(m)}$ in Eq. (2.95) shows that the curves $V = V(sH^{(2)})$ plotted for the values $sH^{(2)} > 0\,(sH^{(2)} < 0)$ can be considered as the "dispersion curves" for the phase velocity determined by the expression $V = (\omega - \Omega)/k$ $(V = (\omega + \Omega)/k)$. It follows from this statement that the definition of the critical velocity used in the present investigation for the case where $\Omega > 0$ is equivalent to that used in papers by Dieterman and Metrikine (1997) and by Metrikine and Vrouwenvelder (2000). The numerical examples for the foregoing discussions will be considered below.

Thus, we come to consider the numerical results obtained within the framework of the solution method discussed above and related to the influence of the oscillation frequency of the moving load, of the initial strain in the layers of the slab, and their mechanical properties on the values of the critical velocity and on the values of the stresses acting on the interface plane between the layers.

2.4.5 Numerical Results and Discussions

Assume that $\lambda^{(1)}/\mu^{(1)} = \lambda^{(2)}/\mu^{(2)} = 1.5$; all numerical investigations for this case have been made. For an illustration of the trustworthiness of the algorithm and PC programs used, first, we consider the case where $\Omega = 0$ which was also consider in paper by Babich et al. (1986) and in the previous sections under $\mu^{(2)}/\mu^{(1)} = 2.0$, $\lambda_1^{(2)} = \lambda_1^{(1)} = 1.0$, $\rho^{(1)}/\rho^{(2)} = 0.5$. The influence of $H^{(1)}/H^{(2)}$ on the values of the critical velocity $c_{cr}(=V_{cr}/c_2^{(2)})$ is investigated. According to the well-known mechanical considerations, for the subsonic velocities of the moving load the values of c_{cr} must approach the corresponding results obtained in Sect. 2.2 and in paper by Babich et al. (1986) with $H^{(1)}/H^{(2)}$. These numerical results are given in Table 2.12, and agree with the foregoing predictions and prove the trustworthiness of the numerical algorithm and PC programs used.

Analyses of the multiple numerical results show that the critical velocity of the moving load occurs in cases where $\mu^{(2)}/\mu^{(1)} > 1$. At the same time, the existence of the critical velocity depends also on the values of $\rho^{(2)}/\rho^{(1)}$ and on the values of

Table 2.12 The values of $c_{cr}(=V_{cr}/c_2^{(2)})$ for various values of $H^{(1)}/H^{(2)}$ under $\mu^{(1)}/\mu^{(2)} = 2$, $\lambda_1^{(2)} = \lambda_1^{(1)} = 1.0$, $\rho^{(1)}/\rho^{(2)} = 0.5$

$H^{(1)}/H^{(2)}$						
0.5	1.0	1.5	2.0	4.0	6.0	∞
0.9084	0.8812	0.8651	0.8556	0.8431	0.8415	0.8451 (Sect. 2.2) 0.8370 (Babich et al. 1986)

Table 2.13 The influence of the parameters $\mu^{(2)}/\mu^{(1)}$, $\rho^{(1)}/\rho^{(2)}$ and $H^{(1)}/H^{(2)}$ on the values of $c_{cr}(=V_{cr}/c_2^{(2)})$ under $\lambda_1^{(2)} = \lambda_1^{(1)} = 1.0$

$\mu^{(2)}/\mu^{(1)}$	$\rho^{(1)}/\rho^{(2)}$	$H^{(1)}/H^{(2)}$			
		0.5	2.0	5.0	7.0
2	$0.5\left(c_2^{(2)} = c_2^{(1)}\right)$	0.9098			
	$2.0\left(c_2^{(2)} > c_2^{(1)}\right)$	–	–	–	–
	$0.25\left(c_2^{(2)} < c_2^{(1)}\right)$	0.9160	0.8906	0.8891	0.8891
3	$1/3\left(c_2^{(2)} = c_2^{(1)}\right)$	0.8777	0.7953	0.7760	0.7753
	$0.5\left(c_2^{(2)} > c_2^{(1)}\right)$	–	0.7663	0.7307	0.7264
	$0.25\left(c_2^{(2)} < c_2^{(1)}\right)$	0.8818	0.8096	0.7970	0.7968
5	$0.2\left(c_2^{(2)} = c_2^{(1)}\right)$	0.8266	0.7146	0.6871	0.6859
	$0.25\left(c_2^{(2)} > c_2^{(1)}\right)$	0.8235	0.7049	0.6728	0.6707
	$1/6\left(c_2^{(2)} < c_2^{(1)}\right)$	0.8287	0.7201	0.6965	0.6957

$H^{(1)}/H^{(2)}$. This statement is illustrated by the data given in Table 2.13. In this table the sign "–" means that in the corresponding case the critical velocity does not exist. Moreover, it follows from Table 2.13 that the values of $c_{cr}(=V_{cr}/c_2^{(2)})$ decrease with $\mu^{(2)}/\mu^{(1)}$.

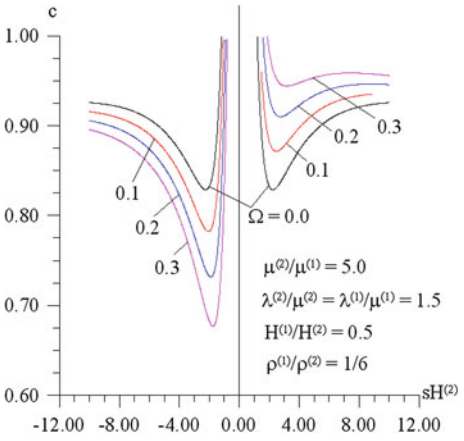

Fig. 2.10 The graphs of the dependencies between c and $sH^{(2)}$ for determination of the values of c'_{cr} and c''_{cr} for various values of Ω under $H^{(1)}/H^{(2)} = 0.5$, $\lambda_1^{(2)} = \lambda_1^{(1)} = 1.0$, $\mu^{(2)} = \mu^{(1)} = 5.0$, $\rho^{(2)} = \rho^{(1)} = 1/6$

The foregoing results agree with the corresponding ones attained in Sect. 2.2 and in papers by Achenbach et al. (1967), Babich et al. (1986). An explanation of why the critical velocity occurs when $\mu^{(2)}/\mu^{(1)} > 1$ can made by analyzing the nature of the dispersion relations of the wave propagation in the system considered. Under $\mu^{(2)}/\mu^{(1)} > 1$ the relations, i.e. the relations between $c/c_2^{(2)}$ and $kH^{(2)}$ (k is a wave number) have a local minimum. But in the case where $\mu^{(2)}/\mu^{(1)} < 1$, these relations do not have a local minimum.

Consider the case where $\Omega \times c \neq 0$. It should be noted that in the case where $\Omega \times c = 0$; taking the symmetry of the $\det\left\|\alpha_{nm}(c(sH^{(2)}))\right\|$ with respect to $sH^{(2)} = 0.0$ into account for analysis of the dependence $c = c(sH^{(2)})$ is sufficient for the consideration of this dependence in the interval $0 \leq sH^{(2)} \leq +\infty$ only. But in the case where $\Omega \times c \neq 0$, according to the term $\Omega c\bar{s}$ in the expression $\psi^{(m)}$ in (2.95), this symmetry is violated. Therefore, in the case where $\Omega \times c \neq 0$ the analyses of the dependence $c = c(sH^{(2)})$ must be done in the interval $-\infty \leq sH^{(2)} \leq +\infty$. For illustration of the foregoing statement we consider the graphs of the dependence given in Fig. 2.10. These graphs are constructed under $\mu^{(2)}/\mu^{(1)} = 5.0$, $\rho^{(1)}/\rho^{(2)} = 1/6$ and $\lambda_1^{(2)} = \lambda_1^{(1)} = 1.0$ for various values of Ω.

It follows from this figure that the graphs constructed in the case where $\Omega = 0$ are symmetric with respect to the straight line determined by the equation $sH^{(2)} = 0$. However, as has been noted above, this symmetry is violated for the graphs constructed under $\Omega > 0$. The analyses of the numerical results show that up to certain Ω (denoted by Ω') the values of the "minimum" critical velocity (denoted by c'_{cr}) are determined by the left branches, i.e. by the branches attained in the region $sH^{(2)} < 0$. The following values (by magnitude) of the critical velocity (denoted by c''_{cr}) are determined by the right branches, i.e. by the branches obtained in the region $sH^{(2)} > 0$. In this case the values c'_{cr} (c''_{cr}) decrease (increase) with Ω. Consequently, up to a certain value of the oscillation frequency (i.e. up to $\Omega = \Omega'$) of the moving load, as a result of the oscillation of this load, the critical velocity decreases. However, in the case where $\Omega > \Omega'$ the left branches of the graphs do not determine the critical velocity; in other words, on these branches, the point for which the equation $dc/d(sH^{(2)}) = 0$ satisfies, as critical velocity does not occur, but the right branches of the graphs to determine the values of c_{cr} for the case where $\Omega > \Omega'$. This procedure continues up to a certain value of Ω (denoted by Ω'') after which the value c''_{cr} goes outside of the framework of the subsonic moving regime. It should be noted that the numerical results shown in Fig. 2.10 in the qualitative sense agree with the corresponding results obtained in papers by Dieterman and Metrikine (1997), Metrikine and Vrouwenvelder (2000). Moreover, these results in the quantitative sense agree with the results obtained in papers by Metrikine and Dieterman (1999), Kim (2004) in which the critical velocity for an infinite Bernoulli-Euler beam resting on an elastic half-space (Metrikine and Dieterman 1999) and on a Winkler type elastic foundation (Kim 2004) when the system is subjected

Table 2.14 The influence of the parameters $\lambda_1^{(2)}$ and $\lambda_1^{(1)}$ on the values of c'_{cr} for various values of $H^{(1)}/H^{(2)}$ in the case where $\Omega = 0.0$

$\lambda_1^{(2)}/\lambda_1^{(1)}$	$H^{(1)}/H^{(2)}$		
	0.5	2.0	5.0
1.0/1.0	0.8266	0.7142	0.6871
1.02/1.0	0.8657	0.7646	0.7393
1.05/1.0	0.9206	0.8326	0.8088
1.07/1.0	0.9551	0.8740	0.8505
1.0/1.02	0.8263	0.7152	0.6998
1.0/1.05	0.8259	0.7037	0.6771
1.0/1.07	0.8393	0.7068	0.6846
1.0/1.10	0.8399	0.7113	0.6937
1.0/1.15	0.8411	0.7184	0.7042
1.0/1.20	0.8427	0.7253	0.7113

Table 2.15 The influence of the parameters $\lambda_1^{(2)}$ and $\lambda_1^{(1)}$ on the values of c'_{cr} for various values of $H^{(1)}/H^{(2)}$ in the case where $\Omega = 0.1$

$\lambda_1^{(2)}/\lambda_1^{(1)}$	$H^{(1)}/H^{(2)}$		
	0.5	2.0	5.0
1.0/1.0	0.7800	0.6270	0.5603
1.02/1.0	0.8204	0.6793	0.6121
1.05/1.0	0.8772	0.7501	0.6805
1.07/1.0	0.9130	0.7932	0.7213
1.0/1.02	0.7794	0.6278	0.5639
1.0/1.05	0.7786	0.6128	0.5190
1.0/1.07	0.7950	0.6158	0.5285
1.0/1.10	0.7953	0.6203	0.5420
1.0/1.15	0.7963	0.6276	0.5625
1.0/1.20	0.7976	0.6348	0.5804

Table 2.16 The influence of the parameters $\lambda_1^{(2)}$ and $\lambda_1^{(1)}$ on the values of c'_{cr} for various values of $H^{(1)}/H^{(2)}$ in the case where $\Omega = 0.2$

$\lambda_1^{(2)}/\lambda_1^{(1)}$	$H^{(1)}/H^{(2)}$		
	0.5	2.0	5.0
1.0/1.0	0.7293	0.5268	0.3729
1.02/1.0	0.7709	0.5800	0.4188
1.05/1.0	0.8294	0.6521	0.4796
1.07/1.0	0.8663	0.6960	0.5161
1.0/1.02	0.7285	0.5272	0.3763
1.0/1.05	0.7273	0.5095	0.3812
1.0/1.07	0.7353	0.5121	0.3165
1.0/1.10	0.7779	0.5161	0.3287
1.0/1.15	0.8444	0.5228	0.3479
1.0/1.20	0.9022	0.5295	0.3658

to a static axial force and a moving load with harmonic amplitude variation was studied.

The influence of the problem parameters $\lambda_1^{(2)}$ and $\lambda_1^{(1)}$ which characterize the magnitude of the initial strains in the layers of the slab is analyzed, and the influence of the parameter $H^{(1)}/H^{(2)}$ on the values of c'_{cr} attained for the various values of Ω. The corresponding results are given in Tables 2.14, 2.15 and 2.16 for the cases where $\Omega = 0.0, 0.1$ and 0.2, respectively. In this case it is assumed that $\mu^{(2)}/\mu^{(1)} = 5$ and $\rho^{(1)}/\rho^{(2)} = 1/6$. The corresponding conclusions followed from these results will be given in the next subsection.

The numerical results regarding the distribution of the stresses $Q_{22}^{(2)}$ and $Q_{22}^{(1)}$ on the planes of the mid-layers are examined with respect to $y_1/H^{(2)}$. However, in this examination the following statements must be taken into account.

According to the discussions made in the previous subsection and the expressions (2.105) and (2.106), in the case where $\Omega \times c = 0$ the relations $\alpha_{ij}^{(m)} = 0$, $\alpha_i^{(m)} = 0$ occur. Consequently, in the case where $\Omega \times c = 0$ the distribution of the stresses $Q_{22}^{(2)}$ and $Q_{22}^{(1)}$ become symmetric with respect to $y_1/H^{(2)} = 0$.

Moreover, in the case where $\Omega \times c = 0$ the distribution of the $\tilde{Q}_{22}^{(2)}$ and $\tilde{Q}_{22}^{(1)}$, in the qualitative sense, also illustrate (simultaneously) the distribution of the $Q_{22}^{(2)}$ and $Q_{22}^{(1)}$, respectively. However, in the case where $\Omega \times c \neq 0$ the functions $\alpha_{ij}^{(m)}$ and $\alpha_i^{(m)}$ appear and these functions are discontinuous with respect to $y_1/H^{(2)} = 0$. This discontinuity is explained by the wave reflection from the planes of the mid-layers. Moreover, in the case where $\Omega \times c \neq 0$, the distribution of the $Q_{22}^{(2)}$ and $Q_{22}^{(1)}$ becomes non-symmetric with respect to the straight line for which the equation is

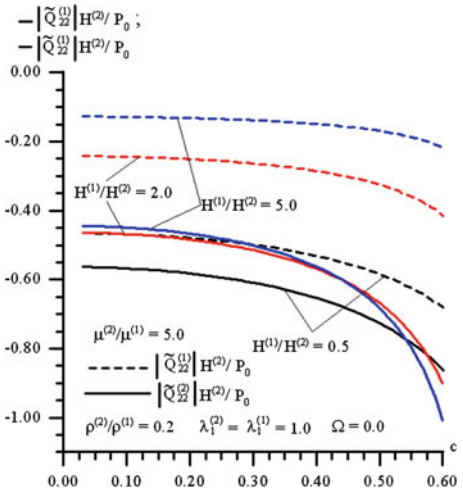

Fig. 2.11 The influence of the moving load velocity on the values of $\left|\tilde{Q}_{22}^{(2)}\right|$ and $\left|\tilde{Q}_{22}^{(1)}\right|$ (at $y_1/H^{(2)} = 0$) for various values of at $H^{(1)}/H^{(2)}$

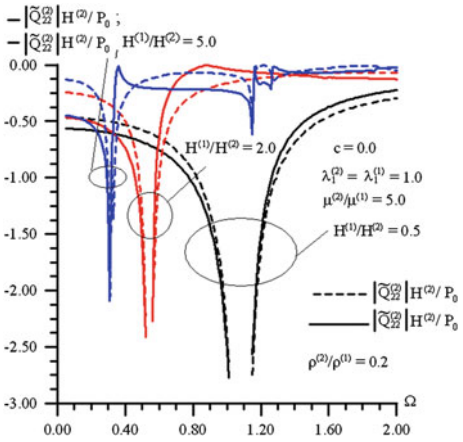

Fig. 2.12 The influence of the oscillating load frequency on the values of $\left|\tilde{Q}_{22}^{(2)}\right|$ and $\left|\tilde{Q}_{22}^{(1)}\right|$ (at $y_1/H^{(2)}=0$) for various values of $H^{(1)}/H^{(2)}$

$y_1/H^{(2)}=0$. Nevertheless, the distribution of the $\left|\tilde{Q}_{22}^{(2)}\right|$ and $\left|\tilde{Q}_{22}^{(1)}\right|$ remain symmetric with respect to the straight line $y_1/H^{(2)}=0$ for the case where $\Omega\times c\neq 0$.

Thus, taking the foregoing discussions into account, consider the numerical results which are attained in the case where $\mu^{(2)}/\mu^{(1)}=5.0$, $\rho^{(2)}/\rho^{(1)}=0.2$. First, we examine the case where the initial strains in the layers of the slab are absent, i.e. in the case where $\lambda_1^{(1)}=\lambda_1^{(2)}=1.0$, and investigate the dependence among the stresses $\tilde{Q}_{22}^{(2)}$ (at $y_2^{(2)}=-H^{(2)}/2$, $y_1=0$), $\tilde{Q}_{22}^{(1)}$ (at $y_2^{(1)}=-H^{(1)}/2$, $y_1=0$) and c under $\Omega=0$, as well as among the foregoing stresses and Ω under $c=0$. The graphs of these dependencies are given in Figs. 2.11 and 2.12 for various values of $H^{(1)}/H^{(2)}$.

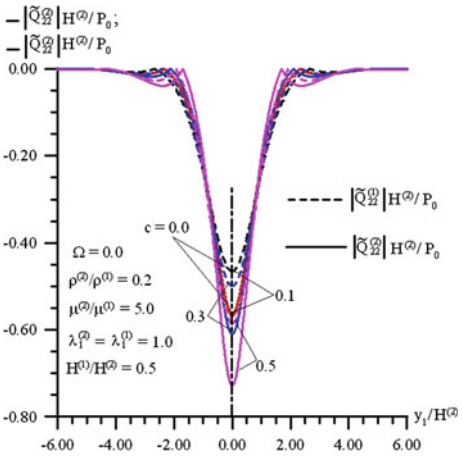

Fig. 2.13 The influence of the moving load velocity c on the distribution of $\left|\tilde{Q}_{22}^{(2)}\right|$ (at $y_2^{(2)}=-H^{(2)}/2$) with respect to $y_1/H^{(2)}$

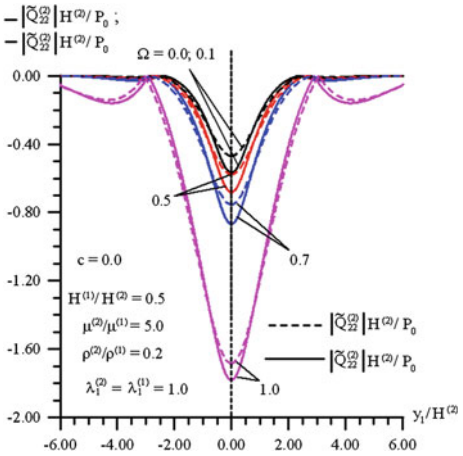

Fig. 2.14 The influence of the oscillating load frequency Ω on the distribution of $\left|\tilde{Q}_{22}^{(2)}\right|$ (at $y_2^{(2)} = -H^{(2)}/2$) with respect to $y_1/H^{(2)}$

It follows from the graphs given in Fig. 2.11 that the absolute values of the stresses $\tilde{Q}_{22}^{(2)}$ and $\tilde{Q}_{22}^{(1)}$ decrease with $H^{(1)}/H^{(2)}$. This result agrees well with the known mechanical considerations. At the same time, these graphs show that for all considered $H^{(1)}/H^{(2)}$ the absolute values of $\tilde{Q}_{22}^{(2)}$ and of $\tilde{Q}_{22}^{(1)}$ increase monotonically with c and $\left|\tilde{Q}_{22}^{(2)}\right|$; $\left|\tilde{Q}_{22}^{(1)}\right| \to \infty$ as $c \to c_{cr}$.

Figure 2.12 shows the resonance values of $\Omega(=\Omega_{res})$ and these values decrease with $H^{(1)}/H^{(2)}$. This decrease can be explained with the decrease in the "stiffness" of the considered system with $H^{(1)}/H^{(2)}$.

Taking the foregoing results into account, we consider the distribution of the stress $\tilde{Q}_{22}^{(2)}$ and $\tilde{Q}_{22}^{(1)}$ on the planes $y_2^{(2)} = -H^{(2)}/2$, $y_2^{(1)} = -H^{(1)}/2$ with respect to $y_1/H^{(2)}$ under $c < c_{cr}$ and $\Omega < \Omega_{res}$. The graphs of the distribution $-\left|\tilde{Q}_{22}^{(2)}\right|H^{(2)}/P_0$

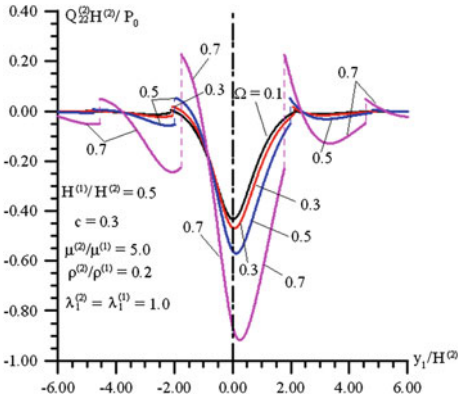

Fig. 2.15 The influence of the oscillating moving load frequency Ω on the distribution of the stress $Q_{22}^{(2)}$ (at $y_2^{(2)} = -H^{(2)}/2$, $\omega t = \pi/4$) with respect to $y_1/H^{(2)}$

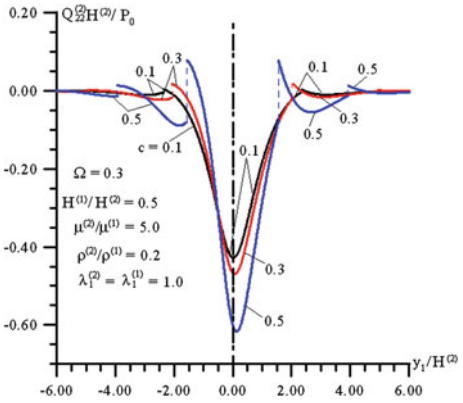

Fig. 2.16 The influence of the moving velocity c on the distribution of the stress $Q_{22}^{(2)}$ (at $y_2^{(2)} = -H^{(2)}/2$, $\omega t = \pi/4$) with respect to $y_1/H^{(2)}$

(at $y_2^{(2)} = -H^{(2)}/2$), $-\left|\tilde{Q}_{22}^{(1)}\right|H^{(2)}/P_0$ (at $y_2^{(1)} = -H^{(1)}/2$) with respect to $y_1/H^{(2)}$ are given in Figs. 2.13 and 2.14 for the case where $\Omega = 0$ and $c = 0$ respectively. It follows from these graphs that the absolute dominant values of the stresses $\left|\tilde{Q}_{22}^{(2)}\right|$ and $\left|\tilde{Q}_{22}^{(1)}\right|$ arise in the region for which $\left|y_1/H^{(2)}\right| \leq 1.0$ under $\Omega = 0.0$ and in the region $\left|y_1/H^{(2)}\right| \leq 2.0$ under $c = 0.0$. At the same time, these values increase monotonically with c and Ω.

Consider the case where $\Omega \times c \neq 0$ and assume that $\omega t = \pi/4$. Figure 2.15 shows the distribution of $Q_{22}^{(2)}H^{(2)}/P_0$ (at $y_2^{(2)} = -H^{(2)}/2$) with respect to $y_1/H^{(2)}$ under $c = 0.3$ for various Ω. The same graphs constructed under $\Omega = 0.3$ for various c are given in Fig. 2.16. It follows clearly from these graphs that the considered distributions are non-symmetric with respect to $y_1 = 0$. The violation of the mentioned symmetries becomes more considerable with Ω (Fig. 2.15) and with c (Fig. 2.16). Moreover, the graphs show that the values of jumps at the

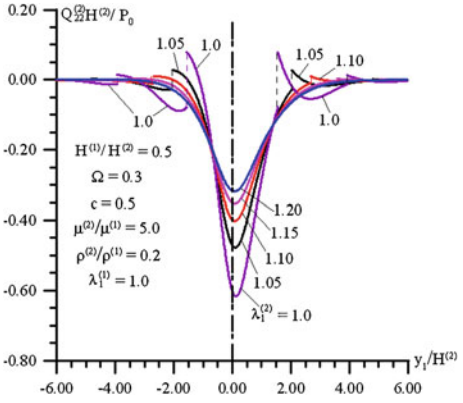

Fig. 2.17 The influence of the initial stretching of the upper layer of the slab, i.e. of the parameter $\lambda_1^{(2)}$ on the distribution of the stress $Q_{22}^{(2)}$ (at $y_2^{(2)} = -H^{(2)}/2$, $\omega t = \pi/4$) with respect to $y_1/H^{(2)}$

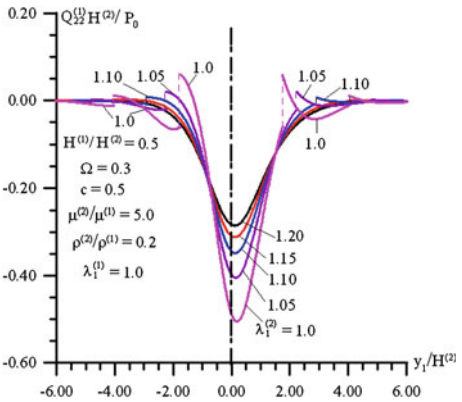

Fig. 2.18 The influence of the initial stretching of the lower layer of the slab, i.e. of the parameter $\lambda_1^{(1)}$ on the distribution of the stress $\tilde{Q}_{22}^{(2)}$ (at $y_2^{(2)} = -H^{(2)}/2$, $\omega t = \pi/4$) with respect to $y_1/H^{(2)}$

discontinuity points increase with Ω and c. In these cases the discontinuity point approaches a point at which the external load acts with Ω as well as with c.

The influence of the initial strain of the upper layer of the slab on the distribution of $Q_{22}^{(2)}H^{(2)}/P_0$ (at $y_2^{(2)} = -\lambda_2^{(2)}H^{(2)}/2$) and $Q_{22}^{(1)}H^{(2)}/P_0$ (at $y_2^{(1)} = -\lambda_2^{(1)}H^{(1)}/2$) with respect to $y_1/H^{(2)}$ is investigated. It is assumed that $\lambda_1^{(1)} = 1.0$. The graphs of these distributions are given in Figs. 2.17 and 2.18 for the stresses $Q_{22}^{(2)}$ and $Q_{22}^{(1)}$, respectively. The graphs show that the aforementioned dominant values of the stresses decrease with $\lambda_1^{(2)}$, i.e. with the initial strains on the upper layer of the slab. Moreover, the results show that the values of a jump in the discontinuity point also decrease with $\lambda_1^{(2)}$, i.e. with the initial strains on the upper layer of the slab. Moreover, the results show that the values of the jump at the discontinuity point also decrease with $\lambda_1^{(2)}$ and this point moves away from the point at which the external force acts. Similar results are also obtained for other values of the problem parameters.

2.4.6 Conclusions

From the results analyzed above the following conclusions have been reached:

- The values of the critical velocity c_{cr} of the oscillating moving load decrease with the thickness of the lower layer of the slab;
- The critical velocity arises only in the cases where the stiffness of the upper layer material is greater than that of the lower layer material. This conclusion agrees with the corresponding results obtained in Sect. 2.2 and in paper by Babich et al. (1986);

- As a result of the oscillation of the moving load, two types of critical velocity occur: one of them (denoted by c'_{cr}) is lesser, but the other one (denoted by c''_{cr}) is greater than the critical velocity attained for the case where the load moves without oscillation. This statement confirms in the qualitative sense the corresponding results obtained in papers by Dieterman and Metrikine (1997), Metrikine and Vrouwenvelder (2000);
- The initial stretching of the upper layer causes an increase in the values of c'_{cr} and c''_{cr}; however, the influence of the initial stretching of the lower layer on the values of c'_{cr} and c''_{cr} is non-monotonic;
- The values of the critical velocity $c'_{cr}\left(c''_{cr}\right)$ decrease (increase) with Ω, i.e. with the frequency of the oscillating moving load;
- The values of c'_{cr} and c''_{cr} decrease with the thickness of the lower layer of the slab and approach the corresponding values attained for the system consisting of a covering layer and half-plane;
- In the case where $c \neq 0$, $\Omega = 0$ (under $c < c_{cr}$) and in the case where $\Omega \neq 0$, $c = 0$ (under $\Omega < \Omega_{res}$), i.e. under action of the moving but non-oscillating load and under action of the oscillating but non-moving load, the dominant absolute values of the stresses $Q_{22}^{(2)}$ and $Q_{22}^{(1)}$ increase with c and Ω; at the same time, in these cases the distribution of the stresses $Q_{22}^{(2)}$ and $Q_{22}^{(1)}$ has no discontinuity and is symmetric with respect to the point $y_1/H^{(2)} = 0$;
- In the case where $\Omega \times c \neq 0$ (under $c < c_{cr}$ and $\Omega < \Omega_{res}$), i.e. in the case where the oscillating moving load acts on the bi-layered slab, the distribution of the stresses $Q_{22}^{(2)}$ and $Q_{22}^{(2)}$ with respect to $y_1/H^{(2)}$ have discontinuity point, the jumps arising at these points increase with c and Ω;
- In the case where $\Omega \times c \neq 0$ the foregoing symmetry of the distribution of the stresses $Q_{22}^{(2)}$ and $Q_{22}^{(1)}$ with respect to $y_1/H^{(2)}$ is violated. As a result of this violation the absolute maximum of considered stresses occurs ahead of the point $y_1/H^{(2)} = 0$;
- The values of Ω_{res}, $Q_{22}^{(2)}$ and $Q_{22}^{(1)}$ decrease with $H^{(1)}/H^{(2)}$ and approach the corresponding ones obtained for the system consisting of a covering layer and half-plane;
- The initial stretching of the upper layer of the slab causes a decrease in the absolute dominant values of the stresses $Q_{22}^{(2)}$ and $Q_{22}^{(1)}$;
- The values of the jump at the discontinuity points decrease and these points go away from the point $y_1/H^{(2)} = 0$ (Fig. 2.9) at which the external load acts with the initial stretching of the upper layer of the slab;
- The results regarding the influence of the initial strains in the upper layer on the values of the critical velocity agree, in the qualitative sense, with the corresponding ones attained in papers by Babich et al. (1986) and in Sect. 2.2. The influence of the initial stretching of the lower layer of the slab on the distribution of the considered stresses is insignificant. Therefore, the numerical results regarding these cases are not considered here.

2.5 Dynamics of a System Comprising a Pre-stressed Orthotropic Layer and Pre-stressed Orthotropic Half-Plane Under the Action of a Moving Load

In the previous sections it has been noted that the critical velocity of the moving load acting of the system consisting of a covering layer and half-space exists in the case where the covering layer material is stiffer than that of the half-space (or half-plane) material. As an example, a system comprising a stiffer layer and soft half-space can be used as a model to simulate an aircraft runway for which the shear modulus of the covering slab material is significantly greater than that for the underlying soil. At the same time, a system comprising a soft covering layer and stiffer half-space, for which the shear modulus of the covering layer material is less than that of the half-space, can be used as a model to simulate an asphalt road on rigid ground.

It should be noted that the foregoing determination of a system consisting of a stiffer layer and soft half-space or soft layer and stiffer layer and soft half-space or soft layer and stiffer half-space is not applicable in cases where the materials of the covering layer or of the half-space are orthotropic, because, in the latter case, there are six independent moduli of elasticity. Therefore, for cases where the materials of the covering layer or of the half-space are orthotropic, whether the system consists of a "stiffer covering layer and soft half-space" or "soft covering layer and stiffer half-space" must be indicated. In the present section within the 'stiffer covering layer and soft half-space" system, the modulus of elasticity of the covering layer material in the moving load direction is greater than that of the mechanical properties of the covering layer material and corresponding numerical results are presented for this case. These results illustrate the influence of the mechanical properties of the covering layer material and the influence of the initial stresses on the values of the moving load's critical velocity and on the stresses acting on the interface plane between the layer and half-plane. In this study, in a mathematical sense, a two-dimensional problem is solved.

The investigations carried out in the present section is based on a paper by Akbarov and Ilhan (2008).

2.5.1 Formulation of the Problem

Taking into consideration the initially stressed half-plane covered by the initially stressed layer, we determine the position of the points of the layer and half-plane by the Lagrangian coordinates in the Cartesian system of coordinates $Ox_1x_2x_3$ (Fig. 2.1). We assume that the layer and half-plane (before the contact) are stressed separately in the direction of the Ox_1 axis and in each of them the uniaxial homogeneous initial stress appears. Note that the covering layer and the half-plane occupy the covering layer and the half-plane occupy the regions $\{-h < x_2 < 0\}$

and $\{-\infty < x_2 < -h\}$, respectively under $\{-\infty < x_1; x_3 < \infty\}$. The direction of the Ox_3 axis is perpendicular to the figure plane and therefore is not shown in Fig. 2.1.

The values related to the layer and half-plane are denoted by the upper indices (1) and (2), respectively. Moreover, the values related to the initial stresses are denoted by the additional upper index 0.

The linearly elastic material of the layer and the half-plane are to be taken as homogeneous and orthotropic with the principal axes Ox_1, Ox_2 and Ox_3. We also assume that the layer and half-plane materials are moderately rigid and initial stress states in those have been determined within the scope of the classical linear theory of elasticity as in (2.1).

Assume that all the relations (except the elasticity relations in (2.4)) written in Sect. 2.2 take place also for the case under consideration. Therefore, we do not repeat here the equation of motion (2.3), strain-displacement relation (2.5), contact (2.11) (complete contact), (2.12) (contact with full slipping), and boundary conditions (2.10) and (2.13). We write here only the following elasticity relations for an orthotropic body under plane-strain state.

$$\begin{aligned} &\sigma_{11}^{(m)} = A_{11}^{(m)}\varepsilon_{11}^{(m)} + A_{12}^{(m)}\varepsilon_{22}^{(m)}, \sigma_{22}^{(m)} = A_{12}^{(m)}\varepsilon_{11}^{(m)} + A_{22}^{(m)}\varepsilon_{22}^{(m)}, \\ &\sigma_{12}^{(m)} = 2\mu^{(m)}\varepsilon_{12}^{(m)}, \end{aligned} \tag{2.113}$$

where

$$\begin{aligned} &A_{11}^{(m)} = \frac{a_{22}^{(m)}}{\det\left\|a_{ij}^{(m)}\right\|}, A_{12}^{(m)} = \frac{-a_{12}^{(m)}}{\det\left\|a_{ij}^{(m)}\right\|}, A_{22}^{(m)} = \frac{a_{11}^{(m)}}{\det\left\|a_{ij}^{(m)}\right\|}, \\ &a_{11}^{(m)} = \frac{1}{E_1^{(m)}}\left(1 - (\nu_{13}^{(m)})^2\frac{E_1^{(m)}}{E_3^{(m)}}\right), a_{12}^{(m)} = \frac{1}{E_2^{(m)}}\left(-\nu_{12}^{(m)} - \nu_{13}^{(m)}\nu_{23}^{(m)}\frac{E_2^{(m)}}{E_3^{(m)}}\right), \\ &a_{22}^{(m)} = \frac{1}{E_2^{(m)}}\left(1 - (\nu_{23}^{(m)})^2\frac{E_2^{(m)}}{E_3^{(m)}}\right). \end{aligned} \tag{2.114}$$

In (2.114) $E_1^{(m)}$, $E_2^{(m)}$ and $E_3^{(m)}$ are the modulus of elasticity of the mth material in the direction of the principal axes Ox_1, Ox_2 and Ox_3, respectively; $\mu_{12}^{(m)}$ is a shear modulus of the mth material in the Ox_1x_2 plane and $\nu_{12}^{(m)}$, $\nu_{13}^{(m)}$, $\nu_{21}^{(m)}$, $\nu_{23}^{(m)}$, $\nu_{31}^{(m)}$, and $\nu_{32}^{(m)}$ are the Poisson coefficients (Lekhnitskii 1981). Note that $\nu_{ij}^{(m)}$ characterizes the shortening (elongation) in the direction of the ith principal axis under stretching (compression) along the jth principal axis. Moreover, three of the six Poisson coefficients are independent ones, because, according to the symmetrical properties of the mechanical constants, the relations $\nu_{12}^{(m)}E_1^{(m)} = \nu_{21}^{(m)}E_2^{(m)}$, $\nu_{13}^{(m)}E_1^{(m)} = \nu_{31}^{(m)}E_3^{(m)}$ and $\nu_{23}^{(m)}E_2^{(m)} = \nu_{32}^{(m)}E_3^{(m)}$ must occur.

This completes the formulation of the problem. It should be noted that in the case where $\sigma_{11}^{(m)} = 0$ $(m = 1, 2)$ the problem formulation described above transforms into the corresponding one within the scope of the classical linear theory of elastodynamics for anisotropic (orthotropic) bodies.

2.5.2 Method of Solution

From Eqs. (2.113), (2.5) and (2.3) we obtain the following equations of motion in terms of displacement:

$$\mu_{12}^{(m)}\left(\frac{\partial^2 u_1^{(m)}}{\partial x_2^2}+\frac{\partial^2 u_2^{(m)}}{\partial x_1 \partial x_2}\right)+A_{11}^{(m)}\frac{\partial^2 u_1^{(m)}}{\partial x_1^2}+A_{12}^{(m)}\frac{\partial^2 u_2^{(m)}}{\partial x_1 \partial x_2}+\sigma_{11}^{(m)0}\frac{\partial^2 u_1^{(m)}}{\partial x_1^2}=\rho^{(m)}\frac{\partial^2 u_1^{(m)}}{\partial t^2},$$

$$\mu_{12}^{(m)}\left(\frac{\partial^2 u_1^{(m)}}{\partial x_1 \partial x_2}+\frac{\partial^2 u_2^{(m)}}{\partial x_1^2}\right)+A_{12}^{(m)}\frac{\partial^2 u_1^{(m)}}{\partial x_1 \partial x_2}+A_{22}^{(m)}\frac{\partial^2 u_2^{(m)}}{\partial x_2^2}+\sigma_{11}^{(m)0}\frac{\partial^2 u_2^{(m)}}{\partial x_1^2}=\rho^{(m)}\frac{\partial^2 u_2^{(m)}}{\partial t^2}. \quad (2.115)$$

By using the coordinate system (2.15) which moves with loading force and introducing the notation

$$c_{12}^{(m)}=\sqrt{\frac{\mu_{12}^{(m)}}{\rho^{(m)}}} \quad (2.116)$$

Equation (2.115) is transformed into the following one:

$$\begin{gathered}\left(\frac{A_{11}^{(m)}+\sigma_{11}^{(m)0}}{\mu_{12}^{(m)}}-\frac{V^2}{(c_{12}^{(m)})^2}\right)\frac{\partial^2 u_1^{(m)}}{\partial x_1^2}+\left(1+\frac{A_{12}^{(m)}}{\mu_{12}^{(m)}}\right)\frac{\partial^2 u_2^{(m)}}{\partial x_1 \partial x_2}+\frac{\partial^2 u_1^{(m)}}{\partial x_2^2}=0,\\ \left(1+\frac{\sigma_{11}^{(m)0}}{\mu_{12}^{(m)}}-\frac{V^2}{(c_{12}^{(m)})^2}\right)\frac{\partial^2 u_2^{(m)}}{\partial x_1^2}+\left(1+\frac{A_{12}^{(m)}}{\mu_{12}^{(m)}}\right)\frac{\partial^2 u_{21}^{(m)}}{\partial x_1 \partial x_2}+\frac{A_{22}^{(m)}}{\mu_{12}^{(m)}}\frac{\partial^2 u_2^{(m)}}{\partial x_2^2}=0\end{gathered} \quad (2.117)$$

In Eq. (2.117) the upper prim in x_1 and x_2 in (2.15) is omitted. In this case, the second boundary condition in (2.10) transforms to the condition (2.17) and the other conditions in (2.10), (2.13) are also valid for the new coordinate system (2.15).

Now we consider the solutions to Eq. (2.117). For this purpose we employ the exponential Fourier transform (2.18) in Eq. (2.117) and given the corresponding

boundary and contact conditions. As a result of this transformation we may obtain from (2.117) the following equation with respect to $u_{1F}^{(m)}(s,x_2)$ and $u_{2F}^{(m)}(s,x_2)$:

$$\begin{aligned} &\frac{d^2u_{1F}^{(m)}}{dx_2^2}+isb^{(m)}\frac{du_{2F}^{(m)}}{dx_2}-s^2a^{(m)}u_{1F}^{(m)}=0,\\ &d^{(m)}\frac{d^2u_{2F}^{(m)}}{dx_2^2}+isb^{(m)}\frac{du_{1F}^{(m)}}{dx_2}-s^2c^{(m)}u_{2F}^{(m)}=0, \end{aligned} \tag{2.118}$$

where

$$\begin{aligned} &i=\sqrt{-1},\quad a^{(m)}=\frac{A_{11}^{(m)}+\sigma_{11}^{(m)0}}{\mu_{12}^{(m)}}-\frac{V^2}{(c_{12}^{(m)})^2},b^{(m)}=\frac{A_{12}^{(m)}}{\mu_{12}^{(m)}}+1,\\ &c^{(m)}=1+\frac{\sigma_{11}^{(m)0}}{\mu_{12}^{(m)}}-\frac{V^2}{(c_{12}^{(m)})^2},d^{(m)}=\frac{A_{22}^{(m)}}{\mu_{12}^{(m)}}. \end{aligned} \tag{2.119}$$

We consider the case where the following inequalities are satisfied.

$$\begin{aligned} &V<\min\left\{c_{12}^{(1)}\sqrt{1+\frac{\sigma_{11}^{(1)0}}{\mu_{12}^{(1)}}};c_{12}^{(2)}\sqrt{1+\frac{\sigma_{11}^{(2)0}}{\mu_{12}^{(2)}}}\right\},\\ &\frac{A_{11}^{(m)}}{\mu_{12}^{(m)}}>1,\frac{A_{12}^{(m)}}{\mu_{12}^{(m)}}>1,\frac{A_{22}^{(m)}}{\mu_{12}^{(m)}}>1. \end{aligned} \tag{2.120}$$

The case determined by relation (2.120) is called the subsonic case.

Taking the relation (2.120) into account and making some mathematical manipulations, we obtain from Eqs. (2.118) and (2.119) the following expression for $u_{2F}^{(1)}$ and $u_{2F}^{(2)}$:

$$\begin{aligned} u_{2F}^{(1)}&=F_1^{(1)}e^{k_1^{(1)}x_2}+F_2^{(1)}e^{-k_1^{(1)}x_2}+F_3^{(1)}e^{k_2^{(1)}x_2}+F_4^{(1)}e^{-k_2^{(1)}x_2},\\ u_{2F}^{(2)}&=F_1^{(2)}e^{k_1^{(2)}x_2}+F_3^{(2)}e^{k_2^{(2)}x_2}, \end{aligned} \tag{2.121}$$

In (2.121) the notation

$$k_{1,2}^{(m)}=\sqrt{-\frac{A^{(m)}}{2}\pm\sqrt{\left(\frac{A^{(m)}}{2}\right)^2-B^{(m)}}} \tag{2.122}$$

is used, where

$$A^{(m)} = (-s^2 a^{(m)} d^{(m)} + s^2 (b^{(m)})^2 - s^2 c^{(m)} (d^{(m)})^{-1},$$
$$B^{(m)} = s^4 a^{(m)} c^{(m)} (d^{(m)})^{-1} \tag{2.123}$$

Thus, from (2.123), (2.118), (2.5) and (2.113) we have completely determined the Fourier transform of all sought values. For determination of the unknowns $F_1^{(1)}$, …, $F_4^{(1)}$, $F_1^{(2)}$ and $F_3^{(2)}$ which enter into these transformations, we obtain from boundary (2.10), (2.13), contact (2.11) (complete contact) and (2.12) (contact with full slipping) conditions corresponding closed system of algebraic equations in the form (2.27). From this algebraic equations we find the expression (2.28) for the aforementioned unknowns and, employing the inverse transform (2.29) we determine the sought stresses and displacements.

Employing the algorithm detailed in Sect. 2.2 we determine the critical velocity of the moving load and the stresses acting on the interface plane between the covering layer and half-plane.

2.5.3 Numerical Results and Discussions

Assume that the material of the half-plane is isotropic, i.e.

$$E_1^{(2)} = E_2^{(2)} = E_3^{(2)} = E^{(2)}, \quad \nu_{12}^{(2)} = \nu_{13}^{(2)} = \nu_{23}^{(2)} = \nu^{(2)},$$
$$\mu_{12}^{(2)} = \frac{E^{(2)}}{2(1+\nu^{(2)})}. \tag{2.124}$$

Taking the relations in (2.124) into account, we introduce the following notation

$$e_1 = \frac{E^{(2)}}{E_1^{(1)}}, \eta_1 = \frac{\sigma_{11}^{(1)0}}{E_1^{(1)}}, \eta_2 = \frac{\sigma_{11}^{(2)0}}{E_1^{(2)}}, \mu_1 = \frac{\mu_{12}^{(1)}}{E_1^{(1)}}. \tag{2.125}$$

Moreover, we assume that

$$\nu_{12}^{(1)} = \nu_{13}^{(1)} = \nu_{23}^{(1)} = 0.3, \nu^{(2)} = 0.3, \frac{\rho^{(2)}}{\rho^{(1)}} = 0.5. \tag{2.126}$$

In the present section we use the notation

$$c = \frac{V}{c_R^{(2)}} \tag{2.127}$$

for the dimensionless velocity c, where $c_R^{(2)}$ is a Rayleigh wave speed of a half-plane material. The critical velocity will be shown as $c_{cr} = V_{cr}/c_R^{(2)}$.

We will now analyze the graphs of the dependencies $c = c(sh)$ which were obtained from the solution to Eq. (2.30) in the case where the expression α_{nm} in this equation is determined according to the Eqs. (2.113), (2.121), (2.123) and (2.118) within the scope of the assumptions (2.124)–(2.127).

Thus, we analyze numerical results, according to which, we can conclude that the dependence $c = c(sh)$ in cases where $e_1(=E^{(2)}/E_1^{(1)}) > 1$ do not have any local maximum or minimum for which $dc/d(sh) = 0$. Such local maxima or minima arise only in cases where $e_1 < 1$, i.e. in cases where the modulus of elasticity of the covering layer material in the direction of the Ox_1 axis (Fig. 2.1) is greater than an elastic modulus of the half-plane material.

Figure 2.19 shows the graphs of $c = c(sh)$ in cases where $e_1 = 0.1$ (Fig. 2.19a) and $e_1 = 0.5$ (Fig. 2.19b) for various $E_2^{(1)}/E_1^{(1)}(=E_3^{(1)}/E_1^{(1)})$ given that $\mu_1 = 0.3846$, $\eta_1 = \eta_2 = 0$. Note that for $E_2^{(1)}/E_1^{(1)} = 1.0$ the considered values of the problem parameters correspond to the case where the material of the covering layer is also isotropic. We recall that this case was already considered in Sect. 2.2. However, in Sect. 2.2 the numerical results were presented with respect to the dimensionless velocity $c = V/c_2^{(1)}$, where $c_2^{(1)}$ is a shear wave velocity of the covering layer material, but in the present section the results are presented with respect to the dimensionless velocity (2.102). Nevertheless, the results obtained for $V = V(sh)$ obtained in the present section in the case where $E_2^{(1)}/E_1^{(1)} = 1.0$ and shown in Fig. 2.19 coincide with corresponding ones obtained in Sect. 2.2.

Note that the graphs shown in Fig. 2.19 are attained for complete contact condition (2.11). Such graphs are also attained for the contact with full slipping (2.12) but these graphs have not been shown here because they have the same character as the graphs given in Fig. 2.19, from which follows that in the case where $e_1 = 0.1$

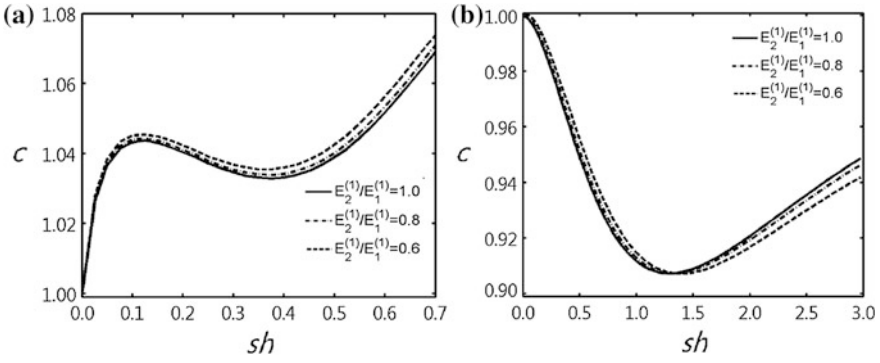

Fig. 2.19 The graphs of the dependencies between c and sh for various values of $E_2^{(1)}/E_1^{(1)} = E_3^{(1)}/E_1^{(1)}$ for $\mu_1 = 0.3846$, under completely contact conditions for the case where $\eta_1 = 0$, $\eta_2 = 0$, $e_1 = 0.1$ (**a**) and $e_1 = 0.5$ (**b**)

the dependencies $c = c(sh)$ have one local maximum and one local minimum, but in the case where $e_1 = 0.5$ these dependencies have only one local minimum. Using the considerations discussed in Sects. 2.2 and 2.3 with respect to definition of the critical velocity we find the critical velocity from the graphs given in Fig. 2.19. Consequently, according to Fig. 2.19, it can be concluded that the values of c_{cr} increase with decreasing $E_2^{(1)}/E_1^{(1)}$, i.e. with a decreasing in the modulus of elasticity of the covering layer material in the direction along its thickness. At the same time, the graphs given in Fig. 2.19 show that the values of c_{cr} increase with a decreasing e_1; i.e. for fixed values of the modulus of elasticity of the half-plane material as the modulus of elasticity along the load moving direction of the layer material increases the values of c_{cr} decrease.

Consider the comparison of the values of the critical velocity attained within the scope of the problem formulation presented in the present section with the corresponding ones attained in Sect. 2.2 and in a paper by Babich et al. (1986). This comparison is illustrated by data given in Table 2.17 which show the values of $V_{cr}/c_{12}^{(1)}$ (where $c_{12}^{(1)} = \sqrt{\mu_{12}^{(1)}/\rho^{(1)}}$) for various e_1. Under obtaining these data we assume that the materials of the covering layer and half-plane are isotropic. These results hold true for the correctness of the approach used, as well as the algorithm that PC programs have produced for this numerical investigation.

Table 2.17 The values of $V_{cr}/c_{12}^{(1)}$ for $\eta_1 = \eta_2 = 0$

e_1	Complete contact conditions (2.11)	Contact conditions with full slipping (2.12)
0.5	0.841 0.839	0.709 0.719
0.1	0.428 0.427	0.373 0.372

Upper (lower) numbers show the values $V_{cr}/c_{12}^{(1)}$ attained in the present section as well as in Sect. 2.2 (in paper by Babich et al. 1986). The case where the materials of the covering layer and half-plane are isotropic

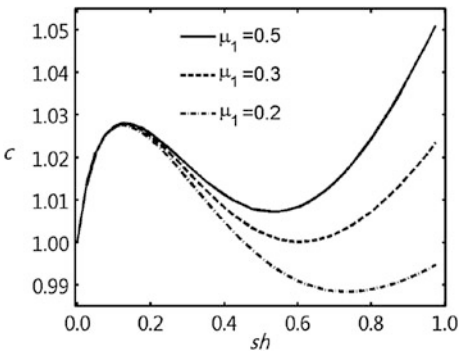

Fig. 2.20 The graphs of the dependencies between c (2.127) and sh for various values of μ_1 under complete contact conditions (2.11) for the case where $\eta_1 = 0$, $\eta_2 = 0$ and $e_1 = 0.2$

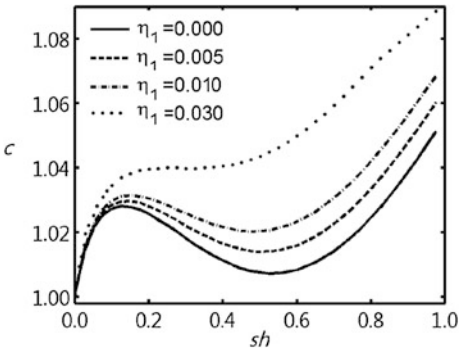

Fig. 2.21 The graphs of the dependencies between c (2.127) and sh for various values of η_1 for $\mu_1 = 0.5$ under complete contact conditions (2.11) for the case $\eta_2 = 0$ and $e_1 = 0.2$

Now, we consider some graphs of dependencies between c (2.127) and sh given in Fig. 2.20 and constructed for various μ_1 in the case where $\eta_1 = \eta_2 = 0$, $e_1 = 0.2$, $E_2^{(1)}/E_1^{(1)} = E_3^{(1)}/E_1^{(1)} = 0.5$. It follows from the graphs that the values of c_{cr} decrease with decreasing μ_1; i.e. the decrease of the shear modulus in the Ox_1x_2 plane of the covering layer material causes a decrease in the values of the critical velocity.

Also we consider the influence of the initial stretching strain of the covering layer on the behavior of the dependencies between c and sh. This influence is illustrated by the graphs given in Fig. 2.21 which are constructed for various η_1 in the case where $\eta_2 = 0$, $e_1 = 0.2$, $E_2^{(1)}/E_1^{(1)} = E_3^{(1)}/E_1^{(1)} = 0.5$ and $\mu_1 = 0.5$. It follows from the graphs that the initial stretching strain of the covering layer causes an increase in the values of c_{cr}.

Note that the foregoing type of numerical results are also obtained for many other values of the problem parameters. These results have been tabulated in Tables 2.18 and 2.19 from which it follows that the critical values of the moving load velocity is controlled mainly with a Rayleigh wave speed of the half-plane material. So that, for the change range considered of the values of the problem parameters the relations

$$0.95c_R^{(2)} < V_{cr} < 1.07c_R^{(2)} \quad \text{(for complete contact (2.11))} \tag{2.128}$$

$$0.81c_R^{(2)} < V_{cr} < 0.96c_R^{(2)} \quad \text{(for contact with full slipping (2.12))} \tag{2.129}$$

occur. Peat, organic clays and soft marine clays which can be taken as the half-plane materials have a Rayleigh wave velocity, as low as 120–200 km/h (see, for example, a paper by Madshus and Kaynia (2000)).

Consequently, in the foregoing and other similar cases numerical results obtained for the critical velocity of the moving load tabulated in Tables 2.18 and 2.19 have a realistic meaning. It should be noted that in a qualitative sense this

Table 2.18 The influence of the initial stretching strain of the covering layer (i.e. of the parameter η_1 under $\eta_1 > 0$) on the values of c_{cr} for the various μ_1, $E_2^{(1)}/E_1^{(1)}(=E_3^{(1)}/E_1^{(1)})$ in the case where $\eta_2 = 0$ under satisfying of the complete contact condition (2.11) (numerator) and contact condition with full slipping (2.12) (denominator)

μ_1	η_1	e_1					
		0.2			0.1		
		$E_2^{(1)}/E_1^{(1)}$					
		0.70	0.50	0.30	0.70	0.50	0.30
0.5	0.000	1.0038 0.8586	1.0073 0.8600	1.0157 0.8644	1.0356 0.9017	1.0378 0.9036	1.0430 0.9091
	0.005	1.0106 0.8677	1.0139 0.8693	1.0221 0.8736	1.0435 0.9140	1.0455 0.9160	1.0499 0.9206
	0.010	1.0170 0.8769	1.0203 0.8784	1.0279 0.8825	1.0501 0.9259	1.0518 0.9275	1.0553 0.9314
	0.030	1.0374 0.9097	1.0398 0.9113	– 0.9148	– 0.9641	– 0.9649	– 0.9671
0.3	0.000	0.9968 0.8545	1.0001 0.8560	1.0082 0.8602	1.0336 0.9003	1.0357 0.9022	1.0408 0.9073
	0.005	1.0046 0.8644	1.0078 0.8659	1.0156 0.8700	1.0419 0.9129	1.0440 0.9148	1.0485 0.9197
	0.010	1.0117 0.8739	1.0148 0.8753	1.0224 0.8795	1.0491 0.9248	1.0506 0.9267	1.0545 0.9305
	0.030	1.0352 0.9079	1.0377 0.9091	1.0430 0.9128	– 0.9638	– 0.9646	– 0.9670
0.2	0.000	0.9855 0.8491	0.9884 0.8504	– 0.8543	1.0305 0.8980	1.0326 0.9003	1.0381 0.9055
	0.005	0.9945 0.8595	0.9973 0.8608	– 0.8646	1.0399 0.9116	1.0418 0.9131	1.0465 0.9180
	0.010	1.0029 0.8696	1.0058 0.8708	– 0.8747	1.0477 0.9236	1.0493 0.9253	1.0533 0.9295
	0.030	1.0310 0.9052	1.0336 0.9064	– 0.9099	– 0.9634	– 0.9642	– 0.9667

concluding agree well with the experimental and theoretical results obtained by Madshus and Kaynia (2000).

In these tables the sign "–" indicates that in the corresponding case, the critical velocity does not exist. At the same time, it follows from these tables and from the relations (2.128) and (2.129) that the incompleteness (i.e. the full slipping of the contact between the constituents) of the contact conditions reduces significantly the values of the critical velocity. In the next subsection, the other conclusions reached on the basis of the data given in Tables 2.18 and 2.19.

Now we consider the distribution of the stresses acting on the interface plane between the covering layer and half-plane. The numerical results show that the effect of the parameter μ_1 (i.e. the effect of shear modulus in the Ox_1x_2 plane) on the aforementioned stress distribution is more significant than that of the parameters $E_2^{(1)}/E_1^{(1)}$ and $E_3^{(1)}/E_1^{(1)}$. Therefore, while obtaining the numerical results (which

Table 2.19 The influence of the initial strain of the half-plane (i.e. of the parameter η_2) on the values of c_{cr} for the various μ_1, e_1 and $E_2^{(1)}/E(=E_3^{(1)}/E_1^{(1)})$ in the case where $\eta_1 = 0$ under satisfying of the complete contact condition (2.11) (numerator) and contact condition with full slipping (2.12) (denominator)

μ_1	η_2	e_1					
		0.2			0.1		
		$E_2^{(1)}/E_1^{(1)}$					
		0.70	0.50	0.30	0.70	0.50	0.30
0.3	0.030	1.0219 0.8829	1.0252 0.8838	1.0334 0.8878	1.0649 0.9331	1.0672 0.9354	1.0732 0.9410
	0.010	1.0055 0.8641	1.0090 0.8655	1.0170 0.8697	1.0442 0.9114	1.0466 0.9137	1.0521 0.9188
	0.005	1.0013 0.8595	1.0046 0.8608	1.0126 0.8650	1.0389 0.9058	1.0413 0.9080	1.0464 0.9131
	−0.005	0.9924 0.8497	0.9957 0.8512	1.0039 0.8554	1.0281 0.8946	1.0302 0.8963	1.0353 0.9016
	−0.010	0.9879 0.8447	0.9912 0.8462	0.9992 0.8504	1.0223 0.8886	1.0244 0.8905	1.0296 0.8958
	−0.030	0.9688 0.8242	0.9719 0.8257	0.9798 0.8301	0.9991 0.8643	1.0012 0.8662	1.0057 0.8713
0.2	0.030	1.0079 0.8758	1.0106 0.8769	0.8948 0.8805	1.0609 0.9310	1.0633 0.9331	1.0696 0.9390
	0.010	0.9932 0.8584	0.9961 0.8595	0.8948 0.8635	1.0411 0.9093	1.0432 0.9114	1.0489 0.9168
	0.005	0.9893 0.8538	0.9922 0.8549	0.8948 0.8590	1.0357 0.9037	1.0380 0.9058	1.0435 0.9112
	−0.005	0.9814 0.8444	0.9845 0.8457	— 0.8496	1.0251 0.8924	1.0272 0.8945	1.0327 0.8996
	−0.010	0.9774 0.8396	0.9803 0.8410	— 0.8450	1.0195 0.8867	1.0218 0.8890	1.0270 0.8938
	−0.030	0.9600 0.8198	0.9630 0.8211	— 0.8253	0.9969 0.8631	0.9990 0.8648	1.0037 0.8698

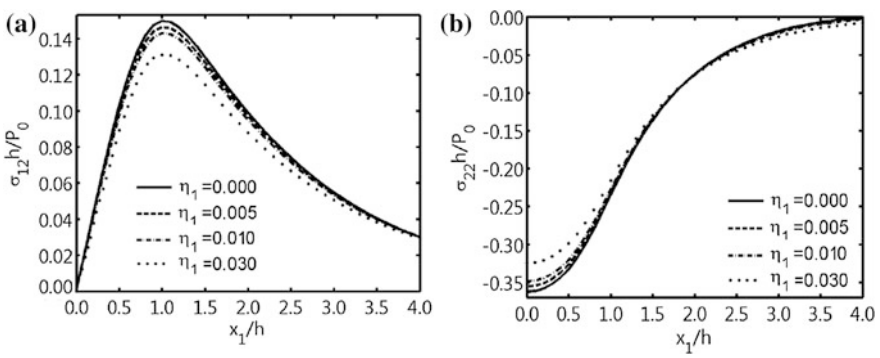

Fig. 2.22 Distribution of the stress on the interface plane with respect to x_1/h for various values of η_1 for $\mu_1 = 0.5$, $c = 0.4$, under complete contact conditions (2.11) for the case where $\eta_2 = 0$, $e = 0.2$. **a** Shear stress $\sigma_{12}(x_1)$; **b** normal stress $\sigma_{22}(x_1)$

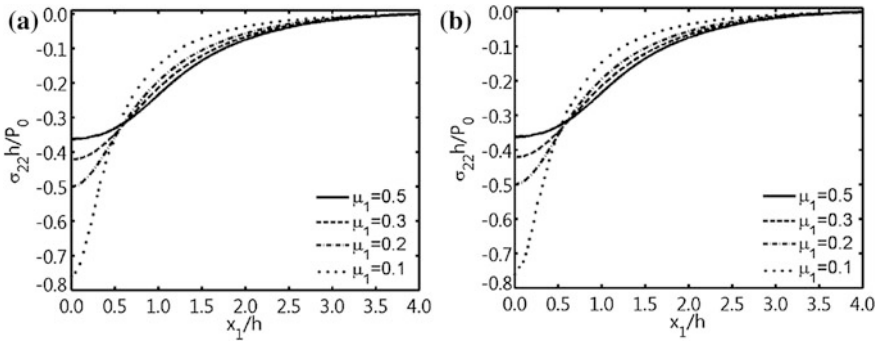

Fig. 2.23 Distribution of the normal stress $\sigma_{22}(x_1)$ on the interface plane with respect to x_1/h for various values of μ_1 for the case where $\eta_1 = 0$, $\eta_2 = 0$, $e_1 = 0.2$ and $c = 0.4$. Complete contact conditions (**a**); incomplete contact conditions (**b**)

will be discussed below) it is assumed that $E_2^{(1)}/E_1^{(1)} = E_3^{(1)}/E_1^{(1)} = 0.5$. Moreover, unless otherwise indicated, it is also assumed that $e_1 = 0.2$, $\eta_1 = \eta_2 = 0$ and $c = 0.4$.

The graphs in Fig. 2.22 show the influence of the initial stretching strain of the covering layer on the distribution of the stresses $\sigma_{12}(=\sigma_{12}^{(1)}(x_1,-h) = \sigma_{12}^{(2)}(x_1,-h))$ (Fig. 2.22a) and $\sigma_{22}(=\sigma_{22}^{(1)}(x_1,-h) = \sigma_{22}^{(2)}(x_1,-h))$ (Fig. 2.22b) for $\mu_1 = 0.5$. According to these graphs, we can conclude that the initial stretching strain of the covering layer causes the absolute values of the stresses to decrease.

Figure 2.23 shows the distribution of the stress $\sigma_{22}(x_1)$ for the complete (2.11) (Fig. 2.23a) and incomplete (2.12) (Fig. 2.23b) contact conditions for various μ_1. It follows from these graphs that in the vicinity of the point $x_1/h = 0$ the absolute values of σ_{22} increase with a decreasing μ_1. Moreover, these graphs show that the influence of the incompleteness of the contact conditions on the distribution of the

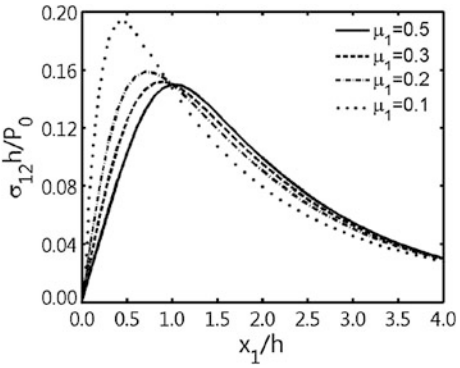

Fig. 2.24 Distribution of the shear stress $\sigma_{12}(x_1)$ on the interface plane with respect to x_1/h for various values of μ_1 under complete contact conditions (2.11) for the case where $\eta_1 = 0$, $\eta_2 = 0$, $e_1 = 0.2$ and $c = 0.4$

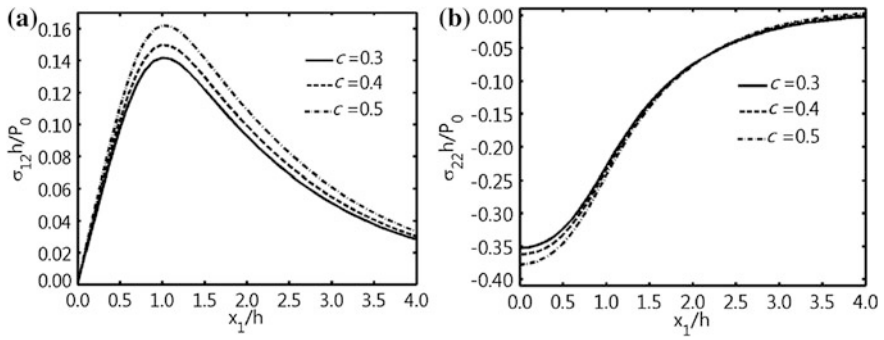

Fig. 2.25 Distribution of the stress on the values on the interface plane with respect to x_1/h for various values of c for $\mu_1 = 0.5$, under completer contact conditions for the case where $\eta_1 = 0$, $\eta_2 = 0$ and $e_1 = 0.2$. Shear stress $\sigma_{12}(x_1)$ (**a**); normal stress $\sigma_{22}(x_1)$ (**b**)

stress σ_{22} is insignificant in the qualitative as well as in the quantitative senses. Therefore, we prefer here to consider only one of the two types of contact conditions, namely the complete contact condition, for the stress distribution analyses.

The influence of μ_1 on the distribution of shear stress σ_{12} is illustrated by the graphs given in Fig. 2.24. In particular, it follows from these graphs that the point at which σ_{12} has its maximum approaches to the point $x_1/h = 0$ as μ_1 decreases.

Consider the influence of the moving load's velocity on the analyzed stress distribution. This influence is illustrated by the graphs given in Fig. 2.25 which show the distribution σ_{12} (Fig. 2.25a) and σ_{22} (Fig. 2.25b) with respect to x_1/h for various c when $\mu_1 = 0.5$. These graphs confirm that in the region where $|x_1/h| \leq 2.5$ the absolute values of σ_{22} increase with c. However, for $|x_1/h| > 2.5$ the absolute values of σ_{22} decrease with c. Note that while obtaining the data in the foregoing graphs it is assumed that $c < c_{cr}$.

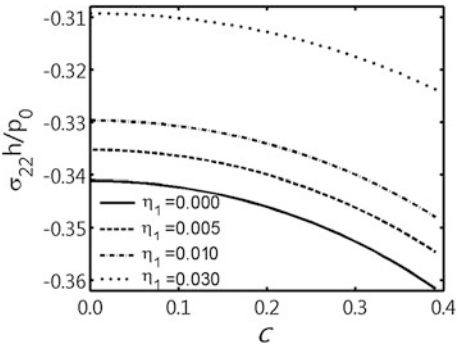

Fig. 2.26 The graphs of the dependencies between normal stress $\sigma_{22}(x_1)$ and c for various values of η_1 for $\mu_1 = 0.5$, under complete contact conditions for the case where $\eta_2 = 0$, $e_1 = 0.2$

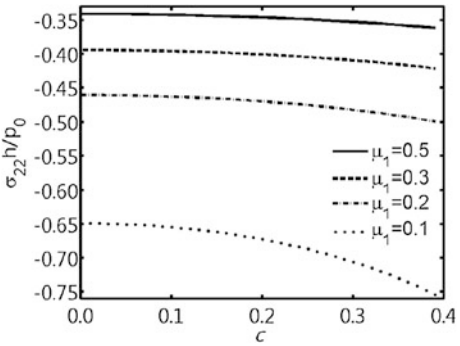

Fig. 2.27 The graphs of the dependencies between normal stress $\sigma_{22}(x_1)$ and c for various values of μ_1 under complete contact conditions for the case where $\eta_2 = 0$, $e_1 = 0.2$

Consider the dependencies between σ_{22} (at $x_1/h = 0.0$) and c. As noted above, the absolute values of all quantities (as well as the absolute values of σ_{22}) which characterize the mechanical behavior of the considered system approach infinity as $c \to c_{cr}$. Therefore, in the construction of these graphs, the values of c are increased up to near vicinity of c_{cr}.

The graphs of the aforementioned dependencies are given in Figs. 2.26 and 2.27. The results illustrated in Fig. 2.26 are attained for various η_1 under $\eta_2 = 0$, $\mu_1 = 0.5$. According to these graphs, we can conclude that the absolute values of σ_{22} (at $x_1/h = 0.0$) increase monotonously with c. In this case the existence of initial stretching strain in the covering layer causes the absolute values of σ_{22} to decrease.

The graphs given in Fig. 2.27 also show the dependencies between σ_{22} (at $x_1/h = 0.0$) and c. However, these graphs are constructed for various μ_1 and again confirm that the absolute values of σ_{22} (at $x_1/h = 0.0$) increase significantly as μ_1 decreases, in other words, as the shear modulus of the covering layer material decreases.

2.5.4 Conclusions

From the results analyzed above the following conclusions were reached:

- The critical velocity was only present in cases where $e_1 < 1$; in other words, the critical velocity arises in cases where the modulus of elasticity of the covering layer material in the moving direction of the external force is more than that of the half-plane material;
- The values of the critical velocity were controlled mainly with a Rayleigh wave velocity of the half-plane material, at the same time, the incompleteness of the contact conditions reduces significantly the values of this critical velocity;

- The values of the critical velocity increased with the modulus of elasticity of the covering layer material in the moving direction of the external force;
- The initial stretching strain of the covering layer and of the half-plane causes an increase in the values of the critical velocity;
- The initial compression strain of the half-plane results in a decrease in the critical velocity values;
- The values of the critical velocity decrease as μ_1 decreases, i.e., as shear modulus of the covering layer material decreases;
- The numerical results obtained for the critical velocity agree well both qualitatively and quantitatively with the known results attained in Sect. 2.2 and in papers by Babich et al. (1986), Madshus and Kaynia (2000);
- The values of $\max|\sigma_{22}|$ and $\max|\sigma_{12}|$ increase with moving load velocity, where $\sigma_{22}(\sigma_{12})$ is a normal (shear) stress acting on the interface plane between the covering layer and half-plane;
- The initial stretching of the covering layer causes to decrease the values of the foregoing stresses;
- The values of $\max|\sigma_{22}|$ and $\max|\sigma_{12}|$ increase with as shear modulus of the covering layer material (i.e. the values of μ_1) decreases.

2.6 Dynamics of a System Comprising on Orthotropic Layer and Orthotropic Half-Plane Under the Action of an Oscillating Moving Load

In the present section, according to papers by Akbarov and Ilhan (2009), Ilhan (2012), we consider a problem related to the dynamics of a system comprising a pre-stressed orthotropic layer and pre-stressed orthotropic half-plane under action of an oscillating moving load. In other words, in the present section we develop the investigation carried out in the previous section for the case where the amplitude of the moving load is time-depend harmonically.

The notation and assumptions accepted in the previous section occur also in the present section.

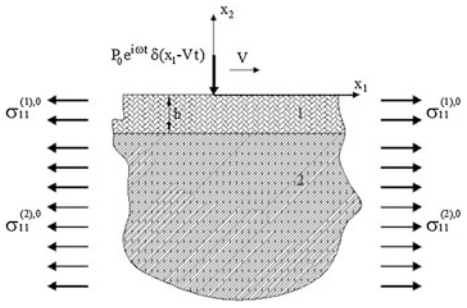

Fig. 2.28 The geometry of the structure of the pre-stressed half-plane covered by the pre-stressed layer

2.6.1 On the Formulation of the Problem and Solution Method

As noted above, the object of the investigation in the present section is the same one which is considered in the previous section and schematically shown in Fig. 2.28. At the same time, the notation, the equation of motion (2.3), the mechanical (2.113) and geometrical (2.5) relations, the contact (2.11) (complete contact), (2.12) (contact with full slipping), and boundary conditions (2.10) (with respect to $\sigma_{12}^{(1)}$) and (2.13) which are used in previous sections occur also in the present section. However the boundary condition with respect to $\sigma_{22}^{(1)}$ in (2.10) is changed and has the following form:

$$\sigma_{22}^{(1)}\Big|_{x_2=0} = -P_0 e^{i\omega t}\delta(x_1 - Vt) \tag{2.130}$$

By using the coordinate system (2.15) which moves with loading force and represent the sought values as $g\left(x_1', x_2', t\right) = \bar{g}\left(x_1', x_2'\right)e^{i\omega t}$ we obtain the following equation from Eqs. (2.3), (2.113) and (2.5) for the amplitude of the displacements:

$$\begin{aligned}
&\left(\frac{A_{11}^{(m)} + \sigma_{11}^{(m)0}}{\mu_{12}^{(m)}} - \frac{V^2}{\left(c_{12}^{(m)}\right)^2}\right)\frac{\partial^2 u_1^{(m)}}{\partial x_1^2} + \left(1 + \frac{A_{12}^{(m)}}{\mu_{12}^{(m)}}\right)\frac{\partial^2 u_2^{(m)}}{\partial x_1 \partial x_2} + \frac{\partial^2 u_1^{(m)}}{\partial x_2^2} \\
&\quad = -\frac{\omega^2}{\left(c_{12}^{(m)}\right)^2}u_1^{(m)} - i\frac{2V\omega}{\left(c_{12}^{(m)}\right)^2}\frac{\partial u_1^{(m)}}{\partial x_1}, \\
&\left(1 + \frac{\sigma_{11}^{(m)0}}{\mu_{12}^{(m)}} - \frac{V^2}{c_{12}^{(m)^2}}\right)\frac{\partial^2 u_2^{(m)}}{\partial x_1^2} + \left(1 + \frac{A_{12}^{(m)}}{\mu_{12}^{(m)}}\right)\frac{\partial^2 u_1^{(m)}}{\partial x_1 \partial x_2} + \frac{A_{22}^{(m)}}{\mu_{12}^{(m)}}\frac{\partial^2 u_2^{(m)}}{\partial x_2^2} \\
&\quad = -\frac{\omega^2}{\left(c_{12}^{(m)}\right)^2}u_2^{(m)} - i\frac{2V\omega}{\left(c_{12}^{(m)}\right)^2}\frac{\partial u_2^{(m)}}{\partial x_1}
\end{aligned} \tag{2.131}$$

where $c_{12}^{(m)}$ is determined through the expression (2.116).

In Eq. (2.131), the upper prime in x_1' and x_2', and over bar in $\bar{u}_1^{(m)}$ and $\bar{u}_2^{(m)}$ are omitted. In this case the boundary condition (2.130) is replaced by the following one:

$$\sigma_{22}^{(1)}\Big|_{x_2=0} = -P_0\delta(x_1) \tag{2.132}$$

As before, we introduce the dimensionless coordinates $\bar{x}_i = x_i/h$ and omit overbar in $\bar{x}_i$. For solution to the equations in (2.131), we employ the exponential Fourier transform (2.18) with respect to the x_1 coordinate. As a result of this transform, we obtain from (2.131) the following equation with respect to $u_{1F}^{(m)}(s, x_2)$ and $u_{2F}^{(m)}(s, x_2)$.

$$\frac{d^2u_{1F}^{(m)}}{dx_2^2}+isb^{(m)}\frac{du_{2F}^{(m)}}{dx_2}-s^2a^{(m)}u_{1F}^{(m)}=0,$$
$$d^{(m)}\frac{d^2u_{2F}^{(m)}}{dx_2^2}+isb^{(m)}\frac{du_{1F}^{(m)}}{dx_2}-s^2c^{(m)}u_{2F}^{(m)}=0, \tag{2.133}$$

where,

$$a^{(m)}=\frac{A_{11}^{(m)}+\sigma_{11}^{(m)0}}{\mu_{12}^{(m)}}-\frac{\omega^2h^2}{s^2\left(c_{12}^{(m)}\right)^2}+\frac{2V\omega h}{s\left(c_{12}^{(m)}\right)^2}-\frac{V^2}{\left(c_{12}^{(m)}\right)^2}$$
$$c^{(m)}=1+\frac{\sigma_{11}^{(m)0}}{\mu_{12}^{(m)}}-\frac{\omega^2h^2}{s^2\left(c_{12}^{(m)}\right)^2}+\frac{2V\omega h}{s\left(c_{12}^{(m)}\right)^2}-\frac{V^2}{\left(c_{12}^{(m)}\right)^2}, \tag{2.134}$$
$$d^{(m)}=\frac{A_{22}^{(m)}}{\mu_{12}^{(m)}},b^{(m)}=1+\frac{A_{12}^{(m)}}{\mu_{12}^{(m)}},i=\sqrt{-1},$$

We assume that the inequalities (2.120) are satisfied, i.e., the subsonic case is considered. Thus, taking the relation (2.120) into account and making some mathematical manipulations, we obtain from Eqs. (2.133) and (2.120) the expressions for $u_{1F}^{(m)}$ and $u_{2F}^{(m)}$ as in (2.121) and (2.122) in the case where $a^{(m)}$, $b^{(m)}$, $c^{(m)}$ and $d^{(m)}$ in (2.123) must be determined through the expressions in (2.134). We introduce the notation

$$\Omega=\frac{\omega h}{c_{12}^{(1)}} \tag{2.135}$$

and note that in the case where $\Omega=0$, which was considered in the previous section, the values of the $k_{12}^{(m)}$ determined by expressions (2.122), (2.123) and (2.134) are real numbers. But in the case where $\Omega>0$, the values of the $k_{12}^{(m)}$ can be real, pure imaginary and complex numbers. This statement follows from the expressions in (2.134), and complicates the solution procedure for the problem considered. Moreover, this statement complicates significantly the composition of the algorithm and PC programs needed to obtain the corresponding results. We recall that similar situations were also analyzed in Sect. 2.4.

Thus, within the noted above preparations by employing the procedure described in the previous sections, we obtain the algebraic system of equations in the form (2.27) for unknown constants in (2.96) from the above noted boundary and contact conditions. Finally, employing the algorithm detailed in Sect. 2.4 we determine the critical velocity of the oscillating moving load and the stresses and displacements are defined from the inverse Fourier transform

$$f(x_1, x_2) = \frac{1}{2\pi} \int\limits_{-\infty}^{+\infty} f_F(s, x_2) e^{isx_1} ds \tag{2.136}$$

Now we consider the calculation of the integral (2.136). In the case where $\Omega = 0$ or in the case where $V = 0$ the integral (2.136) can be reduced to the calculation of either of the integrals $1/\pi \int_0^{+\infty} f_F(s, x_2) \cos(sx_1) ds$ for $u_{2_F}^{(m)}$, $\sigma_{22}^{(m)}$, $\sigma_{11}^{(m)}$, or $1/\pi \int_0^{+\infty} f_F(s, x_2) \sin(sx_1) ds$ for $u_{1_F}^{(m)}$, $\sigma_{12}^{(m)}$. However, in the case where simultaneously $V > 0$ and $\Omega > 0$ this reduction is violated by the term $2V\omega h/s(c_{12}^{(m)})^2$ which enters the expression $a^{(m)}$ and $c^{(m)}$ in (2.134). Therefore in the latter case the calculation of the integral (2.136) must be done without the aforementioned reduction. Consequently, given the calculation of the integral (2.136) we must use the relation

$$\frac{1}{2\pi} \int\limits_{-\infty}^{+\infty} (\bullet) e^{isx_1} ds \approx \frac{1}{2\pi} \int\limits_{-S^*}^{+S^*} (\bullet) \cos(sx_1) ds + \frac{i}{2\pi} \int\limits_{-S^*}^{S^*} (\bullet) \sin(sx_1) ds. \tag{2.137}$$

The values of S^* in (2.137) are determined from the corresponding convergence criterion for the numerical results. At the same time, we use the following notation:

$$\begin{gathered}
\left\{\sigma_{ijc}^{(m)};\ u_{ic}^{(m)}\right\} = \frac{1}{2\pi} \int\limits_{-S^*}^{+S^*} \left\{\sigma_{ijc}^{(m)};\ u_{ic}^{(m)}\right\} \cos(sx_1) ds, \\
\left\{\sigma_{ijs}^{(m)};\ u_{is}^{(m)}\right\} = \frac{1}{2\pi} \int\limits_{-S^*}^{+S^*} \left\{\sigma_{ijs}^{(m)};\ u_{is}^{(m)}\right\} \sin(sx_1) ds, \\
\left\{\tilde{\sigma}_{22}^{(m)};\ \tilde{\sigma}_{11}^{(m)};\ \tilde{u}_2^{(m)}\right\} = \left\{\left|\tilde{\sigma}_{22}^{(m)}\right| e^{i\alpha_{22}^{(m)}};\ \left|\tilde{\sigma}_{11}^{(m)}\right| e^{i\alpha_{11}^{(m)}},\ \left|\tilde{u}_2^{(m)}\right| e^{i\alpha_2^{(m)}}\right\}, \\
\left\{\tilde{\sigma}_{12}^{(m)};\ \tilde{u}_1^{(m)}\right\} = \left\{i\left|\tilde{\sigma}_{12}^{(m)}\right| e^{i\alpha_{12}^{(m)}};\ i\left|\tilde{u}_1^{(m)}\right| e^{i\alpha_1^{(m)}}\right\}
\end{gathered} \tag{2.138}$$

where

$$\begin{gathered}
\left|\tilde{\sigma}_{ij}^{(m)}\right| = \sqrt{(\sigma_{ijc}^{(m)})^2 + (\sigma_{ijs}^{(m)})^2}, \left|\tilde{u}_i^{(m)}\right| = \sqrt{(u_{ic}^{(m)})^2 + (u_{is}^{(m)})^2}, \\
\tan\alpha_{ij}^{(m)} = \frac{\sigma_{ijs}^{(m)}}{\sigma_{ijc}^{(m)}}, \tan\alpha_i^{(m)} = \frac{u_{is}^{(m)}}{u_{ic}^{(m)}}
\end{gathered} \tag{2.139}$$

After the foregoing mathematical preparation, the true (real) values of the sought quantities are determined by the expressions

$$\left\{\sigma_{ij}^{(m)},\, u_i^{(m)}\right\} = \mathrm{Re}\left(\left\{\tilde{\sigma}_{ij}^{(m)},\, \tilde{u}_i^{(m)}\right\} e^{i\omega t}\right), \tag{2.140}$$

according to which, we can write the following expressions.

$$\begin{aligned}
&\sigma_{22}^{(m)} = \left|\tilde{\sigma}_{22}^{(m)}\right| \cos(\alpha_{22}^{(m)} + \omega t);\ \sigma_{11}^{(m)} = \left|\tilde{\sigma}_{11}^{(m)}\right| \cos(\alpha_{11}^{(m)} + \omega t),\\
&\sigma_{12}^{(m)} = -\left|\tilde{\sigma}_{12}^{(m)}\right| \sin(\alpha_{12}^{(m)} + \omega t);\ u_2^{(m)} = \left|\tilde{u}_2^{(m)}\right| \cos(\alpha_2^{(m)} + \omega t),\\
&u_1^{(m)} = -\left|\tilde{u}_1^{(m)}\right| \sin(\alpha_1^{(m)} + \omega t).
\end{aligned} \tag{2.141}$$

Note that similar expressions were also obtained in Sect. 2.4. Moreover, note that the remarks made in Sect. 2.4 on the Doppler Effect occur also for the problem under consideration.

Thus, we now consider the numerical results obtained within the framework of the solution discussed above and related to the influence of the oscillation frequency of the moving load and the mechanical properties of those on the values of the critical velocity and on the values of the displacements and stresses acting on the interface plane between the covering layer and half-plane.

2.6.2 Numerical Results and Discussions

First, we consider the case where the material of the half-plane is isotropic and the notation (2.124), (2.125) and (2.127) take place. Moreover, we assume that the relation (2.126) also takes place and, first, consider the case where the initial stresses in the constituents are absent, i.e. $\eta_1 = \eta_2 = 0.00$. We will now analyze the graphs of the dependence $c = c(sh)$ which was obtained from the equation (2.30) within the scope of the assumption (2.120). Note that the numerical results (not given here) show that, as in the case where an amplitude of the moving load is time independent, also in the case where the moving load amplitude is time-harmonic oscillating one the relation $c = c(sh)$ has a point at which $dc/d(sh) = 0$ occurs only for $e_1 < 1$.

Thus, we investigate the influence of the dimensionless frequency Ω (2.135) on the dependence $c = c(sh)$, consequently on the values of $c_{cr.}$ for various values of parameters e_1, $E_2^{(1)}/E_1^{(1)} (= E_3^{(1)}/E_1^{(1)})$ and μ_1 under $\eta_1 = \eta_2 = 0.00$.

It should be noted that in the case where $\Omega = 0.0$, which was analyzed in the previous section, taking the symmetry of the $\det\left\|\alpha_{nm}(V(sH^{(2)}))\right\|$ in Eq. (2.30) with respect to $sh = 0.0$ into account for analysis of the dependence $c = c(sh)$ it is sufficient to consider this dependence in the interval $0 \leq sh < +\infty$, only. But in the case where $\Omega > 0.0$, according to the Doppler Effect which arises through the term $2V\omega h/s(c_{12}^{(m)})^2$ which enters the expressions $a^{(m)}$ and $c^{(m)}$ in (2.124), this symmetry is violated. Therefore, in the case considered, i.e. in the case where $\Omega > 0.0$ the

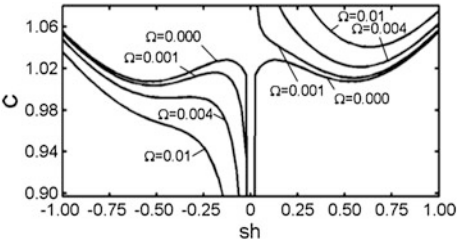

Fig. 2.29 The graphs of the dependencies between c and sh for various values of Ω for $e_1 = 0.2$, $E_2^{(1)}/E_1^{(1)} = 0.5$ and $\mu_1 = 0.5$ under complete contact condition (2.11) and under $\eta_1 = \eta_2 = 0.00$

Table 2.20 The influence of $E_2^{(1)}/E_1^{(1)}$ on the values of c'_{cr} and c''_{cr} for various values of e_1 in the case where $\mu_1 = 0.5$ and $\eta_1 = \eta_2 = 0.00$ under complete (2.11) (upper number) and incomplete (2.12) (lower number) contact conditions

e_1	$\frac{E_2^{(1)}}{E_1^{(1)}}$	$c'_{cr} \times 10^3$ ($\Omega \times 100$)			$c''_{cr} \times 10^3$ ($\Omega \times 100$)		
0.4	1.0	945(0.1) 794(0.1)	942(0.3) 775(1.5)	**915(1.8)** **719(4.9)**	976(2.0) 870(6.0)	1002(4.0) 882(7.0)	**1077(11.0)** **1078(28.3)**
	0.8	947(0.1) 794(0.1)	944(0.3) 774(1.5)	**917(1.8)** **718(4.9)**	970(2.0) 870(6.0)	1003(4.0) 882(7.0)	**10778(10.9)** **10776(27.8)**
	0.6	950(0.1) 792(0.1)	947(0.3) 772(1.5)	**920(1.8)** **714(5.0)**	980(2.0) 870(6.0)	1005(4.0) 882(7.0)	**10781(10.7)** **10776(27.2)**
	0.4	945(0.1) 794(0.1)	952(0.3) 769(1.5)	**925(1.9)** **709(5.1)**	985(2.0) 870(6.0)	1010(4.0) 882(7.0)	**10774(10.2)** **10776(26.0)**
0.3	1.0	971(0.1) 822(0.1)	966(0.3) 795(1.5)	**948(1.0)** **757(3.2)**	1013(2.0) 923(6.0)	1048(4.0) 938(7.0)	**10771(5.80)** **10777(17.8)**
	0.8	972(0.1) 822(0.1)	968(0.3) 795(1.5)	**950(1.0)** **756(3.2)**	1015(2.0) 924(6.0)	1050(4.0) 939(7.0)	**10774(5.70)** **10780(17.6)**
	0.6	975(0.1) 822(0.1)	971(0.3) 794(1.5)	**953(1.0)** **756(3.2)**	1018(2.0) 926(6.0)	1053(4.0) 941(7.0)	**10775(5.50)** **10779(17.2)**
	0.4	981(0.1) 823(0.1)	977(0.3) 794(1.5)	**959(1.0)** **754(3.2)**	1024(2.0) 930(6.0)	1060(4.0) 946(7.0)	**10779(5.10)** **10782(16.4)**
0.2	1.0	998(0.1) 855(0.1)	990(0.3) 811(1.5)	**986(0.4)** **803(1.7)**	1034(1.0) 1002(6.0)	1063(2.0) 1023(7.0)	**10758(2.50)** **10777(9.8)**
	0.8	999(0.1) 855(0.1)	991(0.3) 811(1.5)	**987(0.4)** **803(1.7)**	1036(1.0) 1004(6.0)	1064(2.0) 1025(7.0)	**10777(2.50)** **10765(9.6)**
	0.6	1000(0.1) 856(0.1)	994(0.3) 811(1.5)	**990(0.4)** **804(1.7)**	1038(1.0) 1007(6.0)	1067(2.0) 1029(7.0)	**10781(2.4)** **10773(9.4)**
	0.4	1007(0.1) 858(0.1)	999(0.3) 812(1.5)	**994(0.4)** **804(1.7)**	1044(1.0) 1015(6.0)	1074(2.0) 1037(7.0)	**10763(2.1)** **10773(8.9)**

analyses of the dependence $c = c(sh)$ must be done in the interval $-\infty < sh < +\infty$. For illustration of this statement we consider the graphs of noted dependence given in Fig. 2.29. These graphs are constructed under $e_1 = 0.2$, $E_2^{(1)}/E_1^{(1)} = 0.5$ and $\mu_1 = 0.5$ for various values of Ω under satisfying the complete contact condition (2.11).

It follows from this figure that the graphs constructed in the case where $\Omega = 0$ are symmetric with respect to the straight line determined by the equation $sh = 0.0$. However, this symmetry is violated for the graphs constructed under $\Omega > 0$. The analyses of the numerical results show that up to certain Ω (denoted by Ω') the values of "minimum" critical velocity (denoted by c'_{cr}) are determined by the left branches, i.e. by branches attained in the region $-\infty < sh < 0$. The following (by magnitude) values of the critical velocity (denoted by c''_{cr}) are determined by the right branches, i.e. by the branches attained in the region $0 < sh < +\infty$. In this case the values of $c'_{cr}(c''_{cr})$ decrease (increase) with Ω. Consequently, up to a certain value of the oscillation frequency (i.e. up to $\Omega = \Omega'$) of the moving load, as a result of the oscillation of this load, the critical velocity decreases. However, in the case where $\Omega > \Omega'$ the left branches of the graphs do not determine the critical velocity; in other words, on these branches, the point for which $dc/d(sh) = 0$ does not arise, but the right branches of the graphs determine the values of c_{cr} for the case where $\Omega > \Omega'$. But this procedure continues up to a certain value of Ω (denoted by Ω'') after which the values of c''_{cr} go outside of the framework of the subsonic moving regime.

We recall that the graphs given in Fig. 2.29 are attained for complete contact condition (2.11). Such graphs are also attained for the full slipping contact condition (2.12) but these graphs have not been shown here because they have the same character as the graphs in Fig. 2.29. Note that in this figure the graphs constructed under $\Omega = 0$ coincide with the corresponding ones obtained for the case considered in the previous section.

We continue to discuss the numerical results obtained in the case where $\Omega > 0$. Table 2.20 shows the values of c'_{cr} attained under $0.001 \le \Omega \le \Omega'$ as well as the values of c''_{cr} attained under $\Omega' \le \Omega \le \Omega''$. The results given in Table 2.20 are obtained under complete (2.11) (upper number) and incomplete-full slipping (2.12) (lower number) contact conditions for various values of the parameters e_1 and $E_2^{(1)}/E_1^{(1)}$ in the case where $\mu_1 = 0.5$. Note that in this table the values of Ω are written in parentheses. The values of Ω' and Ω'', and corresponding critical velocities c'_{cr} and c''_{cr} are written in bold. Within the same assumptions and notation the influence of the parameter μ_1 on the values of c'_{cr} and c''_{cr} under $e_1 = 0.2$, $E_2^{(1)}/E_1^{(1)} = 0.5$ are illustrated by data given in Table 2.21.

In Tables 2.20 and 2.21 the values of c''_{cr} corresponding to the $\Omega = \Omega''$ are near to each other, because these values of c''_{cr} almost coincide with $c_2^{(2)}/c_R^{(2)}$ ($\approx$1,0824) which is the upper limit for the velocity of the moving load in the considered cases, for the subsonic case determined by expression (2.120). Therefore the noted values of c''_{cr} do not depend on the mechanical parameters regarding the covering layer

Table 2.21 The influence of the μ_1 on the values of c'_{cr} and c''_{cr} in the case where $e_1 = 0.2$ and $E_2^{(1)}/E_1^{(1)} = 0.5$, $\eta_1 = \eta_2 = 0.00$ under complete (2.11) (upper number) and incomplete (2.12) (lower number)

μ_1	$c'_{cr} \times 10^3$ ($\Omega \times 100$)			$c''_{cr} \times 10^3$ ($\Omega \times 100$)		
0.5	1002(0.1) 856(0.1)	998(0.2) 845(0.5)	**988(0.5)** **803(1.9)**	1047(1.5) 951(4.0)	1059(2.0) 973(5.0)	**10780(2.8)** **10776(10.7)**
0.3	998(0.1) 854(0.1)	995(0.2) 845(0.5)	**981(0.7)** **799(2.3)**	1034(1.5) 934(4.0)	1044(2.0) 952(5.0)	**10766(3.7)** **10771(13.2)**
0.2	987(0.1) 849(0.1)	985(0.2) 842(0.5)	**964(1.3)** **794(0.30)**	1012(1.5) 911(4.0)	1019(2.0) 924(5.0)	**10774(6.9)** **10776(19.5)**

material. However, the values of Ω'' depend significantly on the values of these parameters.

The results tabulated in Tables 2.20 and 2.21 show that the values of the critical velocity of the moving load in the case where $0 \le \Omega \le \Omega'$ as well as in the case where $\Omega' \le \Omega \le \Omega''$ are controlled with a Rayleigh wave speed of the half-plane material. So that, for the change in range considered for the values of the problem parameters, the following relations occur.

For complete contact condition (2.11):

$$\begin{aligned} 0.915\, c_R^{(2)} \le V'_{cr} \le 1.007\, c_R^{(2)},\ V'_{cr} = c'_{cr} c_R^{(2)},\ 0.001 \le \Omega \le \Omega' = 0.019, \\ 0.976\, c_R^{(2)} \le V''_{cr} \le 1.078\, c_R^{(2)},\ V''_{cr} = c''_{cr} c_R^{(2)},\ 0.02 \le \Omega \le \Omega'' = 0.069, \end{aligned} \tag{2.142}$$

For incomplete contact condition with full slipping (2.12):

$$\begin{aligned} 0.719\, c_R^{(2)} \le V'_{cr} \le 0.858\, c_R^{(2)},\ 0.001 \le \Omega \le \Omega' = 0.051, \\ 0.870\, c_R^{(2)} \le V''_{cr} \le 1.078\, c_R^{(2)},\ 0.04 \le \Omega \le \Omega'' = 0.283. \end{aligned} \tag{2.143}$$

Peat, organic clays and soft marine clays which can be taken as the half-plane materials have a Rayleigh wave velocity as low as 120−200 km/h (see, for example, a paper by Madshus and Kaynia (2000)). Consequently, in the foregoing and other similar cases, numerical results obtained for the critical velocity of the moving load and tabulated in Tables 2.20 and 2.21 have realistic meaning. It should be noted that in a qualitative sense this conclusions is in the agreement with the experimental and theoretical results obtained by Madshus and Kaynia (2000). Moreover, if we consider the case where the thickness of the covering layer $h \sim (10^{-2}$ to $1)$ m and $c_{12}^{(1)} \sim (10^3$ to $10^4)$ m/s, then according to the relation $\omega h = c_{21}^{(1)} \Omega$ we obtain that $\omega \sim (10$ to $10^4)$ Hz. According to Degrande and Schillemans (2001), the oscillation frequency of modern high-speed trains is in the region of 10−200 Hz. Consequently, the considered values of Ω, or the values attained for Ω' and Ω'' have also realistic meaning.

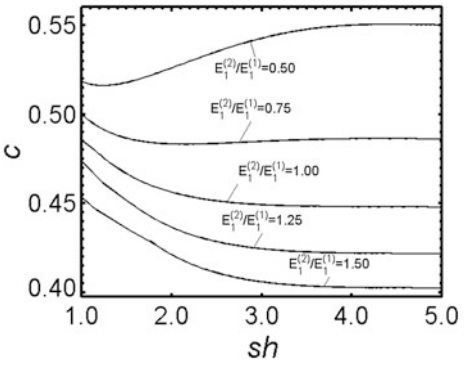

Fig. 2.30 The graphs of the dependencies between c and sh for various $E_1^{(2)}/E_1^{(1)}(=e_1)$ for $E_2^{(1)}/E_1^{(1)} = 0.5$, $E_2^{(2)}/E_1^{(2)} = 0.5$, $\mu_1 = 0.5$, $\mu_2 = 0.5$, under complete contact condition (2.11) for the case where $\eta_1 = \eta_2 = 0.00$

It follows from the relations (2.142) and (2.143) and from the foregoing tables that the full slipping incompleteness of the contact conditions reduces the lower limit of the values of V'_{cr} and V''_{cr}, but increases the upper limit of the values of Ω, namely the values of Ω''. Moreover, it follows from the foregoing tables that in the considered range of the problem parameter, the values of $V'_{cr}(V''_{cr})$ decrease (increase) with the oscillating frequency (i.e. with Ω) of the moving load.

In the all previous investigations related to the case where it was assumed that the materials of the constituents are orthotropic, the concrete numerical results have been presented for the case where the material of the half-plane is an isotropic. Now we consider numerical results related to the case where not only the material of the covering layer is orthotropic, but also the material of the half-plane is orthotropic. Introduce new notation

$$\mu_2 = \frac{\mu_{12}^{(2)}}{E_1^{(2)}}, c = \frac{V}{c_{12}^{(2)}} \tag{2.144}$$

and assume that

$$E_2^{(2)}\Big/E_1^{(2)} = E_3^{(2)}\Big/E_1^{(2)}, v_{12}^{(2)} = v_{13}^{(2)} = v_{23}^{(2)} = 0.3, \rho^{(2)}\Big/\rho^{(1)} = 0.35. \tag{2.145}$$

Analyze the graphs of the dependencies $c = c(sh)$ and first, we consider the numerical results obtained in the case where $\Omega = 0$. Figure 2.30 shows the graphs of $c = c(sh)$ for complete contact condition (2.11) for various values of $E_1^{(2)}/E_1^{(1)}(=e_1)$ in the case where $\mu_1 = 0.5$, $\mu_2 = 0.5$, $E_2^{(1)}/E_1^{(1)} = 0.5$, $E_2^{(2)}/E_1^{(2)} = 0.5$, given that $\eta_1 = 0$, $\eta_2 = 0$. It follows from Fig. 2.30 that in the case where $e_1 \geq 1$ the dependencies $c = c(sh)$ do not have any local maximum or minimum for which $dc/d(sh) = 0$. Such local maximum or minimum arise only in

the case where $e_1 < 1$, i.e. in the case where the modulus of elasticity of the covering layer material in the direction of the Ox_1 (Fig. 2.28) axis is greater than that for the half-plane material. At the same time, these graphs show that the values of critical velocity c_{cr} increase with increasing e_1, i.e. for fixed values of the modulus of elasticity of the covering layer material as the modulus of elasticity of the half-plane material increases along the load moving direction, the values of c_{cr} increase.

We now analyze the graphs of the $c = c(sh)$ constructed in the case where $\Omega \neq 0$. As noted above, in this case the branches attained for $-\infty < sh < 0$ and for $0 < sh < +\infty$ of these graphs are not symmetric with respect to $sh = 0.0$ as shown in Fig. 2.29. As we here consider the case where $\Omega = 0.04$ for which the mentioned left branch has not any minimum or maximum, therefore we will analyze only the graphs of the $c = c(sh)$ constructed for $0 < sh < +\infty$.

Thus, we consider graphs given in Figs. 2.31, 2.32, 2.33 and 2.34 which are constructed under $e_1 = 0.2$, $\mu_1 = 0.5$, $\mu_2 = 0.5$, $E_2^{(1)}/E_1^{(1)} = 0.5$, $E_2^{(2)}/E_1^{(2)} = 0.5$ and $\eta_1 = 0$, $\eta_2 = 0$ unless otherwise stated. The values to ratios of the elastic constants are taken according to Schwartz (1992) and correspond to the real engineering materials. According to definitions of the critical velocity and the graphs given in Fig. 2.31, it can be concluded that the values of c_{cr} increase with increasing $E_2^{(1)}/E_1^{(1)}$, i.e., with a decrease in the modulus of elasticity of the covering layer in the direction along its thickness. Figure 2.32 displays the effect of $E_2^{(2)}/E_1^{(2)}$ on the critical velocities. The values of c_{cr} increase with $E_2^{(2)}/E_1^{(2)}$, i.e., with an increase in the modulus of elasticity of the half-plane material in the direction along its depth. Figures 2.33 and 2.34 show the effect of parameters μ_1 and μ_2 respectively (i.e. the effect of shear modulus of the covering layer and half-plane materials respectively in the Ox_1x_2 plane) on the critical velocity. The solid (dashed) lines in these figures correspond to the complete contact condition (2.11) (to the incomplete contact with full slipping (2.12)). It follows from these figures

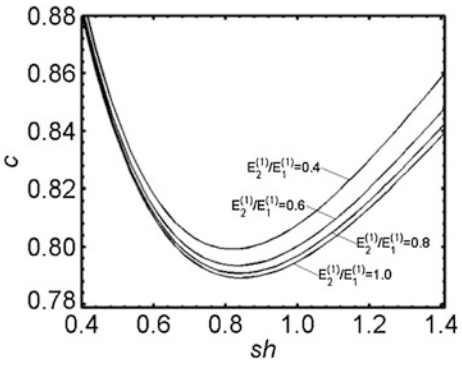

Fig. 2.31 The graphs of the $c = c(sh)$ constructed for various values of $E_2^{(1)}/E_1^{(1)}$ for $e_1 = 0.2$, $E_2^{(2)}/E_1^{(2)} = 0.5$, $\mu_1 = 0.5$, $\mu_2 = 0.5$ and $\eta_1 = 0$, $\eta_2 = 0$. Complete contact condition (2.11)

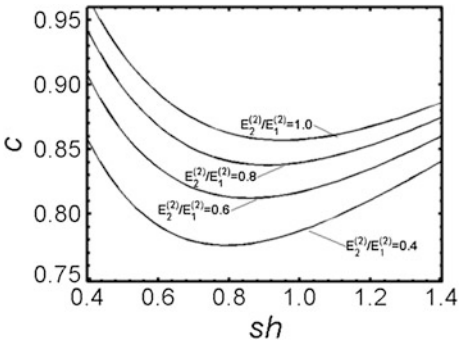

Fig. 2.32 The graphs of the $c = c(sh)$ constructed for various values of $E_2^{(2)}/E_1^{(2)}$ for $e_1 = 0.2$, $E_2^{(1)}/E_1^{(1)} = 0.5$, $\mu_1 = 0.5$, $\mu_2 = 0.5$ and $\eta_1 = 0$, $\eta_2 = 0$. Complete contact condition (2.11)

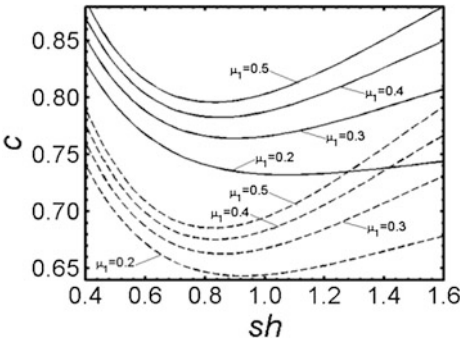

Fig. 2.33 The graphs of the $c = c(sh)$ constructed for various values of μ_1 for $e_1 = 0.2$, $\mu_2 = 0.5$, $E_2^{(2)}/E_1^{(2)} = 0.5$, $E_2^{(1)}/E_1^{(1)} = 0.5$, $\eta_1 = 0$, $\eta_2 = 0$ under complete contact conditions (2.11) (*solid lines*) and incomplete contact conditions with full slipping (2.12) (*dashed lines*)

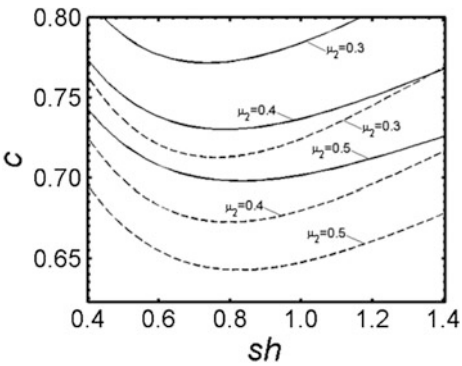

Fig. 2.34 The graphs of the $c = c(sh)$ constructed for various values of μ_2 for $e_1 = 0.2$, $\mu_1 = 0.5$, $E_2^{(2)}/E_1^{(2)} = 0.5$, $E_2^{(1)}/E_1^{(1)} = 0.5$, $\eta_1 = 0$, $\eta_2 = 0$ under complete contact conditions (2.11) (*solid lines*) and incomplete contact conditions with full slipping (2.12) (*dashed lines*)

that the critical velocity increase with increasing (decreasing) μ_1 (μ_2), i.e. with increasing (decreasing) the shear modulus $\mu_{12}^{(1)}$ ($\mu_{12}^{(2)}$) for fixed values of the modulus of elasticity $E_1^{(1)}$ ($E_1^{(2)}$) or with decreasing (increasing) of the modulus of elasticity $E_1^{(1)}$ ($E_1^{(2)}$) for fixed values of the shear modulus $\mu_{12}^{(1)}$ ($\mu_{12}^{(2)}$).

For a wide range of values of the problem parameters, numerical results are found for the critical velocity. These results are given in Tables 2.22, 2.23, 2.24. Table 2.22 shows the influence of the initial stress of the covering layer and half-plane on the values of c_{cr} for the various values of Ω for the case where $\mu_1 = \mu_2 = 0.5$, $E_2^{(2)}/E_1^{(2)} = E_2^{(1)}/E_1^{(1)} = 0.5$ under complete (2.11) (upper number) and incomplete (2.12) (lower number) contact conditions.

Table 2.22 The influence of the initial stress of the covering layer and half-plane on the values of c_{cr} for various values of Ω for the case where $\mu_1 = \mu_2 = 0.5$, $E_2^{(2)}/E_1^{(2)} = E_2^{(1)}/E_1^{(1)} = 0.5$ and $\rho^{(2)}/\rho^{(1)} = 0.35$ under complete (2.11) (upper number) and incomplete (2.12) (lower number) contact conditions contact conditions

e_1	η_1	η_2	Ω				
			0.00	0.04	0.08	0.16	0.20
0.5	0.010	0.000	0.6419 0.5338	0.6675 0.5623	0.6902 0.5888	0.7289 0.6369	0.7455 0.6590
	0.005	0.000	0.6371 0.5284	0.6626 0.5567	0.6851 0.5832	0.7239 0.6313	0.7405 0.6533
	0.000	0.000	0.6323 0.5227	0.6576 0.5511	0.6801 0.5775	0.7188 0.6255	0.7354 0.6475
	0.000	0.010	0.6342 0.5258	0.6592 0.5539	0.6815 0.5800	0.7197 0.6276	0.7361 0.6494
	0.000	0.005	0.6333 0.5243	0.6585 0.5525	0.6342 0.5258	0.7192 0.6266	0.7358 0.6485
	0.000	−0.005	0.6313 0.5212	0.6569 0.5597	0.6795 0.5761	0.7184 0.6244	0.7351 0.6466
	0.000	−0.01	0.6303 0.5196	0.6560 0.5482	0.6788 0.5749	0.7179 0.6233	0.7348 0.6455
0.3	0.010	0.000	0.7021 0.5934	0.7495 0.6409	0.7904 0.6839	0.8602 0.7591	0.8906 0.7930
	0.005	0.000	0.6956 0.5862	0.7427 0.6334	0.7835 0.6759	0.8532 0.7513	0.8835 0.7852
	0.000	0.000	0.6890 0.5787	0.6956 0.5862	0.6956 0.5862	0.6956 0.5862	0.6956 0.5862
	0.000	0.010	0.6920 0.5831	0.7384 0.6295	0.7787 0.6715	0.8477 0.7464	0.8779 0.7801
	0.000	0.005	0.6905 0.5809	0.7371 0.6276	0.7776 0.6698	0.8469 0.7450	0.8773 0.7788
	0.000	−0.005	0.6874 0.5766	0.7345 0.6237	0.7754 0.6663	0.8452 0.7419	0.8758 0.7761
	0.000	−0.01	0.6859 0.5742	0.7332 0.6217	0.7742 0.6645	0.8443 0.7404	0.8750 0.7747

Table 2.23 The influence of $E_2^{(1)}/E_1^{(1)}$ and $E_2^{(2)}/E_1^{(2)}$ on the values c_{cr} for the various e_1 in the case where $\mu_1 = \mu_2 = 0.5$, $\Omega = 0.04$ and $\eta_1 = 0$, $\eta_2 = 0$ under complete (2.11) (upper number) and incomplete (2.12) (lower number) contact conditions

e_1	$\frac{E_2^{(1)}}{E_1^{(1)}}$	$\frac{E_2^{(2)}}{E_1^{(2)}}$			
		1.0	0.8	0.6	0.4
0.3	1.0	0.7899 0.6679	0.7714 0.6530	0.7469 0.6350	0.7121 0.6138
	0.8	0.7902 0.6674	0.7721 0.6530	0.7479 0.6350	0.7134 0.6141
	0.6	0.7908 0.6667	0.7733 0.6524	0.7495 0.6352	0.7156 0.6147
	0.4	0.7916 0.6658	0.7753 0.6523	0.7528 0.6360	0.7201 0.6164
0.2	1.0	0.8519 0.7265	0.8322 0.7108	0.8060 0.6919	0.7690 0.6696
	0.8	0.8531 0.7272	0.8335 0.7116	0.8075 0.6928	0.7707 0.6707
	0.6	0.8552 0.7284	0.8359 0.7130	0.8101 0.6945	0.7735 0.6727
	0.4	0.8596 0.7313	0.8408 0.7163	0.8156 0.6983	0.7794 0.6772
0.1	1.0	0.9631 0.8350	0.9438 0.8194	0.9175 0.8007	0.8799 0.7785
	0.8	0.9652 0.8363	0.9459 0.8215	0.9197 0.8028	0.8821 0.7807
	0.6	0.9652 0.8402	0.9494 0.8248	0.9234 0.8063	0.8860 0.7843
	0.4	0.9762 0.8473	0.9315 0.8140	0.9315 0.8140	0.8943 0.7923

The effect of the orthotropy parameters are tabulated in Tables 2.23 and 2.24. The influence of the $E_2^{(1)}/E_1^{(1)}$ and $E_2^{(2)}/E_1^{(2)}$ on the values of c_{cr} are shown in Table 2.23 for the various values e_1 in the case where $\mu_1 = \mu_2 = 0.5$ and $\Omega = 0.04$ under complete (2.11) (upper number) and incomplete (2.12) (lower number) contact conditions.

The influence of the μ_1 and μ_2 on the values of c_{cr} are shown in Table 2.24 for various values of e_1 in the case where $E_2^{(2)}/E_1^{(2)} = E_2^{(1)}/E_1^{(1)} = 0.5$, and $\Omega = 0.04$ under complete (2.11) (upper number) and incomplete (2.12) (lower number) contact conditions. In these tables the sign "–" indicates that in the corresponding case, the critical velocity does not exist.

This completes the consideration of the results related to the case where not only the material of the covering layer but also the material of the half-plane is orthotropic. Now we again turn to consideration of the numerical results related to the case where the material of the half-plane is isotropic and consider the distribution of the displacement in the Ox_2 axis direction (Fig. 2.28) of the points of the interface

Table 2.24 The influence of the μ_1 and μ_2 on the values of c_{cr} for the various e_1 in the case where $E_2^{(2)}/E_1^{(2)} = E_2^{(1)}/E_1^{(1)} = 0.5$, $\Omega = 0.04$ and $\eta_1 = 0$, $\eta_2 = 0$ under complete (2.11) (upper number) and incomplete (2.12) (lower number) contact conditions

e_1	μ_1	μ_2			
		0.5	0.4	0.3	0.2
0.4	0.5	0.6930 0.5839	0.7518 0.6372	0.8290 0.7095	0.9356 0.8158
	0.4	0.6774 0.5756	0.7263 0.6284	0.8134 0.6998	0.9201 0.8047
	0.3	0.6508 0.5636	0.7109 0.6158	0.7895 0.6863	0.8977 0.7900
	0.2	– 0.5402	– 0.5922	0.7366 0.6627	0.8562 0.7663
0.3	0.5	0.7358 0.6256	0.7964 0.6813	0.8753 0.7565	0.9829 0.8660
	0.4	0.7221 0.6170	0.7822 0.6719	0.7822 0.6719	0.9669 0.8536
	0.3	0.7010 0.6052	0.7611 0.6593	0.8393 0.7321	0.9456 0.8378
	0.2	0.6559 0.5847	0.7188 0.6382	0.8003 0.7101	0.9108 0.8144
0.2	0.5	0.7957 0.6855	0.8601 0.7451	0.9429 0.8252	– – –
	0.4	0.7825 0.6756	0.8457 0.7341	0.9271 0.8125	– 0.9255
	0.3	0.7639 0.6628	0.8262 0.7202	0.9063 0.7966	– 0.9067
	0.2	0.7319 0.6434	0.7939 0.6994	0.8737 0.7741	0.9797 0.8809

plane between the constituents and the distribution of the normal stress acting on that plane. Under these considerations we use the notation $c = V/c_R^{(2)}$ (2.127) and assume that $\eta_1 = \eta_2 = 0$ and $e_1 = 0.2$. Note that we will consider the results attained for the complete contact condition (2.11), only.

Thus, we introduce the notation

$$\begin{aligned} u_2(x_1) &= -\left|u_2^{(1)}(x_1,-h)\right| = -\left|u_2^{(2)}(x_1,-h)\right|, \\ \sigma_{22}(x_1) &= -\left|\tilde{\sigma}_{22}^{(1)}(x_1,-h)\right| = -\left|\tilde{\sigma}_{22}^{(2)}(x_1,-h)\right| \end{aligned} \tag{2.146}$$

and, first, consider the influence of the frequency of the moving load (i.e. the influence of the parameter Ω) on the distribution of the displacement $u_2(x_1)$. In this case we will restrict ourselves with small frequencies, i.e. we will assume that $0 \le \Omega \le 0.03$ because the main interesting effects of the oscillation of the moving load on the $u_2(x_1)$ arises most often for the aforementioned small frequencies. The

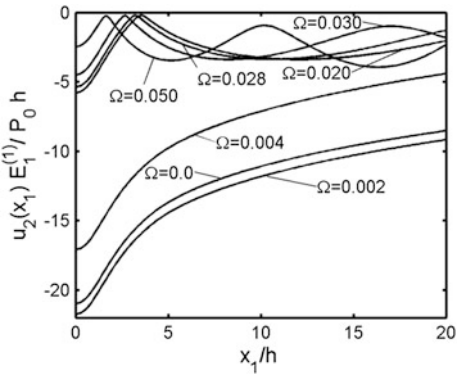

Fig. 2.35 Distribution of the the $u_2(x_1)$ on the interface plane with respect to x_1/h for various values of Ω under $c = 0.6$ for the case where $\mu_1 = 0.5$ and $E_2^{(1)}/E_1^{(1)} = 0.5$

graphs of this distribution are given in Fig. 2.35 under $c = 0.6$, $\mu_1 = 0.5$ and $E_2^{(1)}/E_1^{(1)} = 0.5$ from which it follows that the influence of the Ω on the values of $u_2(x_1)$ is non-monotonic, i.e. before (after) $\Omega = 0.02$ the absolute values of $u_2(x_1)$ increase (decrease) with Ω. It should be noted that this concluding occurs for the considered value of c (i.e. for $c = 0.6$) and for almost all selected Ω (except $\Omega = 0.05$). The maximal absolute value for $u_2(x_1)$ arise at point $x_1/h = 0$. Therefore to illustrate the influence of the Ω on the values of $u_2(x_1)$ for various values of c, it is expedient to consider the graphs of the dependence between $u_2(0)E_1^{(1)}/(P_0h)$ and c for various values of Ω because $u_2(0)$ is a vertical displacement of the interface plane point which is very close to the moving load acting point. These graphs are given in Fig. 2.36. To clarify the illustrations, the graphs are divided into two parts as follows. In the first part (Fig. 2.36a) the load moving velocity c is changed within the interval $[0.0,\ 0.8]$, i.e. before the certain vicinity of the critical velocity, but the second part (Fig. 2.36b) these graphs are given for the interval $[0.85,\ 1.05]$, i.e. before the very near vicinity of the critical velocity. It follows from the foregoing graphs that the jumps arise in the values of $u_2(0)$ with c. The arising of these jumps is characteristic of the considered mechanical processes and is explained with the reflection of the waves from the interface plane between the covering layer and half-plane. At the same time, it clearly follows from the graphs that for such values of Ω, under which there exists critical velocities, Fig. 2.36b shows that the absolute values of $u_2(0)$ increase indefinitely as $c \to c'_{cr}$. The above discussed results in the quantitative sense agree with the corresponding findings attained in Auersch (2008) in which the effect of the moving "strip" loads on the vibrations of soft soil and isolated railway is studied in cases where the moving load velocity is near to the critical velocity. Moreover, it should be noted that the foregoing results are attained for the values $\mu_1 = 0.5$ and $E_2^{(1)}/E_1^{(1)} = 0.5$, but similar ones are also attained for other values of the problem parameters μ_1 and $E_2^{(1)}/E_1^{(1)}$.

We consider the influence of the oscillation frequency of the moving load on the distribution of the normal stress $\sigma_{22}h/P_0$ with respect to x_1/h. In this case we select

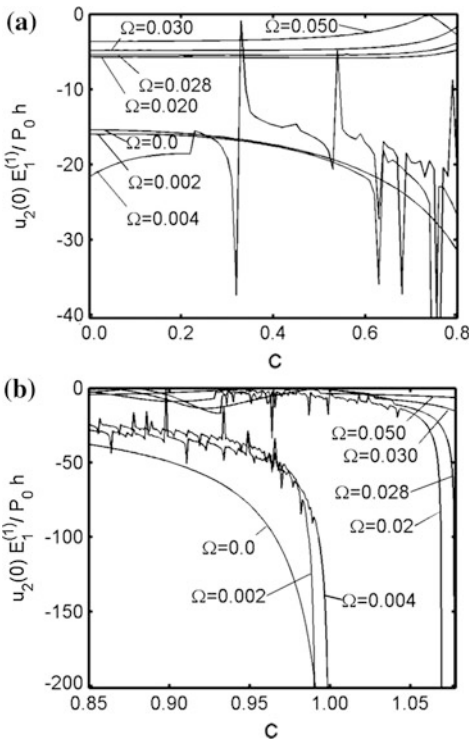

Fig. 2.36 The graphs of the dependence between $u_2(0)$ and c for various Ω under $0 \le c \le 0.8$ (**a**); under $0.85 \le c \le 1.08$ (**b**) in the case where $\mu_1 = 0.5$ and $E_2^{(1)}/E_1^{(1)} = 0.5$

a wider range for the frequency $\Omega\,(0 \le \Omega \le 0.7)$ than that selected for the consideration of the displacement distribution. Because the analyzed stress act on the interface plane and adhesion strength of the system depend directly on the values of this stress. The graphs of these distribution are given in Fig. 2.37 for various values of Ω under $c = 0.4$. It follows from these graphs that in the near vicinity of the load acting point (i.e. in the interval $0 \le x_1/h \le 2.0$) the absolute values of the considered stress decrease with Ω.

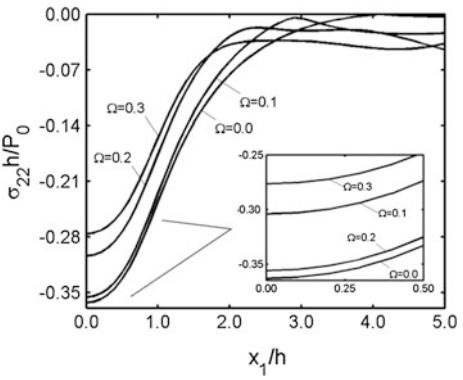

Fig. 2.37 Distribution of the $\sigma_{22}(x_1)$ on the interface plane with respect to x_1/h for various values of Ω under $c = 0.4$

It should be noted that, although the graphs regarding σ_{22} show the distribution of the "amplitude" of the stress $\sigma_{22}^{(1)}(x_1,-h)\left(=\sigma_{22}^{(2)}(x_1,-h)\right)$, the distribution of this and other stresses depend also on the functions $\alpha_{ij}^{(m)}(x_1,x_2)$ in (2.141). Such statement occurs also for the distribution of the displacement. The numerical investigations which are not given here show that, in general, the functions $\alpha_{ij}^{(m)}(x_1,-h)$ and $\alpha_{i}^{(m)}(x_1,-h)$ in (2.116) are discontinuous ones. Consequently this discontinuity causes the discontinuity of the functions $\cos\left(\alpha_{ij}^{(m)}(x_1,-h)+\omega t\right)$ and $\sin\left(\alpha_{ij}^{(m)}(x_1,-h)+\omega t\right)$, and latter ones cause the discontinuity of the distributions of the stresses and displacements with respect to x_1/h. Note that the mentioned discontinuity and jumping is characteristic for dynamical problems and is explained with the wave reflection from the interface planes between the covering layer and half-plane. As an example, we here consider the distribution of the stress $\sigma_{22}^{(1)}(x_1,-h)=-\left|\tilde{\sigma}_{22}^{(1)}\right|\cos\left(\alpha_{22}^{(1)}(x_1,-h)+\omega t\right)$ with respect to x_1/h under $\omega t=\pi/4+2\pi n$ $(n=0,1,2,\ldots)$ $(n=0,1,2,\ldots)$. The graphs of this distribution for various Ω and c are given in Fig. 2.38a, b, respectively. It follows from these graphs that the symmetry of the considered distribution with respect to the straight line determined by equation $x_1=0$ is violated with $\Omega\times c\neq 0$. Consequently, the absolute maximum value of $\sigma_{22}^{(1)}(x_1,-h)$ is attained at the point which is ahead of the moving load acting point but is in the near vicinity of this point, i.e. is in the

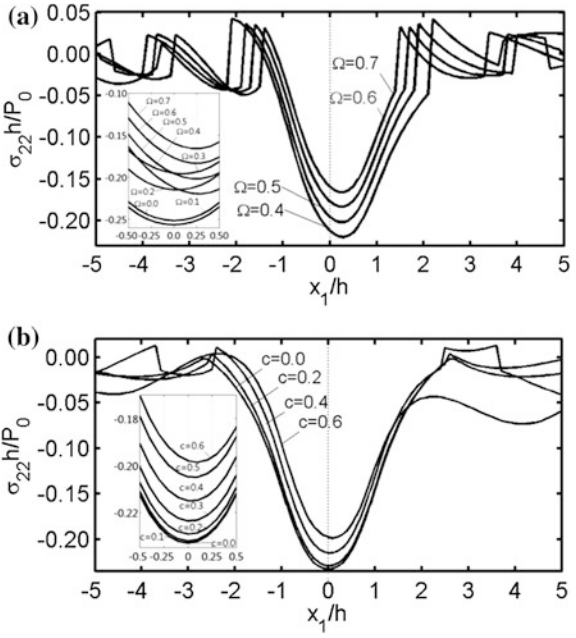

Fig. 2.38 Distribution of the stress $\sigma_{22}^{(1)}(x_1,-h)$ (2.141) with respect to x_1/h under $\omega t=\pi/4+2\pi n$ $(n=0,1,2,\ldots)$ for various values of Ω for $c=0.4$ (**a**), for various values of c for $\Omega=0.2$ (**b**) for the case where $E_2^{(1)}/E_1^{(1)}=0.5$, $\mu_1=0.5$

vicinity for which $x_1/h < 0.5$. Nevertheless these absolute maximum values of $\sigma_{22}^{(1)}(x_1, -h)$ are determined through the values of $\sigma_{22}(x_1, -h)$ which in the quantitative sense have more significance than the function $\cos\left(\alpha_{22}^{(1)}(x_1, -h) + \omega t\right)$. Therefore we turn again to a consideration of the analyses of the numerical results regarding the dependence between $\sigma_{22}(x_1, -h)$ and problem parameters.

It follows from the graphs given in Fig. 2.37 that the absolute values of the stress σ_{22} become significant (in the quantitative sense) at near vicinity of the point $x_1 = 0$. In this case the dependence between $\sigma_{22}h/P_0$ (at $x_1 = 0$) and Ω (for fixed c) is non-monotonic, i.e. there is such a value of Ω (denote it by Ω^*) under which the absolute values of $\sigma_{22}h/P_0$ become maximum. As usual, the frequency is called the "resonance" frequency, and the corresponding values of σ_{22} are called the "resonance" values of the stress. The graphs of the aforementioned dependence are given in Fig. 2.39a, b which are constructed for various values of $E_2^{(1)}/E_1^{(1)}$ and μ_1, respectively. It follows from the graphs that a decrease in the values of the parameter $E_2^{(1)}/E_1^{(1)}$ causes the "resonance" frequency Ω^* to decrease as well as the "resonance" values of σ_{22}, but a decrease in the values of parameter μ_1 causes the "resonance" frequency Ω^* to increase as well as the "resonance" values of the stress σ_{22}. It should be noted that the non-monotonic character of the dependence between $\sigma_{22}h/P_0$ and Ω will be discussed in detail in the next section.

Figure 2.39c shows the influence of the moving load velocity on the dependence between $\sigma_{22}h/P_0$ and Ω under $\mu_1 = 0.5$. According to Fig. 2.39c, there exists such a value of $\Omega(=\Omega_0)$ before (after) which the absolute values of $\sigma_{22}h/P_0$ increase (decrease) with c. This statement can be explained by the existence of a critical velocity under $\Omega < 0.1$. This estimation for Ω follows from relation (2.142).

Now we consider the dependence between the $\sigma_{22}h/P_0$ and c. In this case we must distinguish the following two cases. *Case 1: The critical velocity exists. Case 2: The critical velocity does not exist.* The graphs given in Fig. 2.40a, b which show the mentioned dependencies for various values of the parameters $E_2^{(1)}/E_1^{(1)}$ and μ_1, respectively, portray Case 2. It follows from these graphs that for the considered values of the problem parameters the dependence between $\sigma_{22}h/P_0$ and c is non-monotonic, i.e. before (after) a certain value of c under which the values of $\sigma_{22}h/P_0$ have a jump (denote it by $c_{j\sigma}$). However, under $c > c_{j\sigma}$ the values of $\sigma_{22}h/P_0$ increase with c. Note that the numerical results illustrated in Fig. 2.40a, b agree with the other aforementioned results.

The distinction between aforementioned two cases is illustrated more clearly by the graphs given in Fig. 2.40c, which show the dependence between $\sigma_{22}h/P_0$ and c for various Ω under $\mu_1 = 0.5$. In this figure the graphs regarding the Case 1 and their behavior as $c \to c'_{cr}$ are also illustrated.

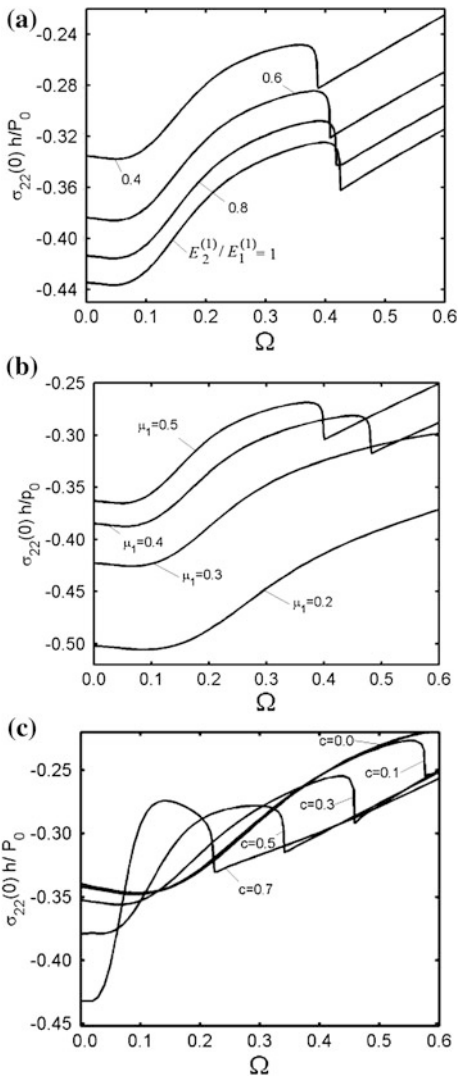

Fig. 2.39 The dependence between $\sigma_{22}(0)h/P_0$ and Ω for the case where $e_1 = 0.2$: **a** for various $E_2^{(1)}/E_1^{(1)}$ under $\mu_1 = 0.5$, $c = 0.4$; **b** for various μ_1 under $c = 0.4$, $E_2^{(1)}/E_1^{(1)} = 0.5$; **c** for various c under $\mu_1 = 0.5$, $E_2^{(1)}/E_1^{(1)} = 0.5$

2.6.3 Conclusions

From the concrete numerical results which are obtained for the case where the material of the covering layer material is orthotropic, but the material of the half-plane is isotropic, and analyzed above the following conclusions were reached:

- There exists a certain limit for oscillation frequency after which the critical velocity does not exist. The interval of the frequency under which the critical velocity exists is divided into two subsequent parts. In the first (second) part of

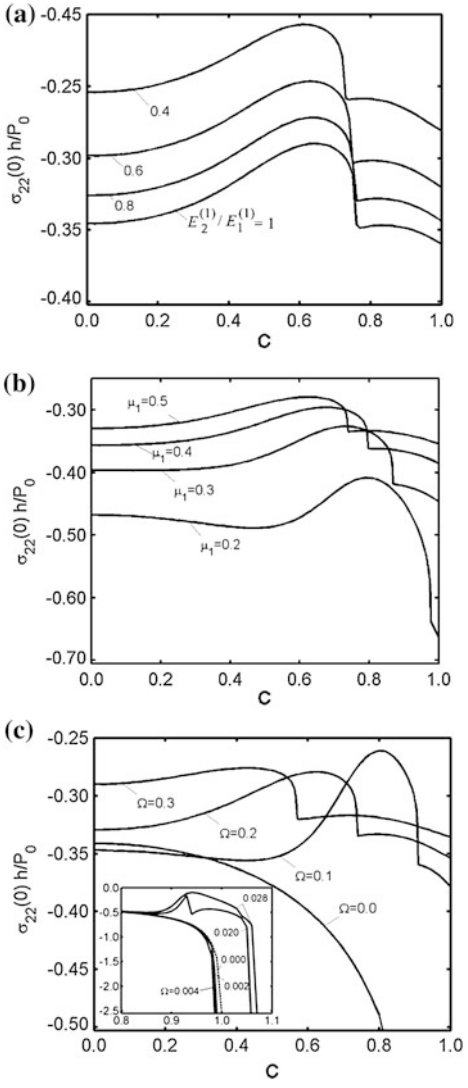

Fig. 2.40 The dependence between $\sigma_{22}(0)h/P_0$ and c for the case where $e_1 = 0.2$: **a** for various $E_2^{(1)}/E_1^{(1)}$ under $\mu_1 = 0.5$, $\Omega = 0.2$; **b** for various μ_1 under $\Omega = 0.2$ $E_2^{(1)}/E_1^{(1)} = 0.5$; **c** for various Ω under $\mu_1 = 0.5$, $E_2^{(1)}/E_1^{(1)} = 0.5$

this interval the values of the critical velocity decrease (increase) with frequency of the oscillation of the moving load.

- The values of the critical velocity are controlled mainly with a Rayleigh wave velocity for the half-plane material; at the same time, the full slipping incompleteness of the contact conditions reduces significantly the values of this critical velocity.
- The limit values of the oscillation frequency after which the critical velocity does not exists, are determined through the values of the critical velocity which are very near to the limit velocity for the subsonic regime. Therefore for the considered values of the problem parameters the mentioned frequency, and

corresponding critical velocity, are determined mainly through the mechanical properties of the half-plane material.

- In the quantitative sense, the values to be considered for the normal stress acting on the interface plane between the covering layer and half-plane and displacement of the points of this plane are attained in the certain near vicinity of the load acting point.
- After the oscillation of the moving load reaches a certain velocity, jumps arise in the stress and displacement values. The magnitude of these jumps depend on the anisotropy of the covering layer material and becomes more considerable for cases where the velocity of the moving load approaches its critical velocity.
- At the same time, as a result of the oscillation of the moving load, the symmetry of the aforementioned distribution with respect to the point at which this load acts is violated for each moment of time.
- Before the aforementioned first jump, there exists the "resonance" value of the oscillation frequency of the moving load under which the stress considered has its absolute local maximum ("resonance") value. The values of the "resonance" stress increase with the velocity of the moving load.

Additionally, in the present section numerical results related to the critical velocity obtained in the case where not only the material of the covering layer, but also the material of the half-plane is orthotropic, are presented and discussed. In this case it was assumed that $\Omega > \Omega'$ and the right branch of the dependence between c and sh is taken into account, only. According to these results it can be made the following conclusions.

- The values of the critical velocity increase with decreasing $E_2^{(1)}/E_1^{(1)}$, i.e. with a decrease in the modulus of elasticity of the covering layer material in the direction along its thickness.
- The values of the critical velocity increase with $E_2^{(2)}/E_1^{(2)}$, i.e. with a increase in the modulus of elasticity of the half-plane material in the direction along its depth.
- The critical velocity increase with increasing (decreasing) the shear modulus $\mu_{12}^{(1)}$ ($\mu_{12}^{(2)}$) for fixed values of the modulus of elasticity $E_1^{(1)}$ ($E_1^{(2)}$) or with decreasing (increasing) of the modulus of elasticity $E_1^{(1)}$ ($E_1^{(2)}$) for fixed values of the shear modulus $\mu_{12}^{(1)}$ ($\mu_{12}^{(2)}$).
- The critical velocity increase with Ω, in other words, in the cases where $\Omega > \Omega'$ the vibration character of the line located moving load causes to increase of the values of the critical velocity.
- The critical velocity increase with tensile stress of the covering layer and half-plane, but decrease with initial compressive stress of the half-plane.
- The critical velocities attained for the complete contact condition (2.11) are greater than those attained for the incomplete contact conditions with full slipping (2.12).

The results attained in the present section agree with the corresponding ones attained in the previous section. Moreover, these results agree, in the qualitative sense, with the results attained in the papers by Auersch (2006, 2008).

2.7 Three-Dimensional Problems on the Dynamics of a System Comprising a Pre-stressed Covering Layer and Pre-stressed Half-Space Under the Action of an Oscillating Moving Load

In all the foregoing sections two-dimensional (with respect to space coordinates) problems, i.e. problems regarding the plane-strain state were considered. In the present section, according to papers by Akbarov et al. (2011, 2015), we will consider the three-dimensional problem on the dynamics of the point-located moving load or point-located oscillation moving load acting on the system consisting of the pre-stressed covering layer and pre-stressed half-space. The investigations are made by utilizing of the second version (see Sect. 2.1) of the small initial deformation theory of the TDLTEWISB. Consequently, the study in the present section can be considered as a development of the study carried out in the previous sections for the corresponding three-dimensional problem.

We recall that the corresponding three-dimensional problem on the dynamics of an oscillating moving load acting on a slab resting on a rigid foundation had been investigated within the scope of classical elastodynamics in the paper by Dieterman and Metrikine (1997). Therefore, in a certain sense the investigations carried out in the present section can be also considered as a development of the investigations made by Dieterman and Metrikine (1997) for a system consisting of a covering layer and half-space.

2.7.1 Formulation of the Problem

Taking into consideration the initially stressed half-space covered by the initially stressed layer, we determine the positions of the points of the layer and half-space by the Lagrangian coordinates in the Cartesian system of coordinates $Ox_1x_2x_3$ (Fig. 2.41a).

We assume that the layer and half-space (before the contact) are stretched or compressed separately in the direction of the Ox_1 and Ox_3 axes and that in each of them bi-axial homogeneous initial stresses appear. Note that the covering layer and the half-space occupy the regions $\{-h < x_2 < 0\}$ and $\{-\infty < x_2 < -h\}$, respectively under $\{-\infty < x_1 < +\infty\}$, $\{-\infty < x_3 < \infty\}$ (Fig. 2.41 a). The values related to the covering layer and half-space are denoted by upper indices (1) and (2), respectively. Moreover, the values related to the initial stresses are denoted by the additional upper index 0.

The linearly elastic material of the layer and half-space materials are to be taken as homogeneous and isotropic. We also assume that the layer and half-space materials are moderately rigid (i.e. the strain related to the yield stress is not more than 0.028) and that their initial stress states are determined within the scope of the classical linear theory of elasticity as follows:

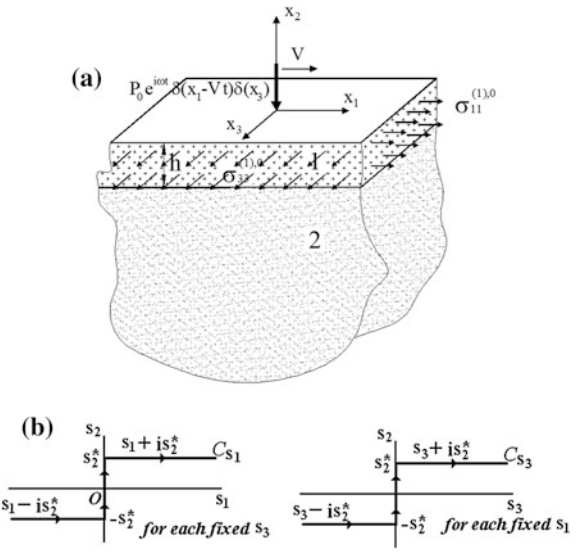

Fig. 2.41 The geometry of the structure of the half-space covered by the layer (**a**); the Sommerfeld contours (**b**)

$$\begin{aligned} &\sigma_{11}^{(m),0} = const_{1m},\ \sigma_{33}^{(m),0} = const_{3m}, \\ &\sigma_{ij}^{(m),0} = 0 \quad \text{for } ij \neq 11, 33, \quad m = 1, 2. \end{aligned} \tag{2.147}$$

The stress state (2.147) can be arise in the case where the system under consideration is loaded at infinity by the uniformly distributed normal forces with intensities p_1 and p_3 acting in the direction of the Ox_1 and Ox_3 axes respectively. According to the well-known mechanical consideration, in the certain distance from the load acting regions the stress state in the system under consideration can be taken as homogeneous one. In this case the stresses in the half-space can be presented as $\sigma_{11}^{(2),0} = p_1$, $\sigma_{33}^{(2),0} = p_3$ and $\sigma_{ij}^{(2),0} = 0$ for $ij \neq 11, 33$. Assuming that the complete contact conditions occur between the covering layer and half-space the stresses in the covering layer are determined as

$$\begin{aligned} \sigma_{11}^{(1),0} &= \frac{E^{(1)}(p_1 + v^{(1)}p_3)}{E^{(2)}(1 - (v^{(2)})^2)} - \frac{E^{(1)}v^{(2)}(p_3 + v^{(1)}p_1)}{E^{(2)}(1 - (v^{(2)})^2)}, \\ \sigma_{33}^{(1),0} &= \frac{E^{(1)}(p_3 + v^{(1)}p_1)}{E^{(2)}(1 - (v^{(2)})^2)} - \frac{E^{(1)}v^{(2)}(p_1 + v^{(1)}p_3)}{E^{(2)}(1 - (v^{(2)})^2)}, \sigma_{ij}^{(1),0} = 0 \quad \text{for } ij \neq 11, 33. \end{aligned}$$

In this way we prove the validity of the expressions in Eq. (2.147). Note that here through $E^{(k)}$ and $v^{(k)}$ the modulus of elasticity and the Poisson's coefficient of the kth material are denoted.

Thus, within the scope of the foregoing statements, we assume that on the upper free face plane of the covering layer the time-harmonic point-located force which

moves with constant velocity V in the direction of the Ox_1 axis is acting (Fig. 2.41a).

According to Guz (2004), the equation of motion of the TLTEWISB for the case under consideration is:

$$\frac{\partial \sigma_{ij}^{(m)}}{\partial x_j} + \sigma_{11}^{(m),0} \frac{\partial^2 u_i^{(m)}}{\partial x_1^2} + \sigma_{33}^{(m),0} \frac{\partial^2 u_i^{(m)}}{\partial x_3^2} = \rho_0^{(m)} \frac{\partial^2 u_i^{(m)}}{\partial t^2} \quad i; j = 1, 2, 3; \quad m = 1, 2. \tag{2.148}$$

In Eq. (2.148) the conventional notation is used.

Note that the Eq. (2.148) can easily be obtained from the non-linear equation of motion (2.6) by employing the linearization procedure described in Sect. 2.2. However, under this linearization procedure it must be taken into consideration the three-dimensionality of the equations and the foregoing initial stresses.

The mechanical relations for the materials of the constituents are taken as follows:

$$\sigma_{ij}^{(m)} = \lambda^{(m)} \theta^{(m)} \delta_{ij} + 2\mu^{(m)} \varepsilon_{ij}^{(m)} \tag{2.149}$$

Note that the component $\varepsilon_{ij}^{(m)}$ of the strain tensor is determined through the components $u_1^{(m)}$, $u_2^{(m)}$ and $u_3^{(m)}$ of the displacement vector as follows:

$$\varepsilon_{ij}^{(m)} = \frac{1}{2} \left(\frac{\partial u_i^{(m)}}{\partial x_j} + \frac{\partial u_j^{(m)}}{\partial x_i} \right), \theta^{(m)} = \varepsilon_{11}^{(m)} + \varepsilon_{22}^{(m)} + \varepsilon_{33}^{(m)} \tag{2.150}$$

Thus, we have the complete system of field Eqs. (2.148)–(2.150) which are satisfied within the covering layer and half-space separately.

Now we consider formulation of the boundary and contact conditions. According to the foregoing discussions, on the upper face plane of the covering layer, the following boundary conditions must be satisfied:

$$\sigma_{32}^{(1)}\Big|_{x_2=0} = \sigma_{12}^{(1)}\Big|_{x_2=0} = 0, \quad \sigma_{22}^{(1)}\Big|_{x_2=0} = P_0 \delta(x_1 - Vt) e^{i\omega t} \delta(x_3) \tag{2.151}$$

Here $\delta(\bullet)$ denotes Dirac's delta function. According to the definition of this function, i.e. according to the relations $\delta(0) = \infty$ and $\delta(x) = 0$ if $x \neq 0$, the presentation $\delta(x_1 - Vt)\delta(x_3)$ means that the oscillating moving load P_0 acts at point of the upper face plane of the covering layer for which $x_1 = Vt$ and $x_3 = 0$.

The following perfect contact conditions occur in the interface plane between the covering layer and half-space:

$$\sigma_{i2}^{(1)}\Big|_{x_2=-h} = \sigma_{i2}^{(2)}\Big|_{x_2=-h},\ u_i^{(1)}\Big|_{x_2=-h} = u_i^{(2)}\Big|_{x_2=-h},\quad i=1,2,3. \tag{2.152}$$

In addition to these, it is supposed that

$$\left|u_i^{(2)}\right|, \left|\sigma_{ij}^{(2)}\right| < M = constant \quad \text{as } x_2 \to -\infty. \tag{2.153}$$

This completes the formulation of the problem. It should be noted that in the case where $\sigma_{11}^{(m),0} = \sigma_{33}^{(m),0} = 0,\ (m=1,2)$ the problem formulation described above transforms into the corresponding one within the scope of the classical linear theory of elastodynamics.

2.7.2 Method of Solution

From Eqs. (2.148) to (2.150) we obtain the following equations of motion in terms of displacement:

$$\begin{aligned}\nabla^2 u_i^{(m)} + \left(1+\frac{\lambda^{(m)}}{\mu^{(m)}}\right)\frac{\partial^2 u_j^{(m)}}{\partial x_j \partial x_i} + \frac{\sigma_{11}^{(m),0}}{\mu^{(m)}}\frac{\partial^2 u_i^{(m)}}{\partial x_1^2} \\ + \frac{\sigma_{33}^{(m),0}}{\mu^{(m)}}\frac{\partial^2 u_i^{(m)}}{\partial x_3^2} = \frac{1}{\left(c_2^{(m)}\right)^2}\frac{\partial^2 u_i^{(m)}}{\partial t^2},\end{aligned} \tag{2.154}$$

$$\nabla^2 = \frac{\partial^2}{\partial x_1^2} + \frac{\partial^2}{\partial x_2^2} + \frac{\partial^2}{\partial x_3^2},\ c_2^{(m)} = \sqrt{\frac{\mu^{(m)}}{\rho_0^{(m)}}} \tag{2.155}$$

where $c_2^{(m)}$ is the speed of the distortion wave. We attempt to use the Lame' representations for the displacements:

$$\begin{aligned}u_1^{(m)} &= \frac{\partial \phi^{(m)}}{\partial x_1} + \frac{\partial \psi_3^{(m)}}{\partial x_2} - \frac{\partial \psi_2^{(m)}}{\partial x_3},\ u_2^{(m)} = \frac{\partial \phi^{(m)}}{\partial x_2} + \frac{\partial \psi_1^{(m)}}{\partial x_3} - \frac{\partial \psi_3^{(m)}}{\partial x_1}, \\ u_3^{(m)} &= \frac{\partial \phi^{(m)}}{\partial x_3} + \frac{\partial \psi_2^{(m)}}{\partial x_1} - \frac{\partial \psi_1^{(m)}}{\partial x_2}.\end{aligned} \tag{2.156}$$

By direct verification we prove that the potentials must satisfy the following equations:

$$\begin{gathered}\nabla^2\phi^{(m)}+\frac{\sigma_{11}^{(m),0}}{\lambda^{(m)}+2\mu^{(m)}}\frac{\partial^2\phi^{(m)}}{\partial x_1^2}+\frac{\sigma_{33}^{(m),0}}{\lambda^{(m)}+2\mu^{(m)}}\frac{\partial^2\phi^{(m)}}{\partial x_3^2}=\frac{1}{\left(c_1^{(m)}\right)^2}\frac{\partial^2\phi^{(m)}}{\partial t^2}\\ \nabla^2\psi_i^{(m)}+\frac{\sigma_{11}^{(m),0}}{\mu^{(m)}}\frac{\partial^2\psi_i^{(m)}}{\partial x_1^2}+\frac{\sigma_{33}^{(m),0}}{\mu^{(m)}}\frac{\partial^2\psi_i^{(m)}}{\partial x_3^2}=\frac{1}{\left(c_2^{(m)}\right)^2}\frac{\partial^2\psi_i^{(m)}}{\partial t^2}\\ \frac{\partial\psi_1^{(m)}}{\partial x_1}+\frac{\partial\psi_2^{(m)}}{\partial x_2}+\frac{\partial\psi_3^{(m)}}{\partial x_3}=0,\end{gathered}\tag{2.157}$$

where $c_1^{(m)}=\sqrt{(\lambda^{(m)}+2\mu^{(m)})/\rho_0^{(m)}}$ is the speed of the dilatation wave.

By the using the coordinate system:

$$x_1'=x_1'-Vt,\ x_2'=x_2,\ x_3'=x_3,\tag{2.158}$$

which moves with the loading force, and presenting the sought values as $g(x_1',x_2',x_3',t)=\bar{g}(x_1',x_2',x_3')e^{i\omega t}$ we obtain the following equations from (2.157):

$$\begin{gathered}\nabla^2\phi^{(m)}+\frac{\sigma_{11}^{(m),0}}{\lambda^{(m)}+2\mu^{(m)}}\frac{\partial^2\phi^{(m)}}{\partial x_1^2}+\frac{\sigma_{33}^{(m),0}}{\lambda^{(m)}+2\mu^{(m)}}\frac{\partial^2\phi^{(m)}}{\partial x_3^2}\\ =\frac{1}{\left(c_1^{(m)}\right)^2}\left[V^2\frac{\partial^2\phi^{(m)}}{\partial x_1^2}-2i\omega\frac{\partial\phi^{(m)}}{\partial x_1}-\omega^2\phi^{(m)}\right],\\ \nabla^2\psi_n^{(m)}+\frac{\sigma_{11}^{(m),0}}{\mu^{(m)}}\frac{\partial^2\psi_n^{(m)}}{\partial x_1^2}+\frac{\sigma_{33}^{(m),0}}{\mu^{(m)}}\frac{\partial^2\psi_n^{(m)}}{\partial x_3^2}\\ =\frac{1}{\left(c_2^{(m)}\right)^2}\left[V^2\frac{\partial^2\psi_n^{(m)}}{\partial x_1^2}-2i\omega\frac{\partial\psi_n^{(m)}}{\partial x_1}-\omega^2\psi_n^{(m)}\right],\\ \frac{\partial\psi_1^{(m)}}{\partial x_1}+\frac{\partial\psi_2^{(m)}}{\partial x_2}+\frac{\partial\psi_3^{(m)}}{\partial x_3}=0.\end{gathered}\tag{2.159}$$

In the Eq. (2.159) the upper prime in x_n and the over bar in $\phi^{(m)}$ and $\psi_n^{(m)}$ $(n=1,2,3)$ are omitted. In this case the second boundary condition in (2.151) is replaced by the following one:

$$\sigma_{22}^{(1)}\Big|_{x_2=0}=P_0\delta(x_1)\delta(x_3).\tag{2.160}$$

The other conditions in (2.151)–(2.153) are also valid for the new coordinate system (2.158).

We introduce the dimensionless coordinates $x_i \to x_i/h$ and for the solution to the system (2.159) we employ the double exponential Fourier transformation with respect to the coordinates x_1 and x_3 defined as:

$$f_{F13}(s_1, x_2, s_3) = \int\limits_{-\infty}^{+\infty} \int\limits_{-\infty}^{+\infty} f(x_1, x_2, x_3) e^{-i(s_1 x_1 + s_3 x_1)} dx_1 dx_3. \tag{2.161}$$

As a result of this transformation we obtain from (2.159) the equation with respect to $\phi_{13F}^{(m)}$ and $\psi_{n13F}^{(m)}$ the solution to which are:

$$\begin{aligned}
\phi_{13F}^{(1)} &= A_1^{(1)}(s_1, s_3) e^{\gamma_1^{(1)}(s_1, s_3) x_2} + A_2^{(1)}(s_1, s_3) e^{-\gamma_1^{(1)}(s_1, s_3) x_2} \\
\phi_{13F}^{(2)} &= A_1^{(2)}(s_1, s_3) e^{\gamma_1^{(2)}(s_1, s_3) x_2}, \\
\psi_{n13F}^{(1)} &= B_{1n}^{(1)}(s_1, s_3) e^{\gamma_2^{(1)}(s_1, s_3) x_2} + B_{2n}^{(1)}(s_1, s_3) e^{-\gamma_2^{(1)}(s_1, s_3) x_2}, \\
\psi_{n13F}^{(2)} &= B_{1n}^{(2)}(s_1, s_3) e^{\gamma_2^{(2)}(s_1, s_3) x_2},
\end{aligned} \tag{2.162}$$

where

$$\begin{aligned}
\left(\gamma_1^{(m)}\right)^2 &= s_1^2 \left[1 + \frac{\sigma_{11}^{(m),0}}{\lambda^{(m)} + 2\mu^{(m)}}\right] + s_3^2 \left[1 + \frac{\sigma_{33}^{(m),0}}{\lambda^{(m)} + 2\mu^{(m)}}\right] \\
&\quad + \frac{\left(c_2^{(1)}\right)^2}{\left(c_1^{(m)}\right)^2} \left[-V^2 s_1^2 - 2\Omega V s_1 + \Omega^2\right], \\
\left(\gamma_2^{(m)}\right)^2 &= s_1^2 \left[1 + \frac{\sigma_{11}^{(m),0}}{\mu^{(m)}}\right] + s_3^2 \left[1 + \frac{\sigma_{33}^{(m),0}}{\mu^{(m)}}\right] \\
&\quad + \frac{\left(c_2^{(1)}\right)^2}{\left(c_1^{(m)}\right)^2} \left[-V^2 s_1^2 - 2\Omega V s_1 + \Omega^2\right].
\end{aligned} \tag{2.163}$$

Substituting the expressions in (2.162) into the last relation in (2.159) we obtain the following relations:

$$B_{12}^{(m)} = -\frac{i}{\gamma_2^{(m)}} (s_1 B_{11}^{(m)} + s_3 B_{13}^{(m)}), \; B_{22}^{(m)} = \frac{i}{\gamma_2^{(m)}} (s_1 B_{21}^{(m)} + s_3 B_{23}^{(m)}). \tag{2.164}$$

In the present investigation we assume that the following inequalities are satisfied:

$$V < \min\left\{c_2^{(1)}\sqrt{1+\frac{\sigma_{11}^{(1),0}}{\mu^{(1)}}};\ \ c_2^{(2)}\sqrt{1+\frac{\sigma_{11}^{(2),0}}{\mu^{(2)}}}\right\}. \tag{2.165}$$

The case determined by the relation (2.165) is called the subsonic case.

Thus, from (2.159), (2.162) to (2.164), we have completely determined the double Fourier transforms of all sought values. For determination of the unknowns $A_1^{(m)}$, $A_2^{(1)}$, $B_{1n}^{(m)}$ and $B_{2n}^{(1)}$ which enter into these transformations, we obtain from boundary condition (2.151) and contact condition (2.152) the corresponding closed system of algebraic equations. From the algebraic equations we find the aforementioned unknowns and, employing the inverse transform:

$$f(x_1,x_2,x_3)=\frac{1}{4\pi^2}\int\limits_{-\infty}^{+\infty}\int\limits_{-\infty}^{+\infty} f_{F13}(s_1,x_2,s_3)e^{i(s_1x_1+s_3x_3)}ds_1ds_3 \tag{2.166}$$

we determine the displacements and stresses in the components of the considered system.

Note that the integrand in relation (2.166), i.e. the expression of $f_{F13}(s_1,x_2,s_3)$ for all the sought quantities can be presented as follows:

$$f_{F13}(s_1,x_2,s_3)=\frac{(\bullet)}{\det\|\alpha_{nm}(s_1h,s_3h,V,\Omega)\|}, \tag{2.167}$$

where $(\bullet)$ is the function which has continuous derivatives in sufficient order. However the function $\det\|\alpha_{nm}(s_1h,s_3h,V,\Omega)\|$ may have the zeroth for certain values of s_1h and s_3h which are determined from the equation:

$$\det\|\alpha_{nm}(s_1h,s_3h,V,\Omega)\|=0,\quad m;n=1,2,\ldots,9. \tag{2.168}$$

It should be noted that the Eq. (2.168) in the case where $\Omega=0$ coincides with the dispersion equation of all the possible subsonic near-surface waves which propagate in the direction of the unit vector $\mathbf{n}\left\{hs_1/\sqrt{(hs_1)^2+(hs_3)^2},\ hs_3/\sqrt{(hs_1)^2+(hs_3)^2}\right\}$, i.e. the equation

$$\det\|\alpha_{nm}(s_1h,s_3h,V,\Omega)\|\|_{\Omega=0}=0 \tag{2.169}$$

is the dispersion equation of the above-noted waves and the relation $V=V(s_1h,s_3h)$ determined from the Eq. (2.169) is the dispersion relation. At the same time, the relation $\Omega=\Omega(s_1h,s_3h)$ determined from the equation:

$$\det\|\alpha_{nm}(s_1h, s_3h, V, \Omega)\|\|_{V=0} = 0 \tag{2.170}$$

is the dispersion diagram of the aforementioned waves.

According to the problem statement, the relations $V = V(s_1h, s_3h)$ and $\Omega = \Omega(s_1h, s_3h)$, as well as the Eqs. (2.169) and (2.170) are symmetric with respect to $s_1h = 0$ and $s_3h = 0$. However the Eq. (2.169) and the relation $V = V(s_1h, s_3h, \Omega)$ or the relation $\Omega = \Omega(s_1h, s_3h, V)$ are symmetric with respect to $s_3h = 0$ only, but the symmetry of these equations and relations with respect to $s_1h = 0$ are violated by the term $2\Omega V s_1$ which enters the expressions in (2.163).

Consequently, in the case under consideration, the order of the roots of the Eq. (2.168) with respect to s_1h and s_3h (denoted by r_1 and r_3 respectively) is also the order of the singularity of the integrand in (2.166). It is known that in the cases where the conditions $0 \le r_1 < 1$ and $0 \le r_3 < 1$ are simultaneously satisfied, the integral (2.166) can be calculated by the use of normal well-known algorithms. In the cases where the condition $r_1 = 1$ or the condition $r_3 = 1$ is satisfied either simultaneously or separately, then the calculation of the integral (2.166) is performed in Cauchy's principal value sense. But in the cases where one of the conditions $r_1 > 1$ or $r_3 > 1$ is satisfied, the integral (2.166) does not have any meaning and the velocity or the frequency corresponding to this case is called the "critical velocity" for fixed frequency or resonance frequency of the moving load. Note that not only under resonance frequency but also under critical velocity the resonance type of phenomenon takes place.

Now we consider the algorithm, according to which, the mentioned orders, i.e. the values of r_1 and r_3 can be determined. To simplify the consideration we separate three cases: in Case 1 (Case 2) we assume that $V > 0$ and $\Omega = 0$ ($V = 0$ and $\Omega > 0$), but in Case 3 we assume that $V > 0$ and $\Omega > 0$. In Case 1 (Case 2) we determine the relation $V = V(s_1h, s_3h)$ from the Eq. (2.169) (the relation $\Omega = \Omega(s_1h, s_3h)$ from the Eq. (2.170)). But in Case 3 we determine the relation $V = V(s_1h, s_3h, \Omega)$ or the relation $\Omega = \Omega(s_1h, s_3h, V)$ from the Eq. (2.168). According to the foregoing determination, the critical velocity corresponds to the cases where:

$$\frac{\partial V}{\partial(s_1h)} = 0 \text{ for fixed } s_3h \quad \text{or} \quad \frac{\partial V}{\partial(s_3h)} = 0 \text{ for fixed } s_1h, \tag{2.171}$$

but the resonance frequency corresponds to the case where:

$$\frac{\partial \Omega}{\partial(s_1h)} = 0 \text{ for fixed } s_3h \quad \text{or} \quad \frac{\partial \Omega}{\partial(s_3h)} = 0 \text{ for fixed } s_1h. \tag{2.172}$$

According to this statement, in Cases 1 and 3 the critical velocity (denoted by V_{cr}) can be determined from the criterion (2.171), but in Case 2 the resonance frequency (denoted by Ω_{res}) can be determined from the criterion (2.172).

The investigations carried out in the previous sections show that if the covering layer material is stiffer than the material of the half-plane (half-space), the relation (2.171) takes place. Otherwise the relation (2.171) does not exist, i.e. there is no

critical velocity for the considered system. It should be noted that in papers by Dieterman and Metrikine (1997), Metrikine and Vrouwenvelder (2000) the critical velocity is defined as the velocity for which the phase and group velocities are equal to each other. In Sect. 2.4 it is proven that the mentioned definition of the critical velocity is equivalent to the definition (2.171).

At the same time, investigations which will be considered in the next chapter show that in Case 2 the resonance frequency does not exist for a system consisting of a covering layer and half-space. However, the results which will be discussed in the next chapter show that in Case 2 such resonance frequencies exist for the system consisting of a "stiff covering layer + soft substrate + absolute rigid half-space".

Thus, taking the foregoing discussions and conclusions into account we will consider below the numerical results obtained within the framework of the solution procedure discussed above and related to the critical velocity and the influence of the oscillation frequency of the moving load on this velocity. In addition, we will consider the numerical results related to the stress distribution on the interface plane between the covering layer and half-space. However, before this we will analyze the Doppler Effect and the algorithm for obtaining the mentioned numerical results.

2.7.3 *Some Notes on the Doppler Effect and the Algorithm for Obtaining the Numerical Results*

First, the improper integral (2.166) is replaced by the corresponding definite integral with

$$\begin{aligned} f(x_1,x_2,x_3) &= \frac{1}{4\pi^2}\int\limits_{-\infty}^{+\infty}\int\limits_{-\infty}^{+\infty} f_{F13}(s_1,x_2,s_3)e^{i(s_1x_1+s_3x_3)}ds_1ds_3 \\ &\approx \frac{1}{4\pi^2}\int\limits_{-S_{1^*}}^{+S_{1^*}}\left(\int\limits_{-S_{3^*}}^{+S_{3^*}} f_{F13}(s_1,x_2,s_3)e^{i(s_1x_1+s_3x_3)}ds_3\right)ds_1. \end{aligned} \tag{2.173}$$

The values of S_{1^*} and S_{3^*} in Eq. (2.173) are defined from the convergence requirement.

To simplify the consideration, we consider the calculation of the values of the displacements $u_i^{(m)}$ and stresses $\sigma_{22}^{(m)}$, $\sigma_{12}^{(m)}$ and $\sigma_{23}^{(m)}$. According to the symmetry and asymmetry of the sought values with respect to x_3, we can write the following relations:

$$\begin{aligned}
\left\{u_{k1F}^{(m)};\sigma_{k21F}^{(m)}\right\} &= \int_{-S_{3^*}}^{+S_{3^*}} \left\{u_{k13F}^{(m)};\sigma_{k213F}^{(m)}\right\} e^{is_3x_3} ds_3 \\
&= 2\int_{0}^{+S_{3^*}} \left\{u_{k13F}^{(m)};\sigma_{k213F}^{(m)}\right\} \cos(s_3x_3) ds_3, \\
\left\{u_{31F}^{(m)};\sigma_{231F}^{(m)}\right\} &= \int_{-S_{3^*}}^{+S_{3^*}} \left\{u_{313F}^{(m)};\sigma_{2313F}^{(m)}\right\} e^{is_3x_3} ds_3 \\
&= 2i\int_{0}^{+S_{3^*}} \left\{u_{313F}^{(m)};\sigma_{2313F}^{(m)}\right\} \sin(s_3x_3) ds_3,
\end{aligned} \tag{2.174}$$

where $k = 1, 2$. At the same time, we use the following notation:

$$\begin{aligned}
\left\{u_{k}^{(m)};\sigma_{k2}^{(m)}\right\} &= \left\{u_{kc}^{(m)};\sigma_{k2c}^{(m)}\right\} + i\left\{u_{ks}^{(m)};\sigma_{k2s}^{(m)}\right\}, \\
\left\{u_{3}^{(m)};\sigma_{32}^{(m)}\right\} &= i\left\{u_{3c}^{(m)};\sigma_{32c}^{(m)}\right\} - \left\{u_{3s}^{(m)};\sigma_{32s}^{(m)}\right\},
\end{aligned} \tag{2.175}$$

where

$$\begin{aligned}
\left\{u_{jc}^{(m)};\sigma_{j2c}^{(m)}\right\} &= \int_{-S_{1^*}}^{+S_{1^*}} \left\{u_{j1F}^{(m)};\sigma_{j21F}^{(m)}\right\} \cos(s_1x_1) ds_1; \\
\left\{u_{js}^{(m)};\sigma_{j2s}^{(m)}\right\} &= \int_{-S_{1^*}}^{+S_{1^*}} \left\{u_{j1F}^{(m)};\sigma_{j21F}^{(m)}\right\} \sin(s_1x_1) ds_1.
\end{aligned} \tag{2.176}$$

Thus, using the notation (2.175) and (2.176) we can write the expressions given below for the complex displacements (denoted by $u_j^{(m)}$) and complex stresses (denoted by $\sigma_{j2}^{(m)}$):

$$\begin{aligned}
\left\{\sigma_{22}^{(m)};\sigma_{32}^{(m)};u_{2}^{(m)};u_{3}^{(m)}\right\} &= \left\{\left|\sigma_{22}^{(m)}\right|e^{i\alpha_{22}^{(m)}};\left|\sigma_{32}^{(m)}\right|e^{i\alpha_{32}^{(m)}};\right. \\
&\quad \left.\left|u_{2}^{(m)}\right|e^{i\alpha_{2}^{(m)}};\left|u_{3}^{(m)}\right|e^{i\alpha_{3}^{(m)}}\right\}, \\
\left\{\sigma_{12}^{(m)};u_{1}^{(m)}\right\} &= \left\{i\left|\sigma_{12}^{(m)}\right|e^{i\alpha_{12}^{(m)}};i\left|u_{1}^{(m)}\right|e^{i\alpha_{1}^{(m)}}\right\},
\end{aligned} \tag{2.177}$$

where

$$\begin{aligned}&\left|\sigma_{j2}^{(m)}\right| = \sqrt{\left(\sigma_{j2c}^{(m)}\right)^2 + \left(\sigma_{j2s}^{(m)}\right)^2},\ \left|u_j^{(m)}\right| = \sqrt{\left(u_{jc}^{(m)}\right)^2 + \left(u_{js}^{(m)}\right)^2},\\ &\tan\alpha_{j2}^{(m)} = \frac{\sigma_{j2s}^{(m)}}{\sigma_{j2c}^{(m)}},\ \ \tan\alpha_j^{(m)} = \frac{u_{js}^{(m)}}{u_{jc}^{(m)}}.\end{aligned} \tag{2.178}$$

After the foregoing mathematical preparation, the true (real) values of the sought quantities are determined by the expressions:

$$\left\{\sigma_{j2}^{(m)}; u_j^{(m)}\right\} = \mathrm{Re}\left\{\sigma_{j2}^{(m)} e^{i\omega t}; u_j^{(m)} e^{i\omega t}\right\}, \tag{2.179}$$

according to which,

$$\begin{aligned}\sigma_{22}^{(m)} &= \left|\sigma_{22}^{(m)}\right| \cos(\alpha_{22}^{(m)} + \omega t),\\ \sigma_{12}^{(m)} &= -\left|\sigma_{12}^{(m)}\right| \sin(\alpha_{12}^{(m)} + \omega t),\ \sigma_{32}^{(m)} = \left|\sigma_{32}^{(m)}\right| \cos(\alpha_{32}^{(m)} + \omega t),\\ u_2^{(m)} &= \left|u_2^{(m)}\right| \cos(\alpha_2^{(m)} + \omega t),\ u_3^{(m)} = \left|u_3^{(m)}\right| \cos(\alpha_3^{(m)} + \omega t),\\ u_1^{(m)} &= -\left|u_1^{(m)}\right| \sin(\alpha_1^{(m)} + \omega t).\end{aligned} \tag{2.180}$$

It follows from expressions (2.178) and (2.180) that the functions $\alpha_{j2}^{(m)}$ and $\alpha_j^{(m)}$ are odd functions with respect to x_1. At the same time, by direct calculation, it is proven that:

$$\begin{aligned}&\alpha_{j2}^{(m)}(x_1, x_2) < 0,\ \alpha_j^{(m)}(x_1, x_2) < 0 \quad \text{for } x_1 > 0,\\ &\alpha_{j2}^{(m)}(x_1, x_2) > 0,\ \alpha_j^{(m)}(x_1, x_2) > 0 \quad \text{for } x_1 < 0.\end{aligned} \tag{2.181}$$

For fixed $x_2 (= x_2^*)$ we can write:

$$\begin{aligned}\alpha_{j2}^{(m)}(x_1, x_2^*) &= \left.\frac{\partial \alpha_{j2}^{(m)}}{\partial x_1}\right|_{x_1=0} x_1 + \alpha_{j2}^{(m)}(x_1, x_2^*),\\ \alpha_j^{(m)}(x_1, x_2^*) &= \left.\frac{\partial \alpha_j^{(m)}}{\partial x_1}\right|_{x_1=0} x_1 + \alpha_j^{(m)}(x_1, x_2^*).\end{aligned} \tag{2.182}$$

It follows from (2.182) and from the foregoing discussions that:

$$k_{j2}^{(m)} = \left.\frac{\partial \alpha_{j2}^{(m)}}{\partial x_1}\right|_{x_1=0} < 0,\ k_j^{(m)} = \left.\frac{\partial \alpha_j^{(m)}}{\partial x_1}\right|_{x_1=0} < 0. \tag{2.183}$$

We introduce the notation:

$$|k| = \min\left\{\left|\alpha_{j2}^{(m)}\right|, \left|\alpha_j^{(m)}\right|\right\}. \tag{2.184}$$

According to equations (2.168), (2.181)–(2.184), the expressions given in (2.180) can be presented through multiplication of two terms, one of which is $e^{i(kx_1+\omega t)}$. This is similar to the expression of the wave propagation along the Ox_1 axis. It should be noted that this "wave propagation" is considered in a moving frame of reference. In this case, as it moves, in propagating a wave with angular frequency ω and wave number $|k|$, the observation point oscillates with angular frequency ω in a moving frame of reference. However, in a fixed frame of reference, according to the foregoing discussions and expressions, it oscillates with angular frequency $\omega = \omega - kV$. This follows from the relationship

$$e^{i(kx_1+\omega t)} = e^{i(k(x_1'-Vt)+\omega t)} = e^{i(kx_1'-\omega t)} \Rightarrow \omega = \omega - kV.$$

Hence, according to the expressions and inequalities (2.181)–(2.183), for a fixed frame of reference, the oscillation frequency $\omega = \omega + |k|V$ ($\omega = \omega - |k|V$) of the observation point determined by coordinates $x_1 > 0$ ($x_1 < 0$) increases (decreases).

This statement is known physically as the Doppler Effect. Consequently, the foregoing discussions and results agree with the well-known results of acoustic-physics and prove the validity of the mathematical modeling used for the problem considered.

Now we turn to the numerical calculation of the integrals in (2.174) and (2.176). Note that these integrals are so-called wave-number integrals and for their numerical calculation two type algorithms were used in the related works of the author of the present book and his students. The first of them is based on Cauchy's principal value sense integration, but the second is based on the use of the Sommerfeld contour for calculation of the wave-number integrals (Tsang 1978; Jensen et al. 2011 and etc.). We attempt to describe briefly here these algorithms and first consider the algorithm which is based on Cauchy's principal value sense integration.

To simplify the consideration we consider the calculation of the integral

$$\sigma_{22c}^{(m)} \approx \frac{1}{2\pi^2} \int_{-S_{1^*}}^{+S_{1^*}} \left(\int_0^{+S_{3^*}} \sigma_{2213F}^{(m)} \cos(s_3 x_3) ds_3 \right) \cos(s_1 x_1) ds_1 \tag{2.185}$$

only. For calculation of the definite integral (2.185), first, the interval $[0, S_{3^*}]$ is divided into shorter intervals $[S_{3i}, S_{si+1}]$, $i = 1, 2, \ldots, N$, $S_{30} = 0$, $S_{3N} = S_{3^*}$, where $\cup_{i=1}^{N}[S_{3i}, S_{si+1}] = [0, S_{3^*}]$ and $\cap_{i=1}^{N}[S_{3i}, S_{si+1}] = \emptyset$. Then, the definite integral becomes:

$$\int_0^{S_{3^*}} \left(\int_{-S_{1^*}}^{+S_{1^*}} (\bullet) ds_1 \right) ds_3 = \sum_{i=0}^{N} \int_{S_{3i}}^{S_{3i+1}} \left(\int_{-S_{1^*}}^{+S_{1^*}} (\bullet) ds_1 \right) ds_3, \tag{2.186}$$

where $(\bullet)$ denotes the integrand.

Consequently, we obtain from (2.185) and (2.186):

$$\int_0^{S_{3^*}} \left(\int_{-S_{1^*}}^{+S_{1^*}} (\bullet) ds_1 \right) ds_3 = \sum_{i=0}^{N} \int_{S_{3i}}^{S_{3i+1}} \sigma_{223F}^{(m)} \cos(s_3 x_3) ds_3. \tag{2.187}$$

For calculation of the integrals on the right side in Eq. (2.187) in the intervals $[S_{3i}, S_{si+1}]$, we use the Gauss integration algorithm, where it is necessary to know the values of $\sigma_{223F}^{(m)}(x_1, x_2, s_3)$ at certain nodal points $s_3 = s'_{3k}$. Thus, calculation of the integral (2.186) is reduced to calculation of the integral:

$$\sigma_{223F}^{(m)}(x_1, x_2, s'_{3k}) = \int_{-S_{1^*}}^{+S_{1^*}} \sigma_{2213F}^{(m)}(s_1, x_2, s'_{3k}) \cos(s_1 x_1) ds_1. \tag{2.188}$$

Now we consider the calculation of the integral (2.188).

For this purpose we determine the roots of the Eq. (2.168) with respect to $s_1 h$ (for $s_3 = s'_{3k}$) which are also the singular points of the integral (2.188). Let us denote these roots as:

$$\begin{aligned} &-S_{1^*} < s_{11}^{-}(s'_{3k}) < s_{12}^{-}(s'_{3k}) < \cdots < s_{1M^-}^{-}(s'_{3k}) < 0 < \\ &s_{11}^{+}(s'_{3k}) < s_{12}^{+}(s'_{3k}) < \cdots < s_{1M^+}^{+}(s'_{3k}) < +S_{1^*} \end{aligned} \tag{2.189}$$

and assume that the order of these roots is not greater than one. The numbers M^- and M^+ in (2.189) depend mainly on the values of s'_{3k} and on the problem parameters: the moving load velocity and its oscillation frequency, the mechanical properties of the constituents of the system under consideration and so forth.

After determining the roots (2.189), the interval of integration $[-S_{1^*}, +S_{1^*}]$ in (2.188) is portioned as follows:

$$\int_{-S_{1*}}^{+S_{1*}}(\bullet)ds_1=\int_{-S_{1*}}^{s_{11}^{-}(s'_{3k})-\varepsilon}(\bullet)ds_1+\int_{s_{11}^{-}(s'_{3k})+\varepsilon}^{s_{12}^{-}(s'_{3k})-\varepsilon}(\bullet)ds_1+\cdots$$
$$+\int_{s_{1M-}^{-}(s'_{3k})+\varepsilon}^{s_{11}^{+}(s'_{3k})-\varepsilon}(\bullet)ds_1+\int_{s_{11}^{+}(s'_{3k})+\varepsilon}^{s_{12}^{+}(s'_{3k})-\varepsilon}(\bullet)ds_1+\cdots+\int_{s_{1M+}^{+}(s'_{3k})+\varepsilon}^{+S_{1*}}(\bullet)ds_1. \tag{2.190}$$

Then, the calculation of the integral (2.190) is performed in Cauchy's principal value sense. Here, ε is a very small value determined numerically from the convergence requirement of the integral (2.188). Each interval $\left[s_{1n}^{\pm}+\varepsilon, s_{1n+1}^{\pm}-\varepsilon\right]$ is further divided into a certain number of shorter intervals, which are used in the Gauss integration algorithm. All these procedures are performed using the programs written in MATLAB. Note that in the above procedure, the values of x_1, x_2 and x_3 are fixed.

Now we consider the second type algorithm which is based on the use of the Sommerfeld contour, i.e. the wave-number integral (2.185) is evaluated along the Sommerfeld contour. In this case, using Cauchy's theorem, the contour $[-\infty,+\infty]$ for s_1 is "deformed" into the contour C_{s_1} in the complex plane $s'=s_1+is_2$ and the contour $[-\infty,+\infty]$ for s_3 is deformed into the contour C_{s_3} (Fig. 2.41b) in the complex plane $s''=s_3+is_2$ and in this way the real roots of the Eq. (2.168) are avoided. Thus, the integral (2.173) in the form $\int_{-\infty}^{+\infty}\int_{-\infty}^{+\infty}f_{F13}(s_1,x_2,s_3)e^{i(s_1x_1+s_3x_3)}ds_1ds_3$ are replaced with corresponding ones in the form $\int_{C_{s_1}}\varphi(s',x_2)e^{is'x_1}ds'$, where $\varphi(s',x_2)=\int_{C_{s_3}}f_{F13}(s',x_2,s'')e^{is''x_3}ds''$ and the stresses and displacements in (2.174) are determined as a real part of this integral, i.e. $\mathrm{Re}\int_{C_{s_1}}\varphi(s',x_2)e^{is'x_1}ds'$. According to Fig. 2.41b, we can write the following relations:

$$\int_{C_{s_3}}f_{F13}(s',x_2,s'')e^{is''x_3}ds''=\int_{-\infty}^{0}f_{F13}(s',x_2,s_3-is_2^*)e^{i(s_3-is_2^*)x_3}ds_3$$
$$+i\int_{-s_2^*}^{+s_2^*}f_{F13}(s',x_2,is_2)e^{-s_2x_3}ds_2$$
$$+\int_{0}^{+\infty}f_{F13}(s',x_2,s_3+is_2^*)e^{i(s_3+is_2^*)x_3}ds_3$$

$$\int\limits_{C_{s_1}} \varphi(s', x_2) e^{is' x_1} ds' = \int\limits_{-\infty}^{0} \varphi(s_1 - is_2^*, x_2) e^{i(s_1 - is_2^*)x_1} ds_1 + i \int\limits_{-s_2^*}^{+s_2^*} \varphi(is_2, x_2) e^{-s_2 x_1} ds_2 + \int\limits_{0}^{+\infty} \varphi(s_1 + is_2^*, x_2) e^{i(s_1 + is_2^*)x_1} ds_1. \tag{2.191}$$

Taking into account the fact that the values of the integral $\int_{C_{s_1}} \varphi(s', x_2) e^{is' x_1} ds'$ are independent of the values of the parameter $s_2^* > 0$, then as usual, in order to simplify the calculation procedure of this integral the parameter s_2^* is assumed to be small. According to this assumption, we can write

$$\left| \int\limits_{-s_2^*}^{+s_2^*} f_{F13}(s', x_2, is_2) e^{-s_2 x_3} ds_2 \right| = O(s_2^*), \quad \left| \int\limits_{-s_2^*}^{+s_2^*} \varphi(is_2, x_2) e^{-s_2 x_1} ds_2 \right| = O((s_2^*)^2). \tag{2.192}$$

Taking the estimation (2.192) into account, for calculation of the integral $\int_{C_{s_1}} \varphi(s', x_2) e^{is' x_1} ds'$ we can use the following approximate expressions:

$$\begin{aligned} \int\limits_{C_{s_3}} f_{F13}(s', x_2, s'') e^{is'' x_3} ds'' &\approx \int\limits_{-\infty}^{0} f_{F13}(s', x_2, s_3 - is_2^*) e^{i(s_3 - is_2^*)x_3} ds_3 \\ &\quad + \int\limits_{0}^{+\infty} f_{F13}(s', x_2, s_3 + is_2^*) e^{i(s_3 + is_2^*)x_3} ds_3 \\ \int\limits_{C_{s_1}} \varphi(s', x_2) e^{is' x_1} ds' &\approx \int\limits_{-\infty}^{0} \varphi(s_1 - is_2^*, x_2) e^{i(s_1 - is_2^*)x_1} ds_1 \\ &\quad + \int\limits_{0}^{+\infty} \varphi(s_1 + is_2^*, x_2) e^{i(s_1 + is_2^*)x_1} ds_1 \end{aligned} \tag{2.193}$$

Note that the accuracy of the expressions in (2.193) with respect to values of the parameter s_2^* will be discussed in the next chapter. Moreover under calculation procedure, the improper integrals $\int_{-\infty}^{0}(\bullet)ds_3$, $\int_{0}^{+\infty}(\bullet)ds_3$, $\int_{-\infty}^{0}(\bullet)ds_1$ and $\int_{0}^{+\infty}(\bullet)ds_1$ in (2.193) are replaced by the corresponding definite integrals $\int_{-S_3^*}^{0}(\bullet)ds_3$, $\int_{0}^{+S_3^*}(\bullet)ds_3$, $\int_{-S_1^*}^{0}(\bullet)ds_1$ and $\int_{0}^{+S_1^*}(\bullet)ds_1$ respectively. The values of S_1^* and S_3^* are determined from the convergence requirement of the numerical results. Note that under calculation of the latter integrals, the integration intervals are further divided into a certain number of shorter intervals, which are used in the Gauss integration algorithm. In this integration procedure it is assumed that in each of the shorter intervals the sampling intervals of the numerical integration Δs_1 and Δs_3 must satisfy the relations $|\Delta s_1| \ll \min\{s_2^*, 1/x_1\}$ and $|\Delta s_3| \ll \min\{s_2^*, 1/x_3\}$ respectively. All these procedures are performed automatically with the PC by use of the corresponding programs constructed by the author and his students in MATLAB.

This completes the discussions related to the algorithms employing for calculation of the wave-number integrals in the form (2.173). Note that numerical results which will be analyzed below are obtained simultaneously with the use of the both above considered algorithms and the comparison show that the results obtained by the use of the algorithm based on the Cauchy's principal value sense coincide almost completely with corresponding ones obtained by the use of the Sommerfeld contour. An example for such comparison will be given below and we will consider here numerical results obtained by the use of the algorithm based on the Cauchy's principal value sense.

2.7.4 Numerical Results and Discussions

Here we consider the numerical results related to Cases 1 ($V > 0,\ \Omega = 0$) and 3 ($V > 0,\ \Omega > 0$). Note that the numerical results related to Case 2 ($V = 0,\ \Omega > 0$) will be analyzed in the next chapter.

Case 1 ($V > 0,\ \Omega = 0$). We consider the cases where $E^{(1)} > E^{(2)}$, and assume that $\rho^{(2)}/\rho^{(1)} = 0.35,\ \nu^{(1)} = \nu^{(2)} = 0.3$. Introduce the notation $c_r = V/c_R^{(2)}$, where $c_R^{(2)}$ is the Rayleigh wave velocity in the half-space material. Consider the dependence $c_r = c_r(s_1 h, s_3 h)$ which is obtained from the solution to the Eq. (2.169) for fixed values of the problem parameters. As it has already been noted, we assume that $c < \min(c_2^{(1)}/c_R^{(2)}, c_2^{(2)}/c_R^{(2)})$. In other words, in the considered case we assume that $c_r < c_2^{(2)}/c_R^{(2)}$, i.e. the subsonic case is considered. For this case the surface-graph of the dependence $c_r = c_r(s_1 h, s_3 h)$ is given in Fig. 2.42. As can be predicted this graph is symmetric with respect to $s_1 h = 0$ and $s_3 h = 0$, and the points for which

$$\frac{\partial c}{\partial (s_1 h)} = 0 \text{ and } \frac{\partial c}{\partial (s_3 h)} = 0 \tag{2.194}$$

are satisfied simultaneously, arise at $s_3 h = 0$.

Note that the critical velocity corresponding to this point coincides with the critical velocity obtained for the corresponding problem regarding the plane-strain state. This statement is proven by direct verification of the values of the critical velocity obtained within the scope of the three dimensional approach with the corresponding values obtained within the scope of the plane-strain state considered in the previous sections. Therefore the critical velocity corresponding to the case (2.194) we denote by $c_{cr.\min}$.

According to the definition (2.171) each of the points of the convex part of the surface $c_r = c_r(s_1 h, s_3 h)$ (Fig. 2.42); (i.e. each value of c for which the inequality $c_{cr.\min} < c_r < c_2^{(1)}/c_R^{(2)}$ is satisfied) is also the critical velocity. This is because, each fixed $s_1 h$ (or $s_3 h$) (i.e. the intersection between the plane $s_1 h = const$ (or $s_3 h = const$) and the surface $c_r = c_r(s_1 h, s_3 h)$) gives the curve which contains the point for which $\frac{\partial c}{\partial (s_3 h)} = 0$ $\left(\text{or } \frac{\partial c}{\partial (s_1 h)} = 0\right)$. But, within the plane-strain approach, the velocity c (the values of which are greater than the critical velocity) is not a critical one.

Now we analyze the question of how the initial stresses act on the values of the critical velocities. Note that the detailing of the numerous numerical results (which are not given here) shows that the initial stresses $\sigma_{33}^{(m),0}$ do not influence the values of the critical velocity and its change range. However, the values of the initial stresses $\sigma_{11}^{(m),0}$ which act along the direction of the moving load velocity, influence the values of the critical velocity and its the change range. This influence is illustrated by the data given in Table 2.25 which show the values of $c_{cr.\min}$

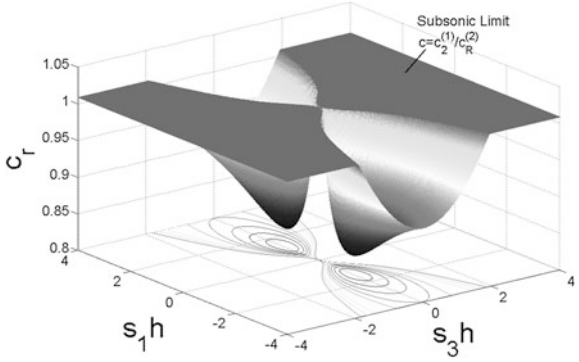

Fig. 2.42 The surface-graph of the dependencies between $c_r = c_r(s_1 h, s_3 h)$ where $c_r = V/c_R^{(2)}$ for the case where $E^{(2)}/E^{(1)} = 0.4$, $\sigma_{11}^{(m)0} = 0$, $\sigma_{33}^{(m)0} = 0$, $\rho^{(2)}/\rho^{(1)} = 0.35$, $\nu^{(1)} = \nu^{(2)} = 0.3$

Table 2.25 The influence of the initial stress of the covering layer $\eta_{11}^{(1)}(=\sigma_{11}^{(1)0}/\mu^{(1)})$ and half-space $\eta_{11}^{(2)}(=\sigma_{11}^{(2)0}/\mu^{(2)})$ on the values of c_{cr} for various $E^{(2)}/E^{(1)}$ in the case where $\rho^{(2)}/\rho^{(1)} = 0.35$, $\nu^{(1)} = \nu^{(2)} = 0.3$

	$E^{(2)}/E^{(1)}$			
		0.4	0.3	0.2
$\eta_{11}^{(1)}$	0.000	0.8256	0.8650	0.9096
	0.015	0.8328	0.8734	0.9201
	0.025	0.8377	0.8790	0.9268
$\eta_{11}^{(2)} = 0$	0.075	0.8610	0.9055	0.9587
$\eta_{11}^{(1)} = 0$	−0.025	0.8218	0.8602	0.9036
	−0.015	0.8234	0.8622	0.9061
	0.015	0.8278	0.8678	0.9132
$\eta_{11}^{(2)}$	0.025	0.8292	0.8697	0.9155

calculated for various values of $E^{(2)}/E^{(1)}$. In other words, the Table 2.25 shows the influence of the initial stresses $\sigma_{11}^{(m),0}$ on the lower limit values of the critical velocity. But the influence of these stresses on the upper limit of the critical velocity can be determined through the expression:

$$c_{cr.\max} = \min\left\{\frac{c_2^{(1)}}{c_R^{(2)}}\sqrt{1+\frac{\sigma_{11}^{(1),0}}{\mu^{(1)}}};\ \frac{c_2^{(2)}}{c_R^{(2)}}\sqrt{1+\frac{\sigma_{11}^{(2),0}}{\mu^{(2)}}}\right\}. \tag{2.195}$$

Introduce the notation $\eta_{11}^{(m)} = \sigma_{11}^{(m),0}/\mu^{(m)}$, $\eta_{33}^{(m)} = \sigma_{33}^{(m),0}/\mu^{(m)}$ and consider the distribution of the normal stress $\sigma_{22} = \sigma_{22}^{(1)}(x_1, x_2, x_3)\Big|_{x_2=-h} = \sigma_{22}^{(2)}(x_1, x_2, x_3)\Big|_{x_2=-h}$ with respect to the point of the inter-medium plane. This distribution is given in Fig. 2.43 for the case where $E^{(2)}/E^{(1)} = 0.4$, $c = 0.4$, $\eta_{11}^{(m)} = 0$, $\eta_{33}^{(m)} = 0$. It follows from this result that the absolute maximal values of the considered stresses appear at the point for which $x_1 = x_3 = 0$. Taking this statement into account consider the change of the values σ_{22} obtained at point $x_1 = x_3 = 0$ with respect to c_r and with respect to the initial stresses. The graphs of the dependence between σ_{22} and c_r constructed for various values of $\eta_{11}^{(1)}$ and $\eta_{33}^{(1)}$ are given in Fig. 2.44a–c for the cases where $E^{(2)}/E^{(1)} = 0.4$, 0.3 and 0.2 respectively. It follows from these results that the absolute values of σ_{22} increase with the velocity of the moving load. A comparison of the values of the stresses obtained here (denoted by σ_{22T}) with the corresponding values of those obtained for the plane strain state (denoted by σ_{22P}) shows that the values of σ_{22T} are less significant than the values of σ_{22P}. Moreover, the results given in Fig. 2.44 show that the initial stretching of the covering layer results in a decrease of the absolute values of the stress σ_{22}. This result can be explained with the fact that as a result of the initial stretching (compressing) stress

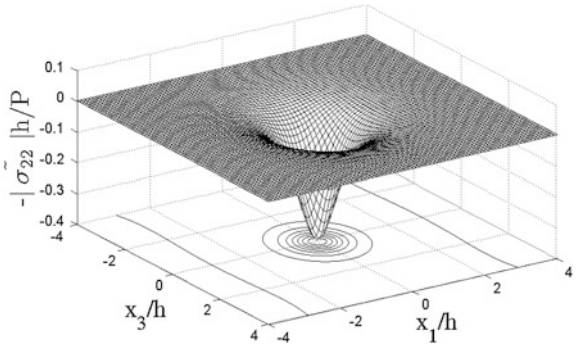

Fig. 2.43 Distribution of the normal stress $\sigma_{22}(x_1, x_3)$ on the interface plane with respect to x_1/h and x_3/h for the case where $\eta_{11}^{(m)} = 0$, $\eta_{33}^{(m)} = 0$ $(m = 1, 2)$, $E^{(2)}/E^{(1)} = 0.4$, $c_r = 0.4$

in structural element made of linear elastic material, causes to increase (to decrease) of the stiffness of this element.

Case 3 ($V > 0,\ \Omega > 0$). We note again that the Case 2 ($V = 0,\ \Omega > 0$) will be considered in the next chapter. Therefore here, we do not consider the numerical results related to Case 2.

Thus, we consider the numerical results related to Case 3. These results are obtained for the following pair of materials selected for a covering layer and half-space: Aluminum (*Al*) with properties $\rho = 2{,}700\,\text{kg/m}^3$, $\nu = 0.35$, $c_1 = 6{,}429\,\text{m/s}$, $c_2 = 3{,}110\,\text{m/s}$; Steel (*St*) with properties $\rho = 7{,}680\,\text{kg/m}^3$, $\nu = 0.29$, $c_1 = 5{,}890\,\text{m/s}$, $c_2 = 3{,}210\,\text{m/s}$, where ρ, ν, c_1 and c_2 are the material density, Poisson coefficient, dilatation and distortion waves' speed, respectively. Numerical investigations are carried out for the following two cases: in case I where the materials of the layer and half-space are selected as *St* and *Al* (denoted by $St + Al$) and in case II where the materials of the layer and half-space are selected as *Al* and *St* (denoted by $Al + St$).

First, we analyze the dependence of the critical velocity on the oscillation frequency Ω. For this purpose we consider the graphs of the function $c_r = c_r(s_1 h, \Omega)$ obtained from the solution to the Eq. (2.168) under $s_3 h = 0$. It should be noted that in the previous subsection, i.e. in the case where $\Omega = 0$, taking the symmetry of the Eq. (2.169) with respect to $s_1 h = 0$ into account, for analyses of the dependence $c_r = c_r(s_1 h)$, it is sufficient to consider this dependence only in the interval $0 \le s_1 h < +\infty$. However, in the present case, i.e. where $\Omega > 0$, according to the Doppler Effect, which arises through the term $2\Omega V s_1$ in expression (2.163), this symmetry is violated. Therefore, in the case where $\Omega > 0$, analyses of the dependence $c_r = c_r(s_1 h, \Omega)$ must be done for $-\infty < s_1 h < +\infty$. For illustration of this statement, we consider the graphs of the noted dependence given in Fig. 2.45 which correspond to the case I, i.e. the case where the covering layer (the half-space) material is $St(Al)$. These graphs are constructed for various values of Ω. It follows from this figure that the graphs constructed in the case where $\Omega = 0$, as expected, are symmetric with

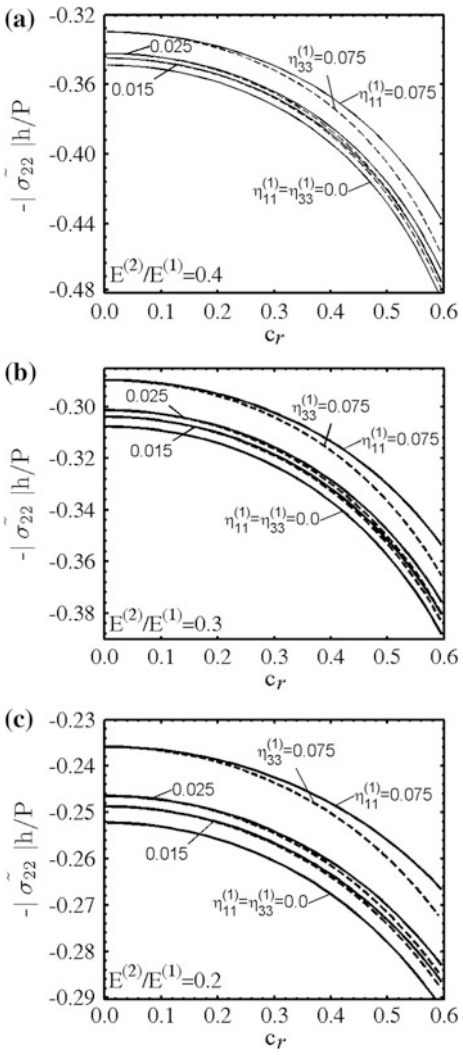

Fig. 2.44 The graphs of the dependencies between the normal stress $\sigma_{22}(0,-h,0)h/P_0$ and c_r for various values of $\eta_{11}^{(1)}$ and $\eta_{33}^{(1)}$: **a** for $E^{(2)}/E^{(1)} = 0.4$, **b** $E^{(2)}/E^{(1)} = 0.3$, **c** $E^{(2)}/E^{(1)} = 0.2$

respect to the straight line determined by the equation $s_1 h = 0$. However, as has been noted above, this symmetry is violated for the graphs constructed under $\Omega > 0$. The analyses of the numerical results show that up to certain Ω (denoted by Ω') the values of the "minimum" critical velocity (denoted by c'_{cr}) are determined by the left branches, i.e. by those branches obtained in the region $s_1 h < 0$.

Figure 2.45 shows that for the certain values of Ω, the following values (by magnitude) of the critical velocity (denoted by $c''_{cr}(>c'_{cr})$) are also determined by the aforementioned left branches. The critical velocities of the moving load determined by the right branches, i.e. by the branches obtained in the region $s_1 h > 0$, we denote through c'''_{cr} which is greater than c''_{cr}. Thus, according to the

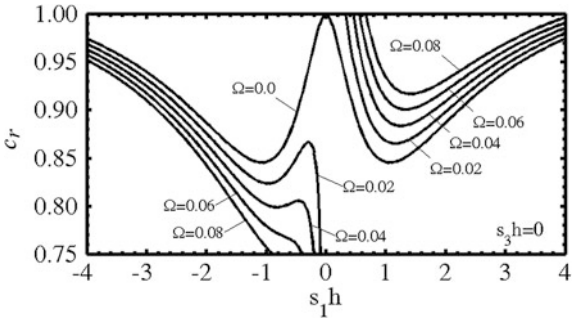

Fig. 2.45 The graphs of the dependencies between c and s_1h constructed under $s_3h = 0$ for various values of Ω in the case where the covering layer (the half-space) material is $St(Al)$

results given in Fig. 2.45 we can conclude that up to certain values of the oscillation frequency (i.e. up to Ω') of the moving load, as a result of the oscillation of this load, the critical velocities c'_{cr} and c''_{cr} decrease with Ω. However, in the case where $\Omega > \Omega'$ the left branches of the graphs do not determine the critical velocity; in other words, on these branches, the point for which the equation $dc/d(s_1h) = 0$ is satisfied, the critical velocity does not occur, but the right branches of the graphs determine the values of c'''_{cr} for the case where $\Omega > \Omega'$. This procedure continues up to a certain value of Ω (denoted by Ω'') after which the value of c'''_{cr} goes outside of the framework of the subsonic moving regime.

It should be noted that the numerical results shown in Fig. 2.45, in the qualitative sense, agree with the corresponding results obtained in Sects. 2.4 and 2.6 and in papers by Dieterman and Metrikine (1997), Metrikine and Vrouwenvelder (2000).

We do not consider here the influence of the initial stresses of the constituents on the values of the critical velocities, because this influence is the same (in the qualitative sense) as the previous subsection. Note that the numerical results discussed above also relate to the corresponding plane-strain state. Consequently, these results are also new ones for the corresponding plane-strain state for the selected pair of materials. However, in the present case, according to the results obtained in the 3D case, all velocities which satisfy the relation:

$$\begin{aligned} c'_{cr} < c_r < \min\left\{\frac{c_2^{(1)}}{c_R^{(2)}}; \frac{c_2^{(2)}}{c_R^{(2)}}\right\} \quad \text{for } \Omega < \Omega', \\ c'''_{cr} < c_r < \min\left\{\frac{c_2^{(1)}}{c_R^{(2)}}; \frac{c_2^{(2)}}{c_R^{(2)}}\right\} \quad \text{for } \Omega' < \Omega < \Omega''. \end{aligned} \tag{2.196}$$

are also critical ones.

We recall that the foregoing numerical results on the critical velocity have been obtained for case I, i.e. for the case where the covering layer (the half-space) material is $St(Al)$. The numerical investigations show that the critical velocity, as

determined above, does not exist for the case II, i.e. for the case where the covering layer (the half-space) material is $Al(St)$. This statement proves again that in the case where the modulus of elasticity of the covering layer is greater than that of the half-space material, the critical velocity of the moving load does not exist.

Now we consider the numerical results related to the distribution of the normal stress which acts on the interface plane between the covering layer and half space. We introduce the notation:

$$\sigma_{22}(x_1, x_3, t) = \sigma_{22}^{(1)}(x_1, x_2 = -h, x_3, t) = \sigma_{22}^{(2)}(x_1, x_2 = -h, x_3, t). \tag{2.197}$$

First we consider the dependence of the values of the modulus of the stress σ_{22} (2.197), i.e. of the $|\sigma_{22}|$ at $x_1 = x_3 = 0$ and Ω obtained for various velocities of the moving load, i.e. for various c. The graphs of this dependence are given in Fig. 2.46. Note that the graphs given in Fig. 2.46a (in Fig. 2.46b) are obtained for the pair of materials $St + Al$ $(Al + St)$. In this figure the results obtained in the case where $c = 0$ coincide with the corresponding ones which will be obtained in the next section.

Moreover in Fig. 2.46b corresponding numerical results obtained under $s_2^* h = 0.01$ by the use of the Sommerfeld contour and these results are indicated by the dashed lines. It follows from the comparison of the results obtained by the use of the Sommerfeld contour with the corresponding ones obtained by the use of Cauchy's principal value sense algorithm that the difference between them is insignificant. Note that this insignificant difference arises only in the case shown in Fig. 2.46b. In other cases which are analyzed here these results coincide with each other almost completely.

It follows from the results that the dependence between $|\sigma_{22}|$ and Ω is non-monotonic for the considered pair of materials. This means that there exists such a value of the oscillation frequency Ω (denoted by Ω_* and called the "resonance" value of Ω) of the moving load under which the modulus of the normal stress σ_{22} (2.194) has its absolute maximum. Note that this result agrees (in the quantitative sense) with the corresponding ones obtained in the previous sections and with the results which will be discussed in the next chapter. Moreover, the non-monotonic character of the dependence between $|\sigma_{22}|$ and Ω agrees with the well-known results by Lamb (1904), Robertson (1966), Gladwell (1968) and others, according to which, the behavior of the half-space under forced vibration is similar to a system which comprises a mass, a parallel connected spring and dashpot. It follows from the graphs given in Fig. 2.46 that the behavior of the half-space covered with the layer under action of the oscillating moving load is also similar to the system which comprises a mass, a parallel connected spring and dashpot.

Now we attempt to explain how the moving velocity of the oscillating load influences the aforementioned character of the mechanical system under consideration. For this purpose we introduce the following notation: through Ω_{I^*} and Ω_{II^*} we denote the resonance value of the Ω obtained for the pair of materials $St + Al$ and $Al + St$, respectively. It follows from the results given in Fig. 2.46 that the values of Ω_{I^*} are less significant than the corresponding values of Ω_{II^*}, i.e.

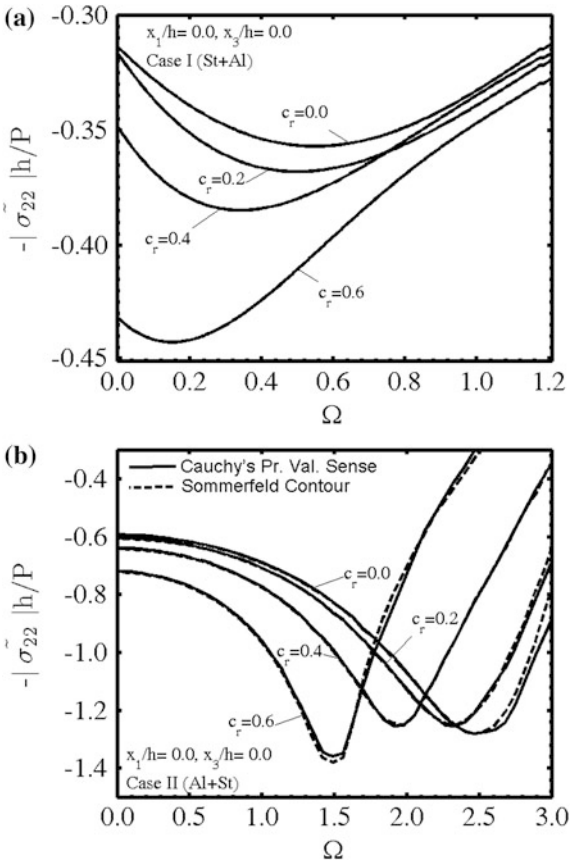

Fig. 2.46 The graphs of dependence between $|\tilde{\sigma}_{22}|$ and Ω constructed for various values of the moving load velocity c_r in the case where: **a** *St* (covering layer) + *Al* (half-space); **b** *Al* (covering layer) + *St* (half-space): *dashed lines* show the results obtained by the use of the Sommerfeld contour

$\Omega_{I^*} < \Omega_{II^*}$. This conclusion agrees with the corresponding one obtained in the paper by Akbarov and Guler (2007) for the plane-strain state, which will be also discussed in the next chapter. Moreover, the results given in Fig. 2.46 show that the values of Ω_{I^*} and Ω_{II^*} decrease with the moving velocity of the external force. This is a new main result which has a great significance in the application sense.

A comparison of the numerical results obtained in the case where $c = 0$ and illustrated in Fig. 2.46 with the corresponding ones given in the paper by Akbarov and Guler (2007) shows that the values of $|\sigma_{22}|$ obtained for the present 3D problem are less significant than the absolute values of that obtained for the plane-strain state.

Consider also the graphs of the dependence between $|\sigma_{22}|$ at $x_1 = 0$ and $x_3 = 0$, and the moving load velocity c constructed for various values of Ω under $\eta_{11}^{(m)} = 0$, $\eta_{33}^{(m)} = 0$. These graphs are given in Fig. 2.47 for the pair of materials $St + Al$ (Fig. 2.47a) and $Al + St$ (Fig. 2.47b). It follows from these graphs that the modulus of the stress σ_{22} increases monotonically with the velocity of the moving load.

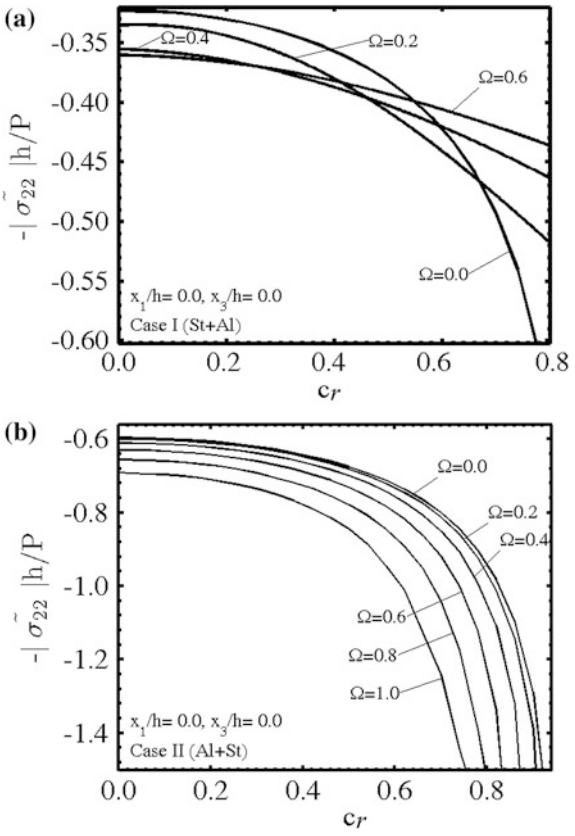

Fig. 2.47 The graphs of dependence between $|\tilde{\sigma}_{22}|$ and c_r constructed for various values of the moving load oscillation frequency Ω in the case where: **a** *St* (covering layer) + *Al* (half-space); **b** *Al* (covering layer) + *St* (half-space)

Now we analyze the influence of the initial stretching of the covering layer, i.e. the influence of the parameters $\eta_{11}^{(1)}\,(>0)$ and $\eta_{33}^{(1)}\,(>0)$ on the values of $|\sigma_{22}|$.

Consider only the case where the material of the covering layer (the half-space) material is $Al(St)$. According to the mechanical consideration the initial stretching of the covering layer must result in a decrease in the values of $|\sigma_{22}|$. This prediction is proven with the graphs given in Fig. 2.48 which show the dependencies between $|\sigma_{22}|$ and Ω (Fig. 2.48a, c) as well as between $|\sigma_{22}|$ and c (Fig. 2.48b, d). Note that the results given in Fig. 2.48a, b (in Fig. 2.48c, d) illustrate the influence of the initial stretching of the covering layer in the direction of the Ox_1 (Ox_3) axis, i.e. the influence of the parameter $\eta_{11}^{(1)}\,(>0)$ under $\eta_{33}^{(1)}=0$ (of the parameter $\eta_{33}^{(1)}\,(>0)$ under $\eta_{11}^{(1)}=0$) on the values of $|\sigma_{22}|$ at $x_1=0$ and $x_3=0$. It follows from these results that the values of $|\sigma_{22}|$ decrease monotonically both with $\eta_{11}^{(1)}$ and $\eta_{33}^{(1)}$.

Now we consider the distribution of the stress σ_{22} (2.197) with respect to the x_1 coordinate under $x_3=0$. Assume that the material of the covering layer (the half-space) is $St(Al)$. Moreover, assume that $\omega t=\pi/4$ in (2.178) and $\eta_{11}^{(m)}=\eta_{33}^{(m)}=0$

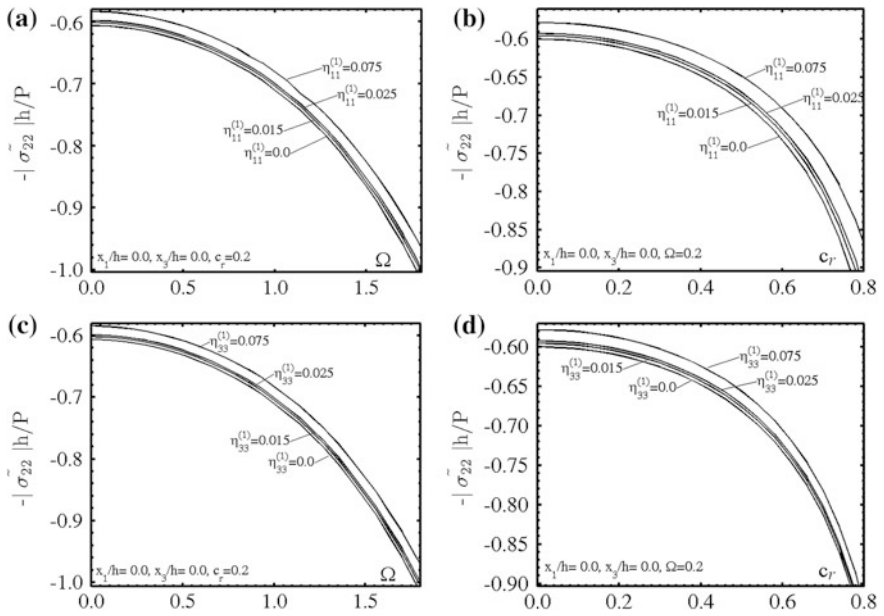

Fig. 2.48 The influence of the pre-stresses of the covering layer in the direction of the Ox_1 axis (Fig. 2.48a, b) and in the direction of the Ox_3 axis (Fig. 2.48c, d) on the dependence between $|\sigma_{22}|$ and Ω as well as between $|\sigma_{22}|$ and c_r. The case where the material of the covering layer (the half-space) is *Al*(*St*)

$(m = 1, 2)$. The graphs of the mentioned distribution are given in Fig. 2.49 which are constructed for various values of Ω under $c = 0.6$ (Fig. 2.49a). Note that Fig. 2.49b shows the zoom of these graphs in the near vicinity of the point $x_1/h = 0$. The graphs show the non-symmetry of the considered distribution with respect to $x_1/h = 0$, which is caused by the Doppler Effect, although the mentioned non-symmetry is slight for the case under consideration.

Finally, we note that the interface plane between the covering layer and half-space acts not only on the normal stress σ_{22} (2.197) but also on the shear stresses and

$$\sigma_{32}(x_1, x_3, t) = \sigma_{32}^{(1)}(x_1, x_2 = -h, x_3, t) = \sigma_{32}^{(2)}(x_1, x_2 = -h, x_3, t).$$

However, the absolute maximum values of these shear stresses are several times less than that of the foregoing normal stress. As an example we consider the graphs given in Fig. 2.50 which show the dependence between $|\sigma_{32}|$ at $x_1/h = 0$, $x_3/h = 0.5$ and Ω under $\eta_{11}^{(m)} = 0$ and $\eta_{33}^{(m)} = 0$. These graphs are constructed for various values of moving load velocity c for the system consisting of *St* (the covering layer) and *Al* (the half-space). A comparison of these results with the corresponding ones given in Fig. 2.46a confirms the foregoing conclusion about the relation between the absolute values of the normal and shear stresses. Moreover, the results given in

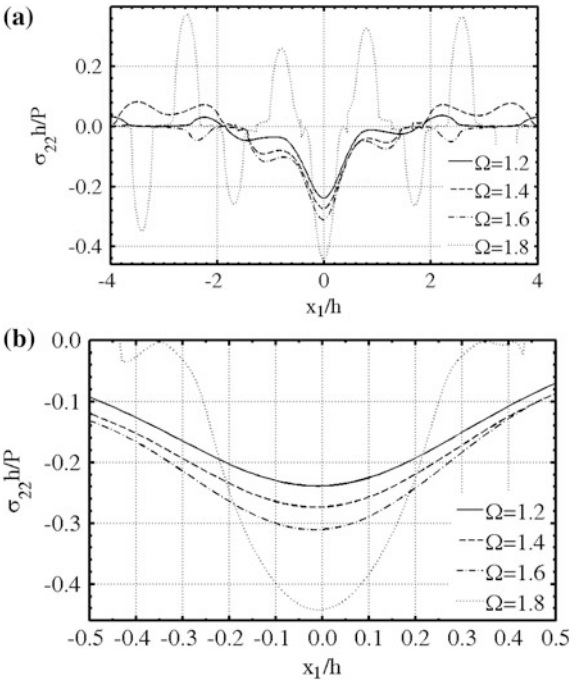

Fig. 2.49 The distribution of the normal stress stress σ_{22} (2.197) with respect to coordinate x_1 (under $x_3 = 0$) obtained for various values of Ω for $c_r = 0.6$ in the case where the material of the covering layer (the half-space) is *St*(*Al*) (**a**). The zoom of the results around the point $x_1/h = 0$ (**b**)

Fig. 2.50 and the results given in Fig. 2.46a show that the "resonance" values Ω_{I^*} of the frequency Ω obtained for the normal stress σ_{22} (denoted by $\Omega_{I^*\sigma_{22}}$) differ from those obtained for the shear stress σ_{32} (denote it by $\Omega_{I^*\sigma_{32}}$), i.e. $\Omega_{I^*\sigma_{32}} > \Omega_{I^*\sigma_{22}}$. This conclusion occurs also for other related quantities and shows the importance of the investigation of the normal stress σ_{22} in the sense of the determination of the adhesion strength of the system under consideration.

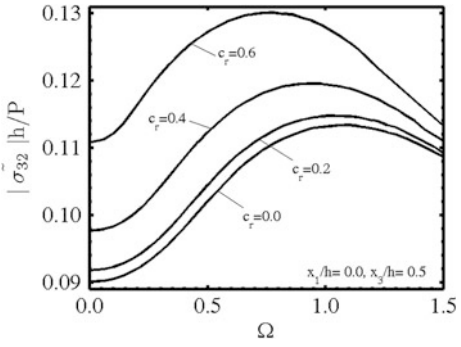

Fig. 2.50 The graphs of the dependence between $|\sigma_{32}|$ and Ω constructed for various values of the moving load velocity c_r

2.7.5 Conclusions

Thus, in the present section the 3D problem of the dynamics of the oscillating moving point-located force acting on the system consisting of the pre-stressed covering layer and pre-stressed half-space has been studied within the scope of the TDLTEWISB. The solution method and the algorithm for obtaining the numerical results are developed and employed. The numerical results on the critical velocity and the stress distribution are presented and discussed. According to this discussion the following conclusions can be reached:

- the minimum (lower limit) of the critical velocity of the point-located moving load acting on the system consisting of the covering layer and half-space coincides with the critical velocity obtained for the corresponding plane-strain state problem;
- each velocity of the point-located moving load which is greater than the minimum (lower limit) value and less than $\min\left(c_2^{(1)}\sqrt{1+\sigma_{11}^{(1)0}/\mu^{(1)}},\ c_2^{(2)}\sqrt{1+\sigma_{11}^{(2)0}/\mu^{(2)}}\right)$ is also the critical velocity, where $c_2^{(1)}\left(c_2^{(2)}\right)$ is the shear wave velocity in the covering layer (half-space) material, $\sigma_{11}^{(1),0}\left(\sigma_{11}^{(2),0}\right)$ is the initial stress in the covering layer (half-space) and $\mu^{(1)}\left(\mu^{(2)}\right)$ is the shear modulus of the covering layer (half-space) material;
- the initial stretching or compressing along the direction which is perpendicular to the moving direction of the load does not have any influence on the values or the change range of the critical velocity;
- the initial stretching (compressing) of the constituents of the considered system along the moving direction of the load results in an increase (a decrease) in the lower and upper limit values of the critical velocity;
- the existence and the values of the critical velocity of the moving load depend significantly on its oscillation frequency: there exists such a value of the frequency Ω (denoted by Ω') before which the minimum value of the critical velocity decreases with Ω, but in the case where $\Omega > \Omega'$ the values of the critical velocity increase with Ω;
- the "resonance" values of the oscillation frequency under which the absolute values of the normal stress acting on the interface plane between the covering layer and half-space has its maximum, decrease with the velocity of the moving load;
- the "resonance" values of the aforementioned normal stress increase with the velocity of the moving load;
- the absolute values of the considered normal stress are less than the corresponding ones obtained for the plane-strain state;
- the initial stretching of the covering layer in the direction which is perpendicular to the moving direction of the external load as well as the initial stretching of the

covering layer in the moving direction of the external load results in a decrease in the absolute values of the aforementioned normal stress;
- numerical results obtained by the use of the algorithm based on the Cauchy's principal value sense coincide almost completely with corresponding ones obtained by the algorithm based on the Sommerfeld contour integration method.

2.8 Oscillating Moving Load Problems Related to Systems Consisting of Viscoelastic Constituents

In the present section, according to a work by Akbarov et al. (2014), we attempt to develop of the investigation carried out in the previous sections to the case where the material of the covering layer and half space are a time-dependent ones. Namely, we assume that these materials are linear viscoelastic. Moreover, for simplicity of the consideration we assume that the constitutive relations of the materials of the constituents of the system under consideration are described through the standard linear solid model. Also, for simplicity of the consideration, all the development mentioned above we will make with respect to the problem considered in Sect. 2.2.

2.8.1 Formulation of the Problem

We consider the system consisting of the pre-stressed covering layer and pre-stressed half-plane, and sketched in Fig. 2.1. Assume that the materials of the covering layer and half-plane are time-dependent, in particular, linear viscoelastic. We use the "own time" conception, according to which, the change of the initial stresses with respect to time is very slow than that related to the perturbation quantities, and therefore the initial stresses in the covering layer and half-plane can be taken as constant under investigation of the response of the system to the moving or oscillating moving load. Consequently, we assume that the relation (2.1) occurs also in the case under consideration and below we use the notation accepted in Sect. 2.2, if otherwise not specified.

For compactness of the consideration here we write again the equation of motion

$$\frac{\partial \sigma_{ij}^{(m)}}{\partial x_i} + \sigma_{11}^{(m)0} \frac{\partial^2 u_j^{(m)}}{\partial x_1^2} = \rho^{(m)} \frac{\partial^2 u_j^{(m)}}{\partial t^2}, \quad i; j; m = 1, 2, \tag{2.198}$$

strain-displacement relation

$$\varepsilon_{ij}^{(m)} = \frac{1}{2}\left(\frac{\partial u_i^{(m)}}{\partial x_j} + \frac{\partial u_j^{(m)}}{\partial x_i}\right) \tag{2.199}$$

boundary condition on the upper face plane of the covering layer

$$\sigma_{12}^{(1)}\Big|_{x_2=0} = 0, \sigma_{22}^{(1)}\Big|_{x_2=0} = -Pe^{i\omega t}\delta(x_1 - Vt), \tag{2.200}$$

complete contact condition on the inter-plane between the covering layer and half-plane

$$\sigma_{i2}^{(1)}\Big|_{x_2=-h} = \sigma_{i2}^{(2)}\Big|_{x_2=-h},\ u_i^{(1)}\Big|_{x_2=-h} = u_i^{(2)}\Big|_{x_2=-h}, \tag{2.201}$$

and the decay condition

$$\left|u_i^{(2)}\right| \to 0,\ \left|\sigma_{ij}^{(2)}\right| \to 0 \quad \text{as} \quad x_2 \to -\infty. \tag{2.202}$$

Thus, now we focus our attention on the constitutive relations of the materials of the constituents. We use the differential form of the constitutive relations related to the "standard linear solid body" model (see Rabotnov 1980). These relations for the plane strain state can be written as follows.

$$\begin{aligned}
&\frac{d\sigma_{11}^{(m)}}{dt} + q^{(m)}\sigma_{11}^{(m)} = \lambda_0^{(m)}\left(\frac{d\theta^{(m)}}{dt} + r_\lambda^{(m)}\theta^{(m)}\right) + 2\mu_0^{(m)}\left(\frac{d\varepsilon_{11}^{(m)}}{dt} + r_\mu^{(m)}\varepsilon_{11}^{(m)}\right),\\
&\frac{d\sigma_{22}^{(m)}}{dt} + q^{(m)}\sigma_{22}^{(m)} = \lambda_0^{(m)}\left(\frac{d\theta^{(m)}}{dt} + r_\lambda^{(m)}\theta^{(m)}\right) + 2\mu_0^{(m)}\left(\frac{d\varepsilon_{22}^{(m)}}{dt} + r_\mu^{(m)}\varepsilon_{22}^{(m)}\right),\\
&\frac{d\sigma_{12}^{(m)}}{dt} + q^{(m)}\sigma_{12}^{(m)} = +2\mu_0^{(m)}\left(\frac{d\varepsilon_{12}^{(m)}}{dt} + r_\mu^{(m)}\varepsilon_{12}^{(m)}\right).
\end{aligned} \tag{2.203}$$

Here $\lambda_0^{(m)}$ and $\mu_0^{(m)}$ are the instantaneous values of the Lame constants, $q^{(m)}$, $r_\lambda^{(m)}$ and $r_\mu^{(m)}$ are rheological parameters of the mth constituent of the system under consideration. It is evident from (2.203) that the long-term values of the Lame constants (denoted by $\lambda_\infty^{(m)}$ and $\mu_\infty^{(m)}$) can be presented through ratio of the rheological parameters $q^{(m)}$, $r_\lambda^{(m)}$ and $r_\mu^{(m)}$ as follows

$$\lambda_\infty^{(m)} = \lambda_0^{(m)}\frac{r_\lambda^{(m)}}{q^{(m)}},\ \mu_\infty^{(m)} = \mu_0^{(m)}\frac{r_\mu^{(m)}}{q^{(m)}}. \tag{2.204}$$

Moreover, it follows from the relation (2.203) that the ratios $1/q^{(m)}$, $1/r_\lambda^{(m)}$ and $1/r_\mu^{(m)}$ have a time dimension. Consequently, these ratios can be taken as characteristic relaxation ($1/q^{(m)}$) and creep ($1/r_\lambda^{(m)}$ or $1/r_\mu^{(m)}$) time for the mth material.

Note that if we take the relations in (2.203) as differential equations with respect to stresses and to solve they, then as a result we obtain the integral form of the constitutive relations with exponential core function $e^{-q^{(m)}t}$.

This completes the formulation of the problem.

2.8.2 Method of Solution

As in Sects. 2.4, 2.6 and 2.7, we use the moving coordinate system (2.15) and represent the sought values as $g(x_1', x_2', t) = \bar{g}(x_1', x_2')e^{i\omega t}$, then we obtain from (2.198) the following equations of motion for amplitudes.

$$\frac{\partial \sigma_{ij}^{(m)}}{\partial x_i} + \sigma_{11}^{(m)0}\frac{\partial^2 u_j^{(m)}}{\partial x_1^2} = \rho^{(m)}\left(-V^2\frac{\partial^2 u_j^{(m)}}{\partial x_1^2} - 2i\omega V\frac{\partial u_j^{(m)}}{\partial x_1} - \omega^2 u_j^{(m)}\right). \tag{2.205}$$

In (2.205) and below we omit the over bar in the notation of amplitudes and prime on the moving coordinates. After employing the foregoing coordinate transform and presentation for the sought values the second condition in (2.200) and the constitutive relations in (2.203) transform to (2.206) and (2.207) respectively

$$\sigma_{22}^{(1)}\Big|_{x_2=0} = -P\delta(x_1), \tag{2.206}$$

$$\begin{aligned}
-V\frac{d\sigma_{11}^{(m)}}{dx_1} + (i\omega + q^{(m)})\sigma_{11}^{(m)} &= \lambda_0^{(m)}\left(-V\frac{d\theta^{(m)}}{dx_1} + (i\omega + r_\lambda^{(m)})\theta^{(m)}\right) \\
&\quad + 2\mu_0^{(m)}\left(-V\frac{d\varepsilon_{11}^{(m)}}{dx_1} + (i\omega + r_\mu^{(m)})\varepsilon_{11}^{(m)}\right), \\
-V\frac{d\sigma_{22}^{(m)}}{dx_1} + (i\omega + q^{(m)})\sigma_{22}^{(m)} &= \lambda_0^{(m)}\left(-V\frac{d\theta^{(m)}}{dx_1} + (i\omega + r_\lambda^{(m)})\theta^{(m)}\right) \\
&\quad + 2\mu_0^{(m)}\left(-V\frac{d\varepsilon_{22}^{(m)}}{dx_1} + (i\omega + r_\mu^{(m)})\varepsilon_{22}^{(m)}\right), \\
-V\frac{d\sigma_{12}^{(m)}}{dx_1} + (i\omega + q^{(m)})\sigma_{12}^{(m)} &= 2\mu_0^{(m)}\left(-V\frac{d\varepsilon_{12}^{(m)}}{dx_1} + (i\omega + r_\mu^{(m)})\varepsilon_{12}^{(m)}\right).
\end{aligned} \tag{2.207}$$

The relations in (2.195), the first condition in (2.200), the contact condition (2.201) and the decay condition (2.202) remain valid also for the amplitudes of the sought values.

Thus, for determination of the amplitude of the sought values we have complete system of equations consisting of equation of motion (2.205), strain-displacement

relation (2.199) and constitutive relation (2.207) under satisfaction the foregoing boundary and contact conditions. For solution to these equations we employ the Fourier transform (2.18) with respect to the coordinate x_1, as a result of which we obtain:the equation of motion

$$\begin{aligned} is\sigma_{11F}^{(m)} + \frac{d\sigma_{12F}^{(m)}}{dx_2} - s^2\sigma_{11}^{(m)0}u_{1F}^{(m)} &= \rho^{(m)}\left(s^2V^2 - 2s\omega V - \omega^2\right)u_{1F}^{(m)}, \\ is\sigma_{12F}^{(m)} + \frac{d\sigma_{22F}^{(m)}}{dx_2} - s^2\sigma_{11}^{(m)0}u_{2F}^{(m)} &= \rho^{(m)}\left(s^2V^2 - 2s\omega V - \omega^2\right)u_{2F}^{(m)}, \end{aligned} \tag{2.208}$$

the strain-displacement relations

$$\varepsilon_{11F}^{(m)} = isu_{1F}^{(m)}, \ \varepsilon_{22F}^{(m)} = \frac{du_{2F}^{(m)}}{dx_2}, \ \varepsilon_{12F}^{(m)} = \frac{1}{2}\left(isu_{2F}^{(m)} + \frac{du_{1F}^{(m)}}{dx_2}\right), \tag{2.209}$$

and the constitutive relations

$$\begin{aligned} &(q^{(m)} - i(sV - \omega))\sigma_{11F}^{(m)} - \lambda_0^{(m)}(r_\lambda^{(m)} - i(sV - \omega))\theta_F^{(m)} \\ &\quad + 2\mu_0^{(m)}(r_\mu^{(m)} - i(sV - \omega))\varepsilon_{11F}^{(m)}, \\ &(q^{(m)} - i(sV - \omega))\sigma_{22F}^{(m)} - \lambda_0^{(m)}(r_\lambda^{(m)} - i(sV - \omega))\theta_F^{(m)} \\ &\quad + 2\mu_0^{(m)}(r_\mu^{(m)} - i(sV - \omega))\varepsilon_{22F}^{(m)}, \\ &(q^{(m)} - i(sV - \omega))\sigma_{12F}^{(m)} = 2\mu_0^{(m)}(r_\mu^{(m)} - i(sV - \omega))\varepsilon_{12F}^{(m)}, \end{aligned} \tag{2.210}$$

In this case the boundary condition (2.206) transforms to the condition

$$\sigma_{22F}^{(1)}\Big|_{x_2=0} = -P \tag{2.211}$$

and the other conditions in (2.200)–(2.202) remain valid also for the Fourier transforms of the corresponding quantities.

After some mathematical manipulations we obtain the relation

$$\begin{aligned} &\sigma_{11F}^{(m)} = \lambda_{com}^{(m)}\theta_F^{(m)} + 2\mu_{com}^{(m)}\varepsilon_{11F}^{(m)}, \ \sigma_{22F}^{(m)} = \lambda_{com}^{(m)}\theta_F^{(m)} + 2\mu_{com}^{(m)}\varepsilon_{22F}^{(m)}, \\ &\sigma_{12F}^{(m)} = 2\mu_{com}^{(m)}\varepsilon_{12F}^{(m)} \end{aligned} \tag{2.212}$$

from (2.210). In (2.212) it is used the following notation.

$$
\begin{aligned}
&\lambda_{com}^{(m)}=\lambda_1^{(m)}+i\lambda_2^{(m)},\ \mu_{com}^{(m)}=\mu_1^{(m)}+i\mu_2^{(m)},\\
&\lambda_1^{(m)}=\lambda_0^{(m)}\frac{d_\lambda^{(m)}+\left(Q^{(m)}\frac{c_2^{(1)}}{c_2^{(m)}}\right)^2((sh)c-\Omega)^2}{1+\left(Q^{(m)}\frac{c_2^{(1)}}{c_2^{(m)}}\right)^2((sh)c-\Omega)^2},\\
&\lambda_2^{(m)}=\lambda_0^{(m)}\frac{Q^{(m)}\frac{c_2^{(1)}}{c_2^{(m)}}((sh)c-\Omega)(d_\lambda^{(m)}-1)}{1+\left(Q^{(m)}\frac{c_2^{(1)}}{c_2^{(m)}}\right)^2((sh)c-\Omega)^2},\\
&\mu_1^{(m)}=\mu_0^{(m)}\frac{d_\mu^{(m)}+\left(Q^{(m)}\frac{c_2^{(1)}}{c_2^{(m)}}\right)^2((sh)c-\Omega)^2}{1+\left(Q^{(m)}\frac{c_2^{(1)}}{c_2^{(m)}}\right)^2((sh)c-\Omega)^2},\\
&\mu_2^{(m)}=\mu_0^{(m)}\frac{Q^{(m)}\frac{c_2^{(1)}}{c_2^{(m)}}((sh)c-\Omega)(d_\mu^{(m)}-1)}{1+\left(Q^{(m)}\frac{c_2^{(1)}}{c_2^{(m)}}\right)^2((sh)c-\Omega)^2},
\end{aligned}
\tag{2.213}
$$

where

$$
c=\frac{V}{c_2^{(1)}},\ \Omega=\frac{h\omega}{c_2^{(1)}},\ Q^{(m)}=\frac{c_2^{(m)}}{hq^{(m)}},\ d_\lambda^{(m)}=\frac{r_\lambda^{(m)}}{q^{(m)}},\ d_\mu^{(m)}=\frac{r_\mu^{(m)}}{q^{(m)}}. \tag{2.214}
$$

Thus, according to the relation (2.212), we can conclude that, the solution procedure developed in Sects. 2.2 and 2.4 can be completely repeated for the solution of the Eqs. (2.208), (2.209) and (2.212). However, in this case the Lame constants $\lambda^{(m)}$ and $\mu^{(m)}$ in Sect. 2.2 must be replaced with the complex constants $\lambda_{com}^{(m)}$ and $\mu_{com}^{(m)}$ respectively determined by expressions (2.213) and (2.214). In the other words, we obtain the equation

$$
\begin{aligned}
&-(sh)^2a^{(m)}u_{1F}^{(m)}+\frac{d^2u_{1F}^{(m)}}{d(x_2/h)^2}+i(sh)b^{(m)}\frac{du_{2F}^{(m)}}{d(x_2/h)}=0,\\
&i(sh)b^{(m)}\frac{du_{1F}^{(m)}}{d(x_2/h)}-(sh)^2c^{(m)}u_{2F}^{(m)}+(b^{(m)}+1)\frac{d^2u_{2F}^{(m)}}{d(x_2/h)^2}=0,
\end{aligned}
\tag{2.215}
$$

for $u_{1F}^{(m)}$ and $u_{2F}^{(m)}$, where

$$
\begin{aligned}
a^{(m)} &= \frac{\bar{\lambda}^{(m)}_{com}}{\bar{\mu}^{(m)}_{com}} + 2 + \frac{\sigma^{(m)0}_{11}}{\bar{\mu}^{(m)}_{com}} - \frac{c^2}{\left(c^{(m)}_{2com}\right)^2} + 2i\frac{\Omega c}{\left(c^{(m)}_{2com}\right)^2} + \frac{\Omega^2}{\left(c^{(m)}_{2com}\right)^2},\\
b^{(m)} &= \frac{\bar{\lambda}^{(m)}_{com}}{\bar{\mu}^{(m)}_{com}} + 1,\\
c^{(m)} &= 1 + \frac{\sigma^{(m)0}_{11}}{\bar{\mu}^{(m)}_{com}} - \frac{c^2}{\left(c^{(m)}_{2com}\right)^2} + 2i\frac{\Omega c}{\left(c^{(m)}_{2com}\right)^2} + \frac{\Omega^2}{\left(c^{(m)}_{2com}\right)^2},\ \bar{c}^{(m)}_{2com}
\end{aligned}
\tag{2.216}
$$

Thus, we can use the expressions (2.22)–(2.226) for the presentation of the solution to the equations in (2.215). In this case the Lame constants $\lambda^{(m)}$ and $\mu^{(m)}$ in in (2.26) must be replaced by the complex constants $\lambda^{(m)}_{com}$ and $\mu^{(m)}_{com}$ (2.213) respectively. In other words, we obtain the following expressions for the displacement and stresses.

$$
\begin{aligned}
u^{(1)}_{2F} &= \mathrm{Re}\Big\{e^{i\omega t}\Big[F^{(1)}_1 e^{k^{(1)}_1 x_2} + F^{(1)}_2 e^{-k^{(1)}_1 x_2} + F^{(1)}_3 e^{k^{(1)}_2 x_2} + F^{(1)}_4 e^{-k^{(1)}_2 x_2}\Big]\Big\},\\
u^{(2)}_{2F} &= \mathrm{Re}\Big\{e^{i\omega t}\Big[F^{(2)}_1 e^{k^{(2)}_1 x_2} + F^{(2)}_3 e^{k^{(2)}_2 x_2}\Big]\Big\},\\
u^{(1)}_{1F} &= \mathrm{Re}\Big\{e^{i\omega t} i\Big[F^{(1)}_1 \alpha^{(1)}_1 e^{k^{(1)}_1 x_2} + F^{(1)}_2 \alpha^{(1)}_2 e^{-k^{(1)}_1 x_2}\\
&\qquad + F^{(1)}_3 \alpha^{(1)}_3 e^{k^{(1)}_2 x_2} + F^{(1)}_4 \alpha^{(1)}_4 e^{k^{(1)}_2 x_2}\Big]\Big\},\\
u^{(2)}_{1F} &= \mathrm{Re}\Big\{e^{i\omega t} i\Big[F^{(2)}_1 \alpha^{(2)}_1 e^{k^{(2)}_1 x_2} + F^{(2)}_3 \alpha^{(2)}_3 e^{k^{(2)}_2 x_2}\Big]\Big\},\\
\sigma^{(1)}_{11F} &= \mathrm{Re}\Big\{e^{i\omega t}\Big[F^{(1)}_1(\lambda^{(1)}_{com}(s\alpha^{(1)}_1 + k^{(1)}_1) + 2\mu^{(1)}_{com} s\alpha^{(1)}_1)e^{k^{(1)}_1 x_2}\\
&\qquad + F^{(1)}_2(\lambda^{(1)}_{com}(s\alpha^{(1)}_2 - k^{(1)}_1) + 2\mu^{(1)}_{com} s\alpha^{(1)}_2)e^{-k^{(1)}_1 x_2}\\
&\qquad + F^{(1)}_3(\lambda^{(1)}_{com}(s\alpha^{(1)}_3 + k^{(1)}_2) + 2\mu^{(1)}_{com} s\alpha^{(1)}_3)e^{k^{(1)}_2 x_2}\\
&\qquad + F^{(1)}_4(\lambda^{(1)}_{com}(s\alpha^{(1)}_4 - k^{(1)}_2) + 2\mu^{(1)}_{com} s\alpha^{(1)}_4)e^{-k^{(1)}_2 x_2}\Big]\Big\},\\
\sigma^{(2)}_{11F} &= \mathrm{Re}\Big\{e^{i\omega t}\Big[F^{(2)}_1(\lambda^{(2)}_{com}(s\alpha^{(2)}_1 + k^{(2)}_1) + 2\mu^{(2)}_{com} s\alpha^{(2)}_1)e^{k^{(2)}_1 x_2}\\
&\qquad + F^{(2)}_3(\lambda^{(2)}_{com}(s\alpha^{(2)}_3 + k^{(2)}_2) + 2\mu^{(2)}_{com} s\alpha^{(2)}_3)e^{k^{(2)}_2 x_2}\Big]\Big\},\\
\sigma^{(1)}_{22F} &= \mathrm{Re}\Big\{e^{i\omega t}\Big[F^{(1)}_1(\lambda^{(1)}_{com}(s\alpha^{(1)}_1 + k^{(1)}_1) + 2\mu^{(1)}_{com} k^{(1)}_1)e^{k^{(1)}_1 x_2}\\
&\qquad + F^{(1)}_2(\lambda^{(1)}_{com}(s\alpha^{(1)}_2 - k^{(1)}_1) - 2\mu^{(1)}_{com} k^{(1)}_1)e^{-k^{(1)}_1 x_2}\\
&\qquad + F^{(1)}_3(\lambda^{(1)}_{com}(s\alpha^{(1)}_3 + k^{(1)}_2) + 2\mu^{(1)}_{com} k^{(1)}_2)e^{k^{(1)}_2 x_2}\\
&\qquad + F^{(1)}_4(\lambda^{(1)}_{com}(s\alpha^{(1)}_4 - k^{(1)}_2) - 2\mu^{(1)}_{com} k^{(1)}_2)e^{-k^{(1)}_2 x_2}\Big]\Big\},
\end{aligned}
$$

$$\begin{aligned}
\sigma_{22F}^{(2)} &= \mathrm{Re}\Big\{e^{i\omega t}\Big[F_1^{(2)}(\lambda_{com}^{(2)}(s\alpha_1^{(2)}+k_1^{(2)})+2\mu_{com}^{(2)}k_1^{(2)})e^{k_1^{(2)}x_2} \\
&\qquad + F_3^{(2)}(\lambda_{com}^{(2)}(s\alpha_3^{(2)}+k_2^{(2)})+2\mu_{com}^{(2)}k_2^{(2)})e^{k_2^{(2)}x_2}\Big]\Big\}, \\
\sigma_{12F}^{(1)} &= \mathrm{Re}\Big\{e^{i\omega t}i\mu_{com}^{(1)}\Big[F_1^{(1)}(\alpha_1^{(1)}k_1^{(1)}-s)e^{k_1^{(1)}x_2}+F_2^{(1)}(-\alpha_1^{(1)}k_1^{(1)}-s)e^{-k_1^{(1)}x_2} \\
&\qquad + F_3^{(1)}(\alpha_3^{(1)}k_2^{(1)}-s)e^{k_2^{(1)}x_2}+F_4^{(1)}(-\alpha_4^{(1)}k_2^{(1)}-s)e^{-k_2^{(1)}x_2}\Big]\Big\}, \\
\sigma_{12F}^{(2)} &= \mathrm{Re}\Big\{e^{i\omega t}i\mu_{com}^{(2)}\Big[F_1^{(2)}(\alpha_1^{(2)}k_1^{(2)}-s)e^{k_1^{(2)}x_2}+F_3^{(2)}(\alpha_3^{(2)}k_2^{(2)}-s)e^{k_2^{(2)}x_2}\Big]\Big\}.
\end{aligned} \tag{2.217}$$

where

$$\begin{aligned}
k_1^{(m)} &= \sqrt{\frac{A^{(m)}}{2}+\sqrt{\left(\frac{A^{(m)}}{2}\right)^2-B^{(m)}}}, k_2^{(m)} = \sqrt{\frac{A^{(m)}}{2}-\sqrt{\left(\frac{A^{(m)}}{2}\right)^2-B^{(m)}}}, \\
A^{(m)} &= \frac{s^2b^{(m)}-s^2c^{(m)}-s^2a^{(m)}(b^{(m)}+1)}{b^{(m)}+1}, B^{(m)} = \frac{s^4a^{(m)}c^{(m)}}{b^{(m)}+1}, \\
\alpha_1^{(1)} &= -s\frac{c^{(1)}}{k_1^{(1)}}+\frac{(b^{(1)}+1)k_1^{(1)}}{sb^{(1)}}, \alpha_2^{(1)} = s\frac{c^{(1)}}{k_1^{(1)}}-\frac{(b^{(1)}+1)k_1^{(1)}}{sb^{(1)}}, \\
\alpha_3^{(1)} &= -s\frac{c^{(1)}}{k_2^{(1)}}+\frac{(b^{(1)}+1)k_2^{(1)}}{sb^{(1)}}, \alpha_4^{(1)} = s\frac{c^{(1)}}{k_2^{(1)}}-\frac{(b^{(1)}+1)k_2^{(1)}}{sb^{(1)}}, \\
\alpha_1^{(2)} &= -s\frac{c^{(2)}}{k_1^{(2)}}+\frac{(b^{(2)}+1)k_1^{(2)}}{sb^{(2)}}, \alpha_3^{(2)} = -s\frac{c^{(2)}}{k_2^{(2)}}+\frac{(b^{(2)}+1)k_2^{(2)}}{sb^{(2)}}.
\end{aligned} \tag{2.218}$$

This completes the consideration of the solution method.

2.8.3 Numerical Results and Discussions

First, we consider the algorithm for determination of the critical velocity in the case under consideration. It is evident that the algorithm for determination of the critical velocity which was employed in the previous sections cannot be applied in the present case. Because, in the present case the determinant $\det\|\alpha_{nm}\|$ in Eq. (2.30) cannot be equated to zero, i.e. in the present case $\det\|\alpha_{nm}\| > 0$. This situation is explained with the fact that the amplitude of the harmonic waves propagated in viscoelastic medium decays, i.e. the dispersion equation $\det\|\alpha_{nm}\| = 0$ with respect to *sh* under fixed *c* and Ω must have complex roots only. As in our investigation the *sh* is the Fourier transformation parameter and has real values only, therefore

$\det\|\alpha_{nm}\| > 0$ takes place. Consequently, the criterion $dc/d(sh) = 0$ which was used in the previous sections for determination of the critical velocity cannot be applied in the case under consideration. Therefore, in the present case for determination of the critical velocity we use the criterion which based on the finding of the absolute maximum values of the sought quantities with respect of the moving load velocity. In the other words, first, we calculate the values, for instance, the values of the $\sigma_{22}^{(1)}$ at $x_2 = -h$ and $x_1/h = 0$, for various values of $c(=V/c_2^{(1)})$ under $0 \le V < \min(c_2^{(1)}, c_2^{(2)})$, as a result of which we have the relation $\sigma_{22}^{(1)} = \sigma_{22}^{(1)}(c)$. If there exits the case where $d\sigma_{22}^{(1)}/dc = 0$. then the velocity c related to this case is a critical velocity. If there is not such cases, then there is not the critical velocity.

Consider the mechanical meaning of the parameters $Q^{(m)}$, $d_\lambda^{(m)}$ and $d_\mu^{(m)}$. According to expression of $Q^{(m)}$ in (2.214), i.e. according to the expression $Q^{(m)} = c_2^{(m)}/(hq^{(m)})$, we can conclude that an increase in the values of the parameter $Q^{(m)}$ means a decrease in the "viscosity properties" of the mth material. Because, $1/q^{(m)}$ is a characteristic relaxation time (consequently, $hq^{(m)}$ can be taken as a characteristic "relaxation speed") and under fixed $c_2^{(m)}$ and h an increase in the values of $Q^{(m)}$ means an increase in the characteristic relaxation time, and a decrease in the viscosity of the mth material.

According to the expressions (2.204) and (2.214), we can write $\lambda_\infty^{(m)} = \lambda_0^{(m)} d_\lambda^{(m)}$ and $\mu_\infty^{(m)} = \mu_0^{(m)} d_\mu^{(m)}$ from which follows that the parameters $d_\lambda^{(m)}$ and $d_\mu^{(m)}$ characterize the long-term values of the Lame constants.

Thus, the influence of the viscosity of the viscoelastic materials on the values of the critical velocity we will investigate through the parameters $Q^{(m)}$, $d_\lambda^{(m)}$ and $d_\mu^{(m)}$. For simplicity of the consideration below we assume that $d_\lambda^{(m)} = d_\mu^{(m)}$ and introduce the notation $d^{(m)}(=d_\lambda^{(m)} = d_\mu^{(m)})$. Moreover, we consider numerical results related to the case where the material of the covering layer is purely elastic, but the material of the half-plane is viscoelastic with the rheological parameters $d^{(2)}$ and $Q^{(2)}$. According to the foregoing discussions, it can be predicted that the results obtained for the viscoelastic case must be approach to the corresponding ones obtained for the purely elastic case with the values of the parameters $d^{(2)}$ and $Q^{(2)}$. For verification this prediction we consider the case which was examined in Sect. 2.2 (or in the paper by Akbarov et al. 2007) for the purely elastic case, that is, the case where $E_0^{(2)}/E_0^{(1)} = 0.1$, $\nu_0^{(2)} = \nu_0^{(1)} = 0.3$, $c_2^{(1)} = c_2^{(2)}$ and $\Omega = 0.0$. Analyze the graphs of the dependence between $\sigma_{22}h/P_0$ calculated at $x_1/h = 0$ and c, where $\sigma_{22}(x_1) = \sigma_{22}^{(1)}(x_1, -h) = \sigma_{22}^{(2)}(x_1, -h)$. These graphs are given in Fig. 2.51 and constructed in the case where $Q^{(2)} = 100$ for various values of $d^{(2)}$.

Thus, it follows from Fig. 2.51 that under the critical velocity of the moving load, that is, under $c = c_{cr}$ for which $|\sigma_{22}| \to \infty$ in the purely elastic case, the absolute values of the $|\sigma_{22}|$ have their maximum and these maximums increase with

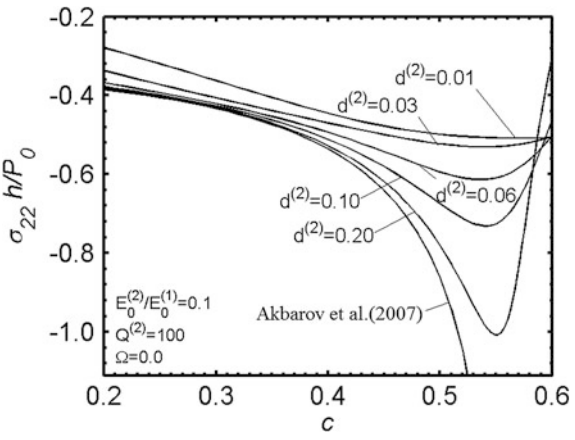

Fig. 2.51 The influence of the parameter $d^{(2)}$ on the values of the dependence between the normal stress σ_{22} and c under $\Omega = 0.0$

$d^{(2)}$. Consequently, the results given in Fig. 2.51 prove the foregoing prediction and validate the correctness of the used algorithm and PC programs for obtaining numerical results.

Now we consider numerical results related to the oscillating moving load and obtained in the case where $E_0^{(2)}/E_0^{(1)} = 0.2$, $\rho^{(2)}/\rho^{(1)} = 0.35$, $\nu_0^{(1)} = \nu_0^{(2)} = 0.3$ and $Q^{(2)} = 100$. These results are given in Figs. 2.52, 2.53 and 2.54 which are obtained in the cases where $\Omega = 0.006$, 0.007 and 0.010 respectively. Note that the results given these figures are obtained for various values of the parameter $d^{(2)}$.

As follows from Figs. 2.52, 2.53 and 2.54 that in the case where $\Omega > 0$ for the purely elastic case there exists two critical velocity which can be denoted as c'_{cr} and $c''_{cr}(>c'_{cr})$. We recall that this conclusion was also noted in the Sects. 2.4, 2.6 and 2.7 of the present chapter. However, in the case where the material of the half-plane is taken as viscoelastic one, the absolute maximum values of the stress σ_{22} are obtained for the moving velocity c (denote it by c_v) for which the relation

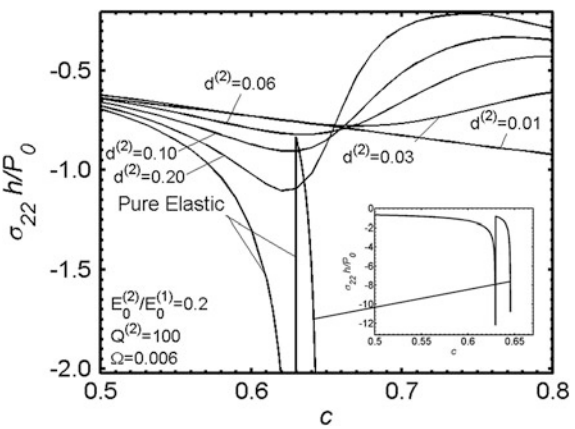

Fig. 2.52 The influence of the parameter $d^{(2)}$ on the dependence between the normal stress σ_{22} and c constructed in the case where $\Omega = 0.006$

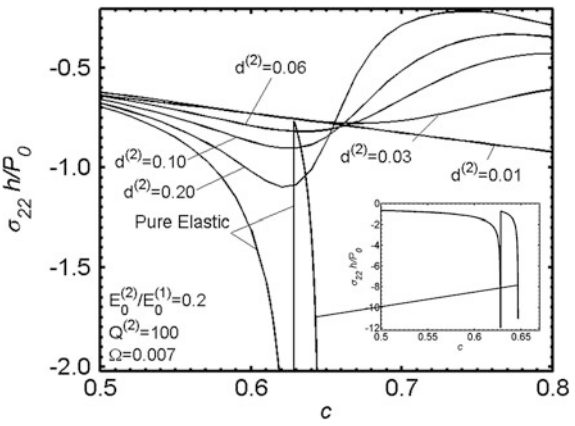

Fig. 2.53 The influence of the parameter parameter $d^{(2)}$ on the dependence between the normal stress σ_{22} and c constructed in the case where $\Omega = 0.007$

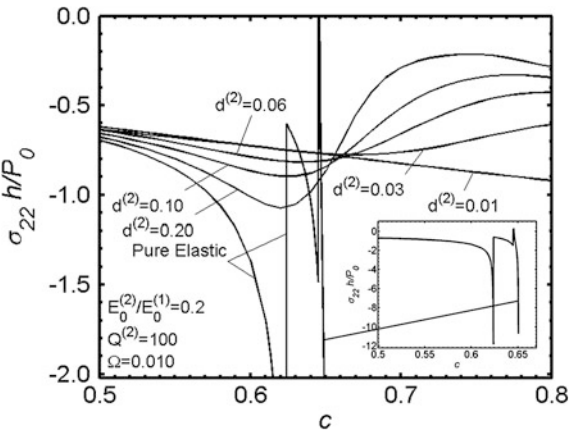

Fig. 2.54 The influence of the parameter $d^{(2)}$ on the dependence between the normal stress σ_{22} and c constructed in the case where $\Omega = 0.010$

$c'_{cr} < c_v < c''_{cr}$ takes place. At the same time, the foregoing numerical results allows us to determine the values of the normal stress acting on the interface plane which have real applicable meaning. Consequently, the approach developed in the present section can be employed for investigation and determination of the other related problems regarding the moving load or oscillating moving load problems.

2.9 On One Analogy Between the Moving Load, Near Surface Wave Propagation and Near Surface Stability Loss Problems Related to the Layered Half-Space

In the present section we attempt to prove that the equations, for instance the Eq. (2.30), from which the critical velocity is determined in the case where the oscillation frequency of the moving load $\omega = 0$, are analog of the dispersion

equation of the near-surface wave propagation problem, if we take the Fourier transformation parameter s as the wave-number and the moving load velocity V as the wave propagation velocity. Moreover, we attempt to prove that the mentioned critical velocity equation is also analog of the equation for determination of the critical force under near-surface stability loss of the layered half-plane, if we take sh as the stability loss form parameter and the moving load velocity V as the external compressive force or stress. Note that the above mentioned analogies take place within the scope of certain restrictions which will be discussed in the present section. For simplicity of the considerations all discussions below, we will make only on the system consisting of the pre-stressed covering layer and pre-stressed half-plane.

2.9.1 The Analogy Between the Near-Surface Wave Propagation Problem and the Corresponding Moving Load Problem

First of all we note that the detail investigations of the near-surface wave propagation problems in the layered half-plane will be investigated in Chap. 4. Here we consider a problem formulation and obtaining of the dispersion equation of the near surface waves propagated in the system consisting of the pre-stressed covering layer and pre-stressed half-plane the sketch of which is shown in Fig. 2.1. Under this consideration and discussions we use all notation and assumptions accepted in Sect. 2.2. Thus, we assume that within the covering layer and half-plane the following field equations are satisfied.

The equations of motion

$$\frac{\partial \sigma_{ij}^{(m)}}{\partial x_i} + \sigma_{11}^{(m)0} \frac{\partial^2 u_j^{(m)}}{\partial x_1^2} = \rho^{(m)} \frac{\partial^2 u_j^{(m)}}{\partial t^2}, \tag{2.219}$$

The elasticity relations

$$\sigma_{ij}^{(m)} = \lambda^{(m)} \theta^{(m)} \delta_i^j + 2\mu^{(m)} \varepsilon_{ij}^{(m)}, \theta^{(m)} = \varepsilon_{11}^{(m)} + \varepsilon_{22}^{(m)}, \tag{2.220}$$

The strain-displacement relations

$$\varepsilon_{ij}^{(m)} = \frac{1}{2} \left(\frac{\partial u_i^{(m)}}{\partial x_j} + \frac{\partial u_j^{(m)}}{\partial x_i} \right). \tag{2.221}$$

We assume that on the upper free plane of the covering layer the conditions

$$\sigma_{21}^{(1)}\Big|_{x_2=0} = 0, \sigma_{22}^{(1)}\Big|_{x_2=0} = 0 \tag{2.222}$$

satisfy. Moreover, we assume that on the interface plane between the covering layer and half-plane the following complete contact conditions take place.

$$\sigma_{i2}^{(1)}\Big|_{x_2=-h} = \sigma_{i2}^{(2)}\Big|_{x_2=-h}, u_i^{(1)}\Big|_{x_2=-h} = u_i^{(2)}\Big|_{x_2=-h}, \quad i = 1, 2. \tag{2.223}$$

For the near surface wave it is necessary to take also into considerations the decay conditions

$$\left|u_i^{(2)}\right| \to 0, \left|\sigma_{i2}^{(2)}\right| \to 0 \quad as \quad x_2 \to -\infty. \tag{2.224}$$

Thus, within the scope of the foregoing equations, contact and boundary conditions we investigate the near surface wave propagation in the direction of the Ox_1 axis in the system under consideration. For this purpose, we represent the displacements as follows.

$$u_1^{(m)} = \varphi_1^{(m)}(x_2)e^{i(kx_1-\omega t)}, u_2^{(m)} = \varphi_2^{(m)}(x_2)e^{i(kx_1-\omega t)}. \tag{2.225}$$

Substituting the expression (2.225) into the Eqs. (2.221), (2.220) and (2.219), we obtain from (2.219) the equations

$$\begin{aligned} -k^2 a'^{(m)}\varphi_1^{(m)} + \frac{d^2\varphi_1^{(m)}}{dx_2^2} + ikb^{(m)}\frac{d\varphi_2^{(m)}}{dx_2} = 0, \\ ikb^{(m)}\frac{d\varphi_1^{(m)}}{dx_2} - k^2 c'^{(m)}\varphi_2^{(m)} + (b^{(m)}+1)\frac{d^2\varphi_2^{(m)}}{dx_2^2} = 0. \end{aligned} \tag{2.226}$$

In (2.226) the notation

$$\begin{aligned} a'^{(m)} &= \frac{\lambda^{(m)}}{\mu^{(m)}} + 2 + \frac{\sigma_{11}^{(m)0}}{\mu^{(m)}} - \frac{c^2}{(c_2^{(m)})^2}, \quad b^{(m)} = \frac{\lambda^{(m)}}{\mu^{(m)}} + 1, \\ c'^{(m)} &= 1 + \frac{\sigma_{11}^{(m)0}}{\mu^{(m)}} - \frac{c^2}{(c_2^{(m)})^2}, \end{aligned} \tag{2.227}$$

is used, where $c = \omega/k$ is a phase velocity of the wave under consideration.

Comparison shows that the expressions of $a'^{(m)}$, $b^{(m)}$ and $c'^{(m)}$ in (2.227) coincide with the expressions of $a^{(m)}$, $b^{(m)}$ and $c^{(m)}$ in (2.20) respectively, if we take V instead of c in (2.227). Consequently, if we take k and c instead of s and V respectively in the expressions (2.22)–(2.26) and in Eq. (2.30), then these

expressions can be taken as a solution and the Eq. (2.30) can be taken as a dispersion equation for the near-surface wave propagation problem under consideration. Since, we prove the analogy between the moving load problem and the near surface wave propagation problem related to the system consisting of the pre-stressed covering layer and pre-stressed half-plane. It is evident that this analogy takes place also for more complicated problems considered in the previous section and related to the cases where the amplitude of the moving load is not oscillating.

Consequently, the graphs of the relation $V = V(sh)$ constructed in the previous sections in the case where $\Omega = 0$ (i.e. in the case where the moving load amplitude does not oscillate) can also be taken as the dispersion curves obtained for the corresponding near-surface wave propagation problems. However, the results obtained in the previous sections were obtained in the cases where the modulus of elasticity of the covering layer material is greater than that of the half-plane. But the near-surface wave propagation problems can be investigated for more wide range of the problem parameters than that considered in the previous sections. Therefore, in Chap. 4 the near-surface wave propagation problems for the pre-stressed layered half-space will be investigated and discussed separately in detail.

2.9.2 The Analogy Between the Near-Surface Stability Loss Problem and the Corresponding Moving Load Problem

Within the scope of the assumptions and notation accepted in Sect. 2.2 we consider the near-surface stability loss of the system consisting of the covering layer and half-plane in the case where this system is compressed by the uniformly distributed normal forces with intensity p in the direction of the Ox_1 axis (Fig. 2.55). Assume that there exists the complete contact conditions between the constituents of the system. In this case the pre-critical stress state in the covering layer and half plane are determined through the following expressions.

$$\sigma_{11}^{(2)0} = p, \sigma_{11}^{(1)0} = \frac{E^{(1)}(1-(\nu^{(2)})^2)}{E^{(2)}(1-(\nu^{(1)})^2)}. \tag{2.228}$$

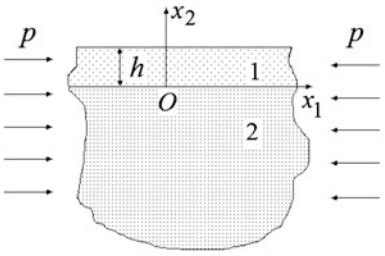

Fig. 2.55 The geometry of the compressed system consisting of the covering layer and half-plane

According to Guz (1999) and Akbarov (2013), the near-surface stability loss of the system under consideration is reduced to the solution of the following eigenvalue problem.

Three-dimensional stability loss equation

$$\frac{\partial \sigma_{ij}^{(m)}}{\partial x_i} + \sigma_{11}^{(m)0} \frac{\partial^2 u_j^{(m)}}{\partial x_1^2} = 0, \tag{2.229}$$

The elasticity relations

$$\sigma_{ij}^{(m)} = \lambda^{(m)} \theta^{(m)} \delta_i^j + 2\mu^{(m)} \varepsilon_{ij}^{(m)}, \theta^{(m)} = \varepsilon_{11}^{(m)} + \varepsilon_{22}^{(m)}, \tag{2.230}$$

The strain-displacement relations

$$\varepsilon_{ij}^{(m)} = \frac{1}{2}\left(\frac{\partial u_i^{(m)}}{\partial x_j} + \frac{\partial u_j^{(m)}}{\partial x_i}\right). \tag{2.231}$$

We assume that the boundary

$$\sigma_{12}^{(1)}\Big|_{x_2=0} = 0, \sigma_{22}^{(1)}\Big|_{x_2=0} = 0 \tag{2.232}$$

and contact

$$\sigma_{i2}^{(1)}\Big|_{x_2=-h} = \sigma_{i2}^{(2)}\Big|_{x_2=-h}, u_i^{(1)}\Big|_{x_2=-h} = u_i^{(2)}\Big|_{x_2=-h}, \quad i = 1, 2. \tag{2.233}$$

conditions are satisfied. For the near-surface stability loss it is also necessary to take into considerations the decay conditions

$$\left|u_i^{(2)}\right| \to 0, \left|\sigma_{ij}^{(2)}\right| \to 0 \quad \text{as} \quad x_2 \to -\infty. \tag{2.234}$$

As the stability loss form is taken as a periodical function with respect to the x_1, therefore the displacements for the foregoing problem are selected as follows.

$$u_1^{(m)} = \phi_1(x_2)\sin(kx_1), u_2^{(m)} = \phi_2(x_2)\cos(kx_1), \kappa = 2\pi/\ell \tag{2.235}$$

where ℓ is a length of the period of the stability loss form.

Thus, substituting (2.235) into the (2.231), (2.230) and (2.229), we obtain the following equations for the displacements.

$$
\begin{aligned}
-\kappa^2 a''^{(m)}\phi_1^{(m)} + \frac{d^2\phi_1^{(m)}}{dx_2^2} + i\kappa b^{(m)}\frac{d\phi_2^{(m)}}{dx_2} = 0,\\
i\kappa b''^{(m)}\frac{d\phi_1^{(m)}}{dx_2} - \kappa^2 c''^{(m)}\phi_2^{(m)} + (b^{(m)}+1)\frac{d^2\phi_2^{(m)}}{dx_2^2} = 0.
\end{aligned}
\tag{2.236}
$$

where

$$
a''^{(m)} = \frac{\lambda^{(m)}}{\mu^{(m)}} + 2 + \frac{\sigma_{11}^{(m)0}}{\mu^{(m)}}, b^{(m)} = \frac{\lambda^{(m)}}{\mu^{(m)}} + 1, c''^{(m)} = 1 + \frac{\sigma_{11}^{(m)0}}{\mu^{(m)}},
\tag{2.237}
$$

Comparison shows that the expressions $a''^{(m)}$, $b^{(m)}$ and $c''^{(m)}$ in (2.237) coincide with the expressions $a^{(m)}$, $b^{(m)}$ and $c^{(m)}$ in (2.20) respectively, if we take $\sigma_{11}^{(m)0}/\mu^{(m)}$ in (2.237) instead of $(\sigma_{11}^{(m)0}/\mu^{(m)} - V^2/(c_2^{(m)})^2)$ in (2.20). Consequently, if we take κ and $\sigma_{11}^{(m)0}/\mu^{(m)}$ instead of s and $(\sigma_{11}^{(m)0}/\mu^{(m)} - V^2/(c_2^{(m)})^2)$ respectively in the expressions (2.22)–(2.26) and in Eq. (2.30), then the expressions (2.22)–(2.26) can be taken as the solution of the stability loss problem (2.228)–(2.234) and the Eq. (2.30) can be taken as the equation from which the relation $p_{cr} = p_{cr}(\kappa h)$ (i.e. the critical force p_{cr}) is determined. It is known that (see Akbarov 2013) under near-surface stability loss of the layered half-plane it is understood the case for which the relation $p_{cr} = p_{cr}(\kappa h)$ has a minimum at $\kappa h \neq 0$ and $\kappa h \neq \infty$. Such type minimum in the relation $p_{cr} = p_{cr}(\kappa h)$ arises namely in the case where the modulus of elasticity of the covering layer material is greater than that of the half-plane material. Consequently, the results obtained for the relation $V = V(sh)$ in the previous sections in the case where moving load is not oscillating, can be taken as the relation $p_{cr} = p_{cr}(\kappa h)$ for the corresponding near-surface stability loss problems.

Since, we have proved the analogy between the moving load problem and near-surface stability loss problem. Although, this proving is made for the system shown in Fig. 2.55, but this procedure can be easily developed for a more complicate systems and problems.

References

Achenbach JD, Keshava SP, Herman G (1967) Moving load on a plate resting on an elastic half space. Trans ASME Ser E J Appl Mech 34(4):183–189

Akbarov SD (2013) Stability loss and buckling delamination: three-dimensional linearized approach for elastic and viscoelastic composites. Springer, Heidelberg, New York, Dordrecht, London

Akbarov SD, Guler C (2007) On the stress field in a half-plane covered by the pre-stretched layer under the action of arbitrary linearly located time-harmonic forces. Appl Math Model 31 (11):2375–2390

Akbarov SD, Guler C, Dincsoy E (2007) The critical speed of a moving load on a prestressed plate resting on a prestressed half-plane. Mech Comp Mater 43(2):173–182

Akbarov SD, Salmanova KA (2009) On the dynamics of a finite pre-strained bi-layered slab resting on a rigid foundation under the action of an oscillating moving load. J Sound Vibr 327 (3–5):454–472

Akbarov SD, Ilhan N (2008) Dynamics of a system comprising a pre-stressed orthotropic layer and pre-stressed orthotropic half-plane under the action of a moving load. Int J Solid Str 45(14–15):4222–4235

Akbarov SD, Ilhan N (2009) Dynamics of a system comprising an orthotropic layer and orthotropic half-plane under the action of an oscillating moving load. Int J Solid Str 46 (21):3873–3881

Akbarov SD, Ilhan N, Temugan A (2011) On the dynamics of the oscillating moving point load acting on the system comprising a pre-stressed layer and pre-stressed half-space. In: Springer Proceedings in Physics, Vibration Problems ICOVP 2011, vol 139, pp 255–260

Akbarov SD, Ilhan N, Sahin NS (2014) Dynamic response to a time-harmonic moving load of a system comprising a viscoelatic layer covering a viscoelastic half-space. In Book of abstract of the XVIII conference on mechanics of composite materials, Riga, Latvia, 2–6 June 2014, p 21

Akbarov SD, Ilhan N, Temugan A (2015) 3D Dynamics of a system comprising a pre-stressed covering layer and a pre-stressed half-space under the action of an oscillating moving point-located load. Appl Math Model. 39:1–18

Auersch L (2006) Ground vibration due to railway traffic-calculation of the effects of moving static loads and their experimental verification. J Sound Vibr 293:599–610

Auersch L (2008) The effect of the critically moving loads on the vibrations of soft soils and isolated railway tracks. J Sound Vibr 310:587–607

Babich SY, Glukhov YP, Guz AN (1986) Dynamics of a layered compressible pre-stressed half-space under the influence of moving load. Int Appl Mech 22(6):808–815

Babich SY, Glukhov YP, Guz AN (1988) To the solution of the problem of the action of a live load on a two-layer half-space with initial stress. Int Appl Mech 24(8):775–780

Babich SY, Glukhov YP, Guz AN (2008a) Dynamics of a pre-stressed incompressible layered half-space under load. Int Appl Mech 44(3):268–285

Babich SY, Glukhov YP, Guz AN (2008b) A dynamic for a pre-stressed compressible layered half-space under moving load. Int Appl Mech 44(4):388–405

Biot MA (1965) Mechanics of incremental deformations. Wiley, New York

Degrande G, Schillemans L (2001) Free fields vibration during the passage of a Thals high-speed train at variable speed. J Sound Vibr 247(1):131–144

Dieterman HA, Metrikine AV (1997) Critical velocities of a harmonic load moving uniformly along an elastic layer. Trans ASME J Appl Mech 64:596–600

Dincsoy E, Guler C, Akbarov SD (2009) Dynamical response of a prestrained system comprising a substrate and bond and covering layers to a moving load. Mech Comp Mater 45(5):527–536

Eringen AC, Suhubi ES (1975) Elastodynamics, vol 1. Finite motions. Academic press, New York, London

Gladwell GML (1968) The calculation of mechanical impedances related with the surface of a semi-infinite elastic body. J Sound Vibr 8:215–219

Green AE, Rivlin RS, Shied RT (1952) General theory of small elastic deformations superposed on finite elastic deformation. Proc R Soc Lond A 211:128–154

Guz AN (1999) Fundamentals of the three-dimensional theory of stability of deformable bodies. Springer, Berlin

Guz AN (2002) Elastic waves in bodies with initial (residual) stresses. Int Appl Mech 38(1):35–78

Guz AN (2004) Elastic waves in bodies with initial (residual) stresses. A.C.K, Kiev (in Russian)

Ilhan N (2012) The critical speed of a moving time-harmonic load acting on a system consisting a pre-stressed orthotropic covering layer and a pre-stressed half-plane. Appl Math Model 36 (8):3663–3672

Jensen FB, Kuperman WA, Porter MB, Schmidt H (2011) Computational ocean acoustic. Springer, Berlin

Hussein MFM, Hunt HEM (2006) Modeling of floating-slab tracks with continuous slabs under oscillating moving loads. J Sound Vibr 297(1/2):37–54

Kerr AD (1983) The critical velocity of a load moving on a floating ice plate that is subjected to in-plane forces. Cold Reg Sci Technol 6(3):267–274

Kim SM (2004) Vibration and stability of axial loaded beams on elastic foundation under moving harmonic loads. Eng Struct 26:95–105

Lamb H (1904) On the propagation of tremors over the surface of an elastic solid. Philos Trans R Soc Lond Ser A 203:1–42

Lekhnitskii SG (1981) Theory of elasticity an anisotropic body. Mir Publishers, Moscow

Madshus C, Kaynia AM (2000) High speed railway lines on soft ground: dynamic behavior at critical train speed. J Sound Vibr 231(3):689–701

Metrikine AV, Vrouwenvelder ACWM (2000) Surface ground vibration due to a moving train in a tunnel: two-dimensional model. J Sound Vibr 234(1):43–66

Metrikine AV, Dieterman HA (1999) Lateral vibration of an axially compressed beam on an elastic half-space due to a moving lateral load. Eur J Mech A/Solids 18:147–158

Schwartz MM (1992) Composite materials handbook, 2nd edn. McGraw-Hill, New York

Rabotnov YuN (1980) Elements of hereditary solid mechanics. Mir Publishers, Moscow

Robertson IA (1966) Forced vertical vibration of a rigid circular disc on a semi-infinite solid. Math Proc Cambridge Philos Soc 62:547–553

Truesdell C, Noll W (1965) The nonlinear field theories of mechanics. In: Flugge E (ed) Handbuch der Physik, vol III/3. Springer, Berlin, New York

Tsang L (1978) Time-harmonic solution of the elastic head wave problem incorporating the influence of Rayleigh poles. J Acoust Soc Am 65(5):1302–1309

Vesnitskii AI, Metrikine AV (1993) Parametric instability in the oscillations of a body moving uniformly in a periodically inhomogeneous elastic system. J Appl Mech Tech Phys 34: 226–271

http://www.springer.com/978-3-319-14459-7

Dynamics of Pre-Strained Bi-Material Elastic Systems
Linearized Three-Dimensional Approach
Akbarov, S.
2015, XXI, 1004 p. 477 illus., Hardcover
ISBN: 978-3-319-14459-7